# Mixed in place permeability reductive layer through Al and OM precipitation

M.P.A. Kaptein

Technical University Delft

TU Delft

de Vries & van de Wiel

# Mixed in place permeability reductive layer through Al and OM precipitation

by

M.P.A. Kaptein

To obtain the degree of Master of Science in:
**Geo-Engineering**
Faculty of Civil Engineering and Geosciences,
Delft University of Technology

To be defended publicly on Tuesday February 9, 2021 at 12:00 AM.

| | | |
|---|---|---|
| Student number: | 4321448 | |
| Project duration: | March 1, 2020 – February 9, 2021 | |
| Thesis committee: | Prof. dr. ir. T.H. Heimovaara, | TU Delft, supervisor and committee chair |
| | Dr. Sc. A. Askarinejad, | TU Delft, supervisor |
| | Dr. M. Hrachowitz, | TU Delft, supervisor |
| | Ir. D. Jumelet, | DEME-group, supervisor |

TU Delft

de Vries & van de Wiel

# Abstract

The control of infiltration and seepage of water is one of the most challenging tasks in water management and civil-engineering and, in an attempt to control this, methods for forming a water-impermeable layer in the soil have been widely practised in soil engineering (Laumann et al., 2018; Proto et al., 2016).The use of natural processes to modify the engineering properties of the subsurface could help to develop cost-effective, robust and sustainable engineering technologies and is attracting increasing attention from the industry (Zhou, 2020). This research aims to reduce the permeability by using aluminium (Al) and organic matter (OM) precipitates mixed ex-situ with porous media to create a horizontal barrier. The Al-OM precipitates were expected to clog the pore space with a reduction in permeability and hydraulic conductivity as result. To find out if it is feasible to use Al-OM precipitates mixed ex-situ with porous media for a permeability reductive layer, the Al-OM precipitates and the permeability of the medium were researched.

To characterise the flocculation reaction, experiments on the flocculation were performed. The yield of the reaction was obtained by adding certain amounts of Al and OM solutions to form particular amounts of dry mass of flocs. This experiment confirmed the hypothesis that 85% of the added mass of OM will result in dry mass of flocs. The concept of a critical metal to carbon ratio (M/C-ratio), indicating flocculation regardless of the input concentrations, was tested by measuring the pH over an increasing M/C-ratio. From this titration curve, the found critical M/C ratio is between 0.023-0.031, and the pH stabilises at a level lower than pH 4. This result proves the concept behind the numerical scenarios describing the titration of OM solutions with $Al^{3+}$, with a critical molar M/C ratio independent of the input concentrations (Veerkamp, 2018; Zhou, 2020). After determining the yield of the reaction and concluding that the concentration of Al and OM was not of influence, the by-products of the Al-OM reaction were quantified. The ionic strength of the supernatant of an increasing density of flocs in solution was determined by measuring the electrical conductivity (EC). The results showed that the ionic strength increased linearly with an increasing density of flocs. The relationship between the ionic strength and the density of flocs was coupled to the linear relationship between concentrations potassium chloride (KCl) and its EC. From the results, the measured EC can be used as a tracer since the $K^+$ and $Cl^-$ are non-reactive.

The hydraulic conductivity measurements were conducted by a falling head test to be able to make an indication of the change in permeability when adding the Al-OM precipitates to the sand. To find the optimal method to mix the Al, OM and porous media, the influence of different methods of producing, adding and mixing the materials on the permeability reduction is explored. In the first mixing method, the Al and OM were added in solution, the solution containing Al-OM precipitates was centrifuged until the reduced ionic strength was at an EC value less than 700 µm/cm. The hydraulic conductivity measurements were used to obtain the relationship between the hydraulic conductivity reduction over an increasing concentration of flocs retained by one kilogram of sand. The hydraulic conductivity was reduced exponentially over an increasing concentration of flocs up to a magnitude of 3. The results imply a large variability in the achieved reduction dominated by the amount of retained flocs. The second method is using Al and OM in powder format and adding them to the dry sand and adding 500 ml of water to this mixture. This mixing method resulted in a completely different floc structure. The flocs produced by mixing in solution have a shear dependency feature, while dry mixing created particles that have a constant size. For this method, the increase of the reduction is linear over an increase of concentration of flocs retained by the soil. The highest reduction for this method was found to be of a magnitude of two, measured at 50 grams of flocs retained by one kilogram of sand. Finally, this research gave proof of principle of using Al-OM precipitates mixed directly with sand could reduce the permeability up to a magnitude of 3. These results present a new road to research on this Al-OM-sand mixture's strength parameters and compaction over time over an increasing floc density, since these parameters are critical for using the layer in practice.

# Aknowledgements

In this section, I would like to thank those who made it possible to work on this study. First of all, I would like to thank Timo Heimovaara for the inspiration and confidence he has had in my work overtime. Secondly, I would like to thank Daan Jumelet. During this strange time of COVID, graduating from home and working from home, he kept his finger on the pulse. He always painted the bigger picture in which I could perhaps see my graduation in practice—making me see the bigger picture has always been a great motivation for me to continue with smaller things. I would also like to thank GSE's technical support, thank you for making the Department's working environment vivid and encouraging, especially during this pandemic. Jolanda van Haagen, without you I would never have been able to do a chemical experiment. Mark Friebel, Jens van den Berg, Karel Heller, Roland Klasen and Michiel Slob thank you for your technical support. But also especially for the conviviality this summer. Of course, I will not forget to thank you, Mohammed Jafar. I found it very educational to work together on my setup, and I won't soon forget the magical water. I would also like to thank Jiani Zhou. Your help came at the perfect moment for me. Thank you for your tremendous help with my writing, in making me understand some aspects of Al-OM better and for cheering me on. Also, to my other exam committee members, Amin Askarinejad and Markus Hrachowitz, I would like to show my gratitude. Besides my exam committee, Barend van den Bosch and Jauk Stroo from the company de Vries & van de Wiel deserve to be mentioned here as they have helped along the way in the form of interesting discussions, meetings and insights.

Lastly, I want to thank everyone who supported me throughout the project on a personal level. A big thanks to my roommates and friends. They have dealt with me through my study time, kept me distracted when necessary and going through the pandemic and my thesis with me. A big thanks to my parents. I love you. Luckily, you'll never have to go to your notes to remember what my study is called. And a special thanks to my sister Fleur, who's always there, not only personal but also to spelling check my emails, documents, presentations and this thesis.

# Contents

# Nomenclature

**Abbreviations**

| | |
|---|---|
| Al | Aluminium |
| C | Carbon |
| Demi water | Demineralized water |
| DOC | Dissolved Organic Carbon |
| DOM | Dissolved Organic Matter |
| EC | Electrical Conductivity |
| FA | Fulvic Acid |
| Fe | Iron |
| HA | Humic Acid |
| HCR | Hydraulic Conductivity Reduction |
| KCl | Potassium Chloride |
| M/C ratio | Molar Metal to Carbon ratio |
| MICP | Microbially Induced Calcite Precipitation |
| MIP | Mixed In Place |
| OM | Organic Matter |
| PSD | Particle Size Distribution |

| **Symbols** | **Description** | **Unit** |
|---|---|---|
| $\frac{dh}{dt}$ | Rate with which burette level falls | [L/T] |
| $\frac{dP}{dx}$ | Pressure gradient | [M/T$^2$] |
| $\gamma$ | Stable floc size exponent | [-] |
| $\varkappa$ | Permeability | [L$^2$] |
| $\mu$ | Viscosity of the fluid | [M/LT] |
| $\varphi$ | Sphericity | [-] |
| $\rho$ | Density of the fluid | [M/L$^3$] |
| $\rho_s$ | The density of the sediment | [M/L$^3$] |
| $\rho_w$ | The density of the water | [M/L$^3$] |
| A | Cross-sectional area of the sample | [L$^2$] |
| a | Cross-sectional area of the burette | [L$^2$] |
| C | Floc strength constant | [-] |

| | | |
|---|---|---|
| $C_u$ | Uniformity Coefficient | [-] |
| $D_{10}$ | the sieve opening size (mm) through which 10% of aggregate passes | [L] |
| $d_{10}$ | Characteristic particle diameter | [L] |
| $D_{60}$ | the sieve opening size (mm) through which 60% of aggregate passes | [L] |
| $d_{floc}$ | Floc diameter | [L] |
| $D_p$ | Particle diameter | [L] |
| G | Average velocity gradient | [1/T] |
| G | The submerged weight | $[MLT^{-2}]$ |
| g | Accelaration due to gravity | $[L/T^2]$ |
| g | Gravitational acceleration | $[L/T^2]$ |
| h | Piezometric head | [L] |
| $h_0$ | Initial head | [L] |
| K | Hydraulic conductivity | [L/T] |
| p | Porosity | [-] |
| Q | Discharge | $[L^3/T]$ |
| t | Time | [T] |
| v | Apparent velocity of flow | [L/T] |
| $V_{permeameter}$ | The volume of the permeameter | $[L^3]$ |
| $V_{pore}$ | The pore volumes | $[L^3]$ |
| $V_{sand}$ | The volume of the sand | $[L^3]$ |

# List of Figures

# List of Tables

# 1 Introduction

## 1.1. Soil sealing: a general overview

Controlling infiltration or seepage of water is one of the most challenging tasks in water management and civil-engineering (Laumann et al., 2018; Proto et al., 2016). The magnitude of the leakage flow is controlled by the permeability of the soil (Bear and Cheng, 2010; Fitts, 2013; Vis, 2015). Permeability is a crucial characteristic of the soil and can be defined as the porous medium's ability to allow passage of water through itself. The most common material used for watertight purposes is clay, due to the fact that it is considered impermeable. Generally, clays have numerous problems due to their low strength, high compressibility and high level of volumetric changes (i.e., shrinking and swelling) (Ural, 2018). In soil remediation, containment retaining barriers are often made with low permeability material, such as clay. However, additional treatment to the clays is often needed (i.e., by adding soluble polymer) to ensure the function of the barrier (Met et al., 2005). For example, dike sealing is often done by compacting the clay or using geosynthetic clay liners. Geosynthetic liners are mostly clay layers, sandwiched between geotextiles or glued to a geomembrane (Daniel, 1993). Another example, i.e., containment resistant barriers, is the treatment of the bentonite clay by soluble polymers in order to create a clay-polymer fabric that is able to resist different classes of chemical contaminants (McRory, 2005). Other soil improvement techniques or horizontal soil sealing methods include spreading asphalt and plastic resin over the selected area (Holtz, 1974; Owa and Husar, 1987). The disadvantage of these methods is that they generally are not that environmentally friendly and rarely feasible when practised on large areas (Owa and Husar, 1987). Therefore, more interest is shown for in-situ treatments. For example, for dike improvement, impermeable sheet pile barriers can be placed within the dike, or an alternative is to create a flow barrier using injection (Zhou et al., 2019).

In-situ projects are generally done by providing the soil with soil treatment agents such as cement milk, water glass, urethane, acrylamide, salt or acrylic acid (Owa and Husar, 1987). These methods may become cost-prohibitive, and environmental concerns regarding traditional methods persist (Proto et al., 2016). In addition, these methods require bulk amounts of treatment agents since the location of the leak is not always precisely known. As a result, the large material usage is perceived as a disadvantage. Much research has been done for using microorganisms or utilising naturally-occurring processes to induce the bioclogging of the leakages at the location (Blauw et al., 2016). The effectiveness of these in-situ methods are often highly dependent on the microorganisms (Blauw et al., 2016), the preparation of the liquid agents, the injection conditions and the efficiency of the injection (Owa and Husar, 1987).

Developing a nature-based geo-engineering technique to reduce soil permeability can provide a solution to a wide range of engineering challenges. The use of natural processes to modify the engineering properties of the subsurface could help to develop cost-effective, robust and sustainable engineering technologies, and thus it is attracting increasing attention from the industry (Zhou, 2020). One example is Microbially Induced Calcite Precipitation (MICP), which relies on in-situ calcite precipitation to reduce soil permeability and to strengthen the soil (Chu et al., 2012). Another example is the SOil Sealing by Enhanced Aluminium and DOM Leaching (SoSEAL) method. The inspiration for this technique comes from the understanding of natural Podzol soils (Zhou, 2017). During Podzolization, the complexation of organic matter (OM) with

polyvalent metals, such as iron (Fe) and aluminium (Al) that are naturally present in the soil, leads to the formation of organo-metallic complexes. The solubility of organo-metallic complexes depends on the local environment such as pH and redox potential (Zhou, 2020). The precipitation and accumulation of organo-metallic complexes in soil reduces the local soil permeability.

### 1.1.1. SoSEAL

The SoSEAL project started at the TU Delft in 2014, and since then much scientific research has been done on the SoSEAL concept. Within SoSEAL, permeability reduction is obtained by pumping an Al solution and dissolved organic matter (DOM) into the soil (Popma, 2017). Al ions can bind to deprotonated functional groups of DOM to form Al-OM complexes (Nierop et al., 2002; Tipping, 2002). Complexation and subsequent precipitation of OM by Al results in the formation of soil layers with reduced permeability; a process that is well known from podzols (Laumann et al., 2018). The SoSEAL concept was mainly investigated as a preventive measure against piping to enhance the stability of dikes (Bonfiglio, 2016; Hopman, 2016; Vis, 2015). Field-scale tests have shown that it is possible to create a vertical cylindrical flow barrier after an injection period of 8 days, where the permeability of the treated sand was reduced to 2% of its original value. This first full-scale field test demonstrates that applying Al-OM precipitates is a suitable bio-based engineering tool to reduce soil permeability in-situ (Zhou et al., 2019). Although the feasibility of creating a vertical flow barrier using Al-OM precipitates has been proven, a horizontal flow barrier is also be of great interest, which can provide a solution to leakage of contaminants, infiltration and leakage in general. Popma (2017) studied the proof of principle of creating a horizontal layer of reduced permeability by applying horizontal drains. Although the precipitation took place, the reduction in hydraulic conductivity was less than expected (i.e., between 25-30% instead of order of magnitudes). The results from this research show that it is possible to use Al-OM precipitation to create a horizontal layer of reduced permeability, but that it is a challenge to make this layer area-covering due to the occurrence of preferential flow (Popma, 2017). This is also why the overall permeability reduction is not as profound as hoped for.

## 1.2. Project relevance

Methods for creating a water-impermeable layer in the soil have been widely excised in soil engineering practices. These methods include horizontal spreading of an impermeable layer over the desired area, which is not environmentally friendly and rarely feasible practised over large areas (Owa and Husar, 1987). The in-situ processes are generally carried out by creating coagulated soil layers with soil treatment agents. The liquid agent is injected into the soil through a nozzle that is inserted into the soil, at which location the agent reacts and coagulates (Owa and Husar, 1987). In this case, the liquid injection agent's preparation, the flow paths, and the injection efficiency are the limiting factors for the quality of the permeability reducing layer of the entire desired treatment zone. Since the utilisation of natural processes for engineering purposes has been widely discussed in recent years, the question arose if it was possible to use the Al-OM precipitates mixed with soil ex-situ to create a horizontal barrier, without using injection.

## 1.3. Research objective

The main objective of this research is to obtain proof of principle that permeability can be reduced by direct mixing between Al-OM precipitates and porous media. From this objective the overall research question is formulated as:

*Is it feasible to apply Al-OM precipitates mixed ex-situ with porous media for a permeability reductive layer?*

To answer the overall research question, sub-objectives are identified and listed below:

- How to characterise the complexing behaviour of the Al-OM precipitates under measurable macro conditions (i.e., pH, molar metal to carbon ratio (M/C-ratio) and ionic strength)?
- What is the most effective method to mix the Al-OM and porous media?
- What is the relationship between the mass of Al-OM precipitates on the permeability reduction of the porous media?
- Is it feasible to upscale the Al-OM-porous media mixture application to use as a geo-engineering tool in the field?

The structure of this thesis is as follows: Chapter 2 is a literature review. This chapter gives insight in the natural process of podzolisation and the chemical/physico-chemical characteristics of the Al-OM complexation, the empirical relations describing the hydraulic conductivity and theories on particle retention that could influence the hydraulic conductivity. Chapter 3 lists and explains the chemicals and (small scale) experiments needed to answer the research questions. In chapter 4, the experiments' results are presented and described. In chapter 5, the results and the effectiveness of the ex-situ mixing of the flocs and the porous media as a permeability reductive layer is discussed. In chapter 6, the research questions are answered, and the remaining knowledge gaps for further research and the use of the layer in practice are identified.

# 2

# Theoretical Background

The permeability reduction method proposed, is hydraulic conductivity reduction by Al and OM precipitates. In this chapter a literature review is given on the Al-OM precipitates, the empirical and experimental background of hydraulic conductivity and the theories on hydraulic conductivity reduction by particles.

## 2.1. Aluminium-organic matter complexes

The Al-OM precipitates are inspired by the podzolization process. The Al-OM complexation is highly investigated by Zhou in his thesis on SoSEAL. In this section the podzolization process, the Al-OM precipitation and the factors influencing this precipitation will be discussed.

### 2.1.1. Podzolisation

The inspiration for the Al-OM precipitates is the natural process responsible for forming the impermeable B-horizon during podzolisation. Podzols mainly occur in cool, humid climates under forest or heath vegetation in medium textured to coarse material (Lundstrom et al., 2000). At the top of the soil, plant organic matter accumulates and slowly humifies. DOM leaches as an acidic solution into the soil and dissolves the ground's existing metals. The dissolved metals and OM translocate to the lower soil forming an impermeable spodic B-horizon by the precipitation and accumulation of the Al-Fe-OM precipitates in the pore spaces (Lundstrom et al., 2000; Zhou et al., 2019).

### 2.1.2. The chemical characteristics of OM

Natural OM in soils consist of litter, other plant residues, soil biomass and humus (Stevenson, 1995). Due to their various organic complexes and high level of intrinsic complexity it is difficult to describe the chemical characteristics of OM (Zhou, 2020). The conventional humification theory focuses therefore on the overall characteristics of unidentifiable organic compounds i.e., humic substances. The humic substances are subdivided based on the solubility of the OM in alkaline extracts into humic acid (HA) , fulvic acid (FA) and humin. The solubility and ion-binding characteristics of OM in water depends on the polarities of its functional groups and whether they can ionize (Zsolnay, 2003). The two functional groups that are often considered as the dominating binding sites are the carboxylic and phenolic groups (Alice Gomes de Melo et al., 2016) shown in Figure 2.1.1. The ionization of phenol and carboxylic acid are given by the following equations and constants:

Carboxylic group:

$$\mathrm{RCOOH} \overset{+\mathrm{H_2O}}{\rightleftharpoons} \mathrm{RCOO}{-}^{+}\,\mathrm{H}^{+} \qquad logK = -4 \tag{2.1}$$

Phenolic group:

$$\mathrm{ROH} \overset{+\mathrm{H_2O}}{\rightleftharpoons} \mathrm{RO}{-}^{+}\,\mathrm{H}^{+} \qquad logK = -10 \tag{2.2}$$

It can be concluded that the carboxylic groups are relatively strong acids that ionize at low pH. The solubility of humic substances (and the molecular size distribution of the soluble components) is dependent on pH, ionic strength and the nature of the electrolyte ions (Kipton et al., 1992). Humin P775 is a potassium humate.

When a potassium humate is brought in an aqueous solution, the non-reactive potassium dissociates and some functional groups protonate again. As a result a potassium humate solution has a high pH (Kipton et al., 1992).

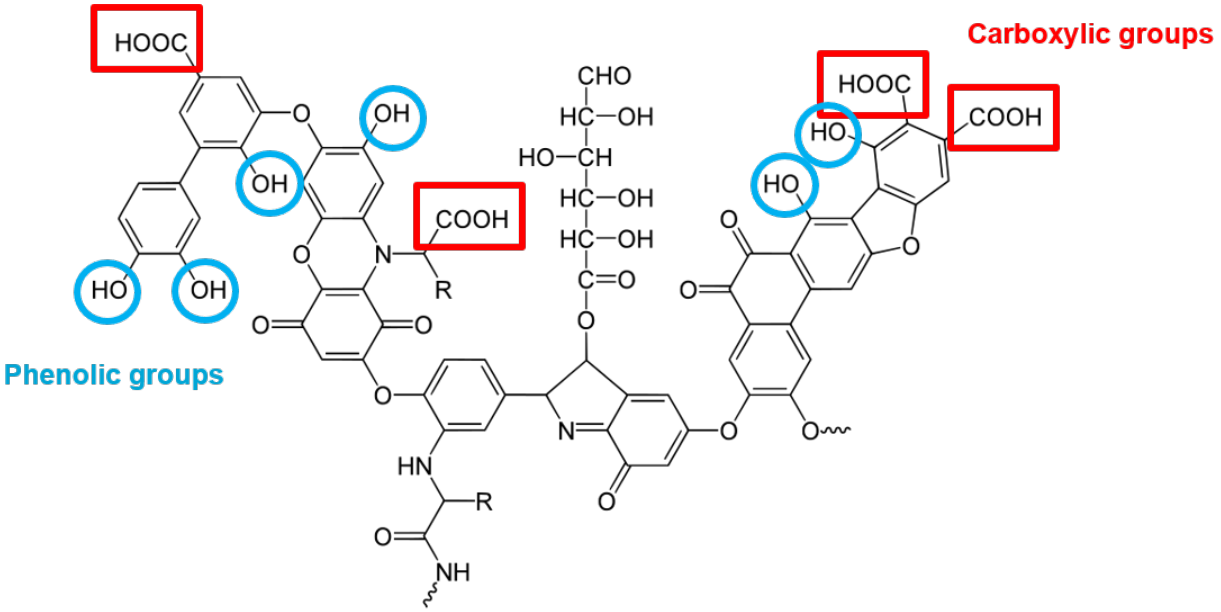


Figure 2.1.1: Mineral composition of OM with its functional groups, carboxylic and phenolic groups highlighted (Laumann et al., 2018).

### 2.1.3. The chemical characteristics of Al

Al and Fe form the most rigid complexes with OM (Tipping, 2002), and due to their high valence they are able to bind more than one organic molecule at the time (Nierop et al., 2002). When metals, like Al, are dissolved in water, the metal will react with water molecules and form metal-hydroxide (ions). In this thesis Aluminium Chloride Hexahydrate (AlCl3 · 6H2O, Sigma Aldrich, Germany) is used as a source of Al. $Al^{3+}$ is known to have a primary hydration shell consisting of six water molecules in octahedral coordination (Richens, 1997). The water molecules in this primary hydration shell are polarised. Depending on the pH this can lead to the loss of protons. This means that water molecules in the hydration shell can be progressively replaced by hydroxyl ions, giving the so-called monomeric Al species:

$$Al^{3+} \longrightarrow Al(OH)^{2+} \longrightarrow Al(OH)_2{}^{+} \longrightarrow Al(OH)_3 \longrightarrow Al(OH)_4{}^{-}$$

The successive deprotonations can then be given by the following equations and their corresponding equilibrium constants (Duan and Gregory, 2003):

$$Al^{3+} + H_2O \rightleftharpoons Al(OH)^{2+} + H^+ \qquad pK_1 = 4.95 \tag{2.3}$$

$$Al(OH)^{2+} + H_2O \rightleftharpoons Al(OH)_2{}^{+} + H^+ \qquad pK_3 = 5.6 \tag{2.4}$$

$$Al(OH)_2{}^{+} + H_2O \rightleftharpoons Al(OH)_3 + H^+ \qquad pK_3 = 6.7 \tag{2.5}$$

$$Al(OH)_3 + H_2O \rightleftharpoons Al(OH)_4{}^{-} + H^+ \qquad pK_4 = 5.6 \tag{2.6}$$

$$Al(OH)_3 \rightleftharpoons Al^{3+} + 3\,OH^- \qquad pK_5 = 31.5 \tag{2.7}$$

Using these hydrolysis constants and logK=10.5, Duan and Gregory (2003) plotted the concentrations of the various species in equilibrium with amorphous hydroxide as a function of pH (Figure 2.1.2). It can be seen that the hydrolysis of Al is strongly influenced by the background pH, under acidic conditions $Al^{3+}$ predominates whereas under neutral and base conditions $Al(OH)_4^-$ predominates.

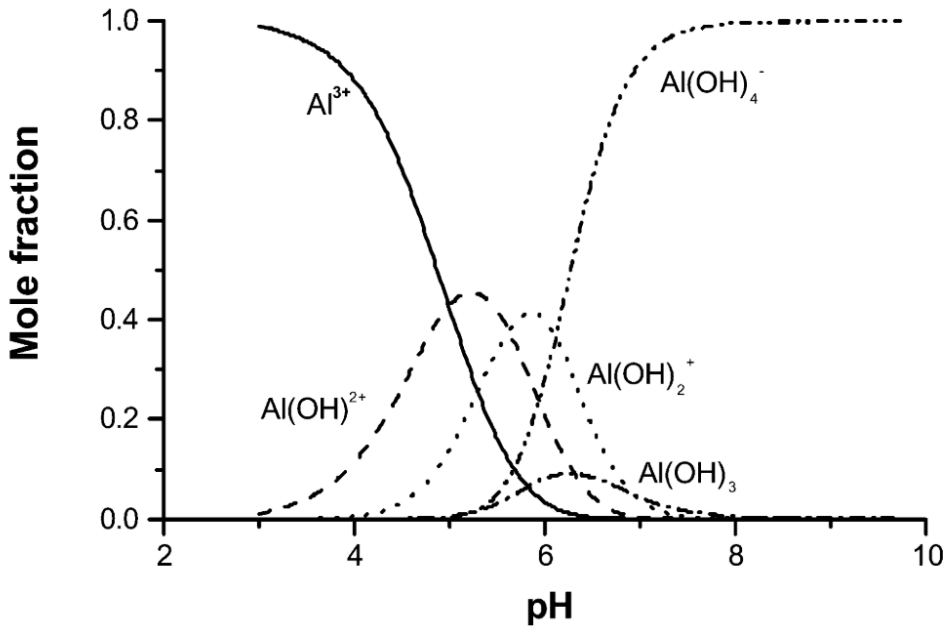


Figure 2.1.2: Proportions (mole fractions) of dissolved hydrolysis products in equilibrium with amorphous hydroxides. Edited from: Duan and Gregory (2003).

## 2.1.4. Complexation and Flocculation of OM and Al

Coagulation and flocculation processes are mainly due to charge neutralisation and sweep flocculation mechanisms (Ghernaout and Ghernaout, 2012). One of the theories that has been often cited to explain the flocculation of OM using metal salts is the DLVO theory (Zhou, 2020). Generally OM is conceptualised as negatively charged particles which due to their electrical repulsion of the colloids are considered thermodynamically stable (Wiersma, 2019). The addition of positively charged metal cations neutralises the negative charge of the OM particles, leading to charge neutralisation. These destabilised colloids can bind together to form larger particles through van der Waals forces which we call precipitation/flocculation (Duan and Gregory, 2003; Wiersma, 2019; Zhou, 2020). Increasing the metal concentrations leads to a decrease of the Donnan potential on OM molecules (Zhou, 2020). Weng et al. found that coagulation of humic acid occurs when the Donnan potential is less negative than -0.08 V.

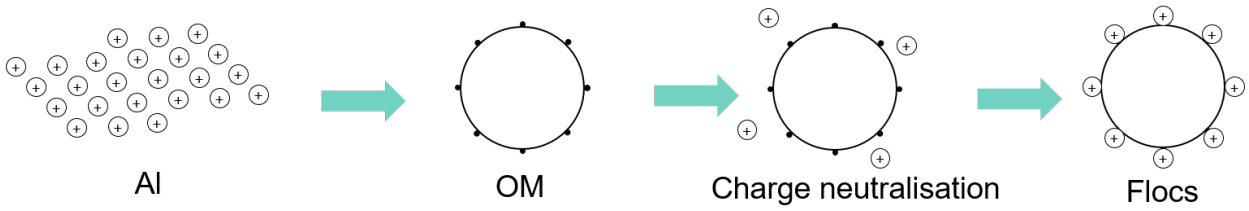


Figure 2.1.3: Schematic representation of flocculation.

From Nierop et al. (2002),Jansen et al. (2002) and Zhou (2020) it was found that the pH is related to the charge neutralisation mechanism. At higher pH (generally pH>7), amorphous aluminium hydroxides will be formed affecting the solubility of OM via another mechanism, sweep flocculation. This mechanism is called sweep flocculation due to the fact that the growing precipitates have an open structure and capture particles in their matrix, sweeping them from the water (Duan and Gregory, 2003). Instead of ion-OM interaction, sweep flocculation attributes to formation of amorphous aluminium hydroxides, which are very small in size and thus have a very large surface area (Zhou, 2020). At low pH-values (<4) the $H^+$ ions outcompete $Al^{3+}$ ions for the binding sites on OM because of their relatively high concentration, so that extremely high concentrations of $Al^{3+}$ ions are required to reduce the negative surface charge on OM (Zhou, 2020). The pH determines the number of acidic functional groups on a given OM molecule that is deprotonated and

available for binding metals (Jansen et al., 2002). In addition the pH values determine whether $Al^{3+}$ predominates or $Al(OH)_4^-$ predominates shown in Figure 2.1.2. The higher the valence, the more binding sites there are with OM, and the more stable the complex becomes. From Figure 2.1.2 it shows that a lower pH, below 5, $Al^{3+}$ is present. From section 2.1.2 the carboxylic group tends to bind metals in a pH range from 3 to 5 and phenolic groups in a pH range of 7 to 9. The carboxylic groups dissociate more easily, which makes them very prone to changes in pH or metal concentrations.

Jansen et al. (2002) demonstrated that the insoluble complexation is dependent on the Al/C ratio and the pH. A critical molar metal to carbon ratio (M/C ratio) has often been used to describe the flocculation of OM induced by metal ions (Nierop et al., 2002). From Zhou (2020), flocculation takes place at approximately the same M/C ratio, regardless of the input of OM concentration. Experiments of Jansen et al. (2002) reveal that insoluble Al-OM complexes precipitate instantaneously when the M/C ratio is above 0.06. The M/C ratio determines to what extent the negative charge on the OM molecules resulting from deprotonation is compensated by the positive charge on metal cations, with a net zero charge inducing precipitation of the complex (Jansen et al., 2002). At higher M/C ratios, it will be increasingly difficult for cations to find unoccupied binding sites, and also there will be an increasing electrostatic repulsion by residual positive charge left on cations that are already bound to OM (Jansen et al., 2002). This means that there is a decrease in particle size and precipitation observed. Previous work from Bonfiglio (2016); Sanna (2020); Wiersma (2019); Zhou et al. (2019) has shown that there is a value of M/C ratio of 0.03 at which precipitation occurs. The optimal value for floc size and amount of precipitation and the size of precipitated flocs is the largest at a M/C ratio of 0.06.

### 2.1.5. Physico-chemcial behaviour of Al-OM flocs

Flocs may be defined as highly porous, irregularly shaped and loosely connected cloud-like aggregates formed by the constant collision between smaller particles (Jarvis et al., 2006; Zhou, 2020). Research showed that organo-metallic precipitates occur as floc-like structures with sizes ranging from 17 µm up to 1000 µm (Jarvis et al., 2005). From the Al-OM laboratory research for the SoSEAL concept, Laumann et al. (2018) found the size of the Al-OM flocs (M/C ratio 0.1, pH 4.8) exposed to an increasing stirring rate from 150, 300 to 400 rpm, which first decreased in diameter from 750, 250 and then decreased further to 125 µm, respectively, as shown in Figure 2.1.4 (right) (Zhou, 2017).

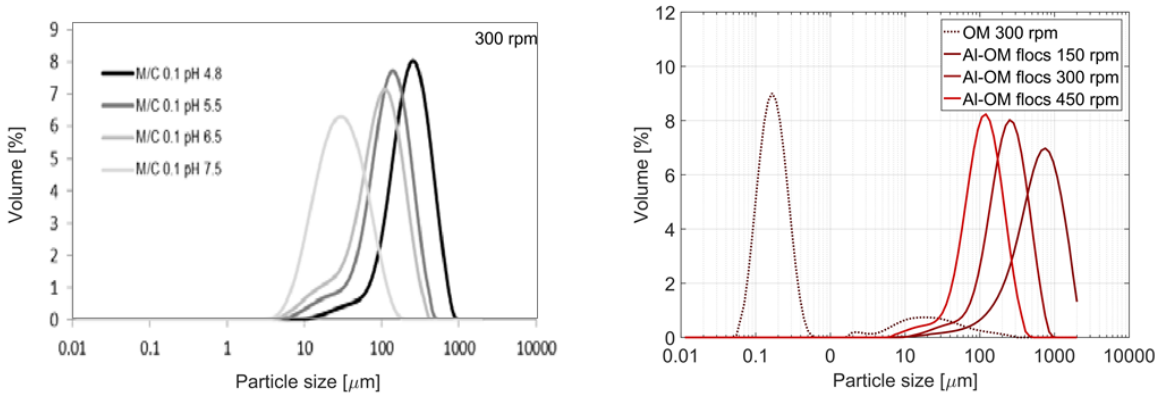


Figure 2.1.4: Al-OM floc size distribution for a M/C ratio of 0.1 and a varying pH for a stirring rate of 300 rpm (left (Zhou, 2020)). Changes in Al-OM floc size distributions for different stirring rates (right) (Laumann et al., 2016).

The knowledge of floc formation and kinetics from colloid science is essential to understand the clogging potential of the Al-OM flocs. Floc strength generally increases with a decreasing floc size due to the fact of floc compaction and the number of internal bounds. It is difficult to measure the floc strength due to the fragility and complexity of floc structure (Jarvis et al., 2005). The fact that the regrowth, floc size and flocculation are shear dependent, a variable that can be measured, research has been done on the effect of the shear on the regrowth of the floc (Wiersma, 2019). Floc dimension decreases with the increase in shear rate, since it influences the stability of flocs (Jarvis et al., 2006). In addition, the collision efficiency decreases

as the floc size gets bigger (Zhou, 2020).The floc size as a function of shear is expressed mathematically by Jarvis et al. (2005) by equation 2.8:

$$\log d_{floc} = \log C - \gamma \log G \tag{2.8}$$

Where $d_{floc}$ is the floc diameter [L]; C is the floc strength constant [-]; $\gamma$is the stable floc size exponent and G is the average velocity gradient [1/T], which is equivalent of shear (Zhou, 2020).

Though high shear conditions lead to the breakage of large sized flocs almost instantaneously, this breakage is reversible, meaning that small flocs will regrow in size when the imposed shear conditions become low again (Jarvis et al., 2005). From Jarvis et al. (2005), the flocculation follows a certain pattern of a rapid growth phase, a steady state, a breakage phase and a re-form state. Especially the part of the breakage and regrowth is very interesting for the effect of mixing on the floc sizes. If the shear rate is too high, it can destroy the flocs to such a small size that they are not able to regrow anymore (Yu et al., 2010). From the results of Wiersma (2019) it was found that flocs, even when broken at the highest shear, are still > 100 µm. From the total floc concentration and the relative sizes and number of flocs, it could be concluded that regrown flocs are more dense than flocs which had not been broken (Wiersma, 2019). Overall, these results can be used to predict a broken floc size of 100-300 µm depending on the shear rate, with limited regrowth of max 15%.

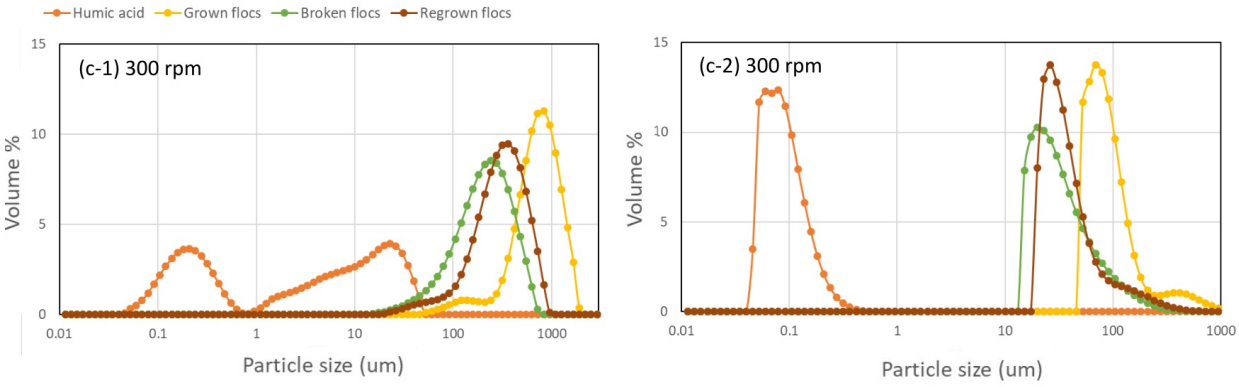


Figure 2.1.5: The comparison between volume-based and number based floc size distributions for shear rate of 300 rpm (Wiersma, 2019).

## 2.2. Hydraulic conductivity

The aim of the research is to reduce the hydraulic conductivity of the soil by adding particles to the soil structure. In this chapter the terms hydraulic conductivity and permeability are used interchangeably. To prevent confusion, the hydraulic conductivity is the ability or ease of fluid to pass through material (Head and Epps, 2011). The permeability is the ability of material allowing fluid to pass through. Permeability is a property of the porous medium itself, while hydraulic conductivity is the property of the whole system including both porous medium and the flowing fluid. For deriving the hydraulic conductivity, density and viscosity of the fluid are considered along with the permeability of the porous medium. Permeability is essentially synonymous with hydraulic conductivity, although this term may be more strictly interpreted as correct only if water is the permeant (Davies and Mander, 2007). Some researchers interpret this reduction in permeability as the direct consequence of a reduction of porosity, which is caused by the precipitates in the pore spaces (Zhou, 2020). By measuring the hydraulic conductivity an indication of the change in permeability can be made. In this chapter, the theoretical background for this thesis is presented by giving a review on the hydraulic conductivity and the laboratory tests to measure the hydraulic conductivity.

### 2.2.1. The falling head test

Soils consist of solid particles with voids between them. These voids are interconnected which enables water or other fluid to pass through the soils, that is, if soils are permeable. There are several laboratory tests for

determining the coefficient of the permeability, such as the constant head test, falling head test, capillary permeability test and consolidation test (Nagy et al., 2013). The capillary permeability tests are mostly used in partially saturated fine grained soils. The consolidation tests can be indirectly used to determine the permeability coefficient of clays and the constant head test is most suitable for coarse grained soils, such as gravels and sands. In this research the falling head test is used, which is the test that is mostly used for low permeability soils. In the test the head difference and the discharge through the sample decrease with time. The discharge is given by 2.9:

$$Q = -a\frac{dh}{dt} \tag{2.9}$$

Where Q is the discharge [$L^3$/T]; a the cross-sectional area of the burette [L]; $\frac{dh}{dt}$ is the rate with which the burette level falls [L/T]. When combining equation 2.9 with Darcy's flow equation:

$$Q = KA\frac{h}{L} \tag{2.10}$$

Where Q is the discharge [$L^3$/T]; K the hydraulic conductivity [L/T]; A is the cross-sectional area of the sample [$L^2$]; h is the piezometric head [L] and L is the flow length [L]. Combining equation 2.9 and 2.10 the hydraulic conductivity, K, can be calculated as:

$$K = \frac{aL}{At}ln\frac{h_0}{h} \tag{2.11}$$

In which $h_0$ [L] is the initial head and h the head at time t [T]. A schematic description of the falling head test set-up is given in 2.2.1.

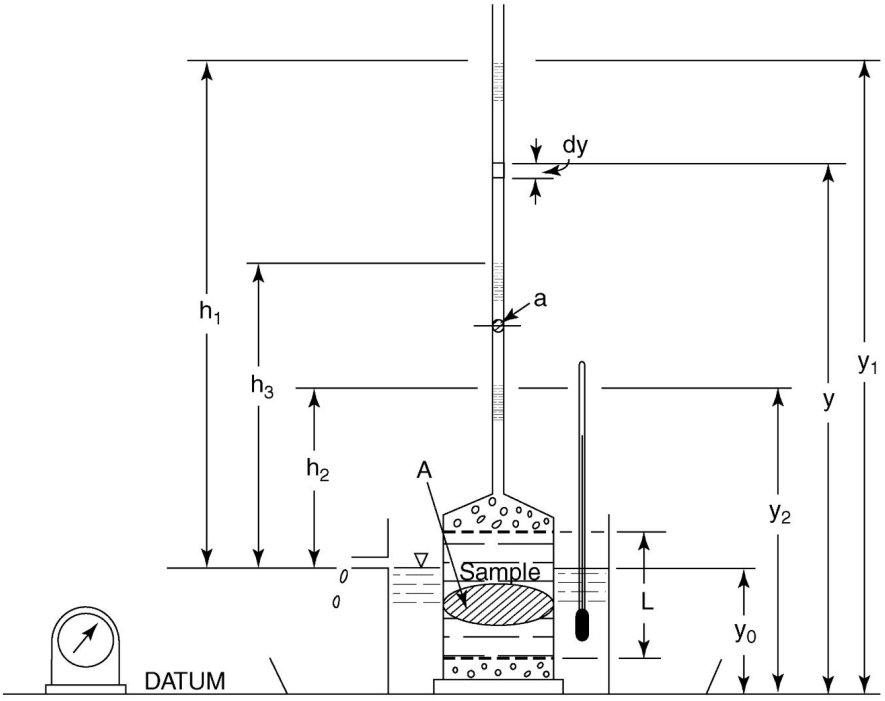


Figure 2.2.1: Schematic diagram of the falling head permeability test setup (Head, 2018).

### 2.2.2. Empirical relations

The saturated hydraulic conductivity of a soil can be predicted using empirical relationships. In section 2.2.1 an example of the experimental method for measuring the hydraulic conductivity is given. This experimental method is based on the empirical relationship proposed by Darcy in 1856, often referred to as Darcy's law. Hazen introduced the effect temperature and grain size on the apparent velocity of flow by relating the hydraulic conductivity to the characteristic particle diameter $d_{10}$ . Another well-known relationship between permeability and the properties of pores was proposed by Kozeny and later modified by Carman by the following semi-empirical, semi-theoretical formula for the relationship between the pressure gradient and the velocity (Hommel et al., 2018):

$$\frac{dP}{dx} = \frac{180\mu}{\phi^2 D_p^2} \frac{(1-p)^2}{p^3} v \tag{2.12}$$

where $\frac{dP}{dx}$ is the pressure gradient [M/T$^2$]; μ is the viscosity of the fluid [M/LT]; φ is the sphericity [-]; $D_p$ is the particle diameter [L]; p is the porosity of the medium [-] and v is the velocity of flow [L/T] defined by:

$$v = \frac{Q}{A} \tag{2.13}$$

which is the discharge [L$^3$/T] over the area A [L$^2$].

Substituting equation 2.12 with Darcy's law equation 2.13 and the relation between permeability and hydraulic conductivity given by:

$$\kappa = K \frac{\mu}{\rho g} \tag{2.14}$$

$$Q = A \frac{\kappa}{\mu} \frac{dP}{dx} \tag{2.15}$$

where ϰ is the permeability of the medium that the water is flowing through [L$^2$] ;μ is the viscosity of the fluid [M/LT]; ρ is the density [M/L$^3$] and g gravitational acceleration [L/T]. The equation becomes:

$$v \frac{\mu}{\kappa} = \frac{180\mu}{\phi^2 D_p^2} \frac{(1-p)^2}{p^3} v \tag{2.16}$$

which can be simplified and rewritten as an equation for the permeability of the porous medium that water is flowing through by:

$$\kappa = \frac{\phi^2 D_p^2}{180} \frac{p^3}{(1-p)^2} \tag{2.17}$$

where ϰ is the permeability of the medium that the water is flowing through [L$^2$] ;$D_p$ is the particle diameter [L] and p is the porosity [-].

### 2.2.3. Hydraulic conductivity reduction by particles

The reduction of porous media by particles is researched extensively due to the fact that the colloidal matter can either block or partially restrict fluid flow. Multiple fields are dependent on the existence or lack of existence of fluid flow. In this section, the reason multiple fields are dependent on the hydraulic conductivity and the mechanisms of particle retention are described.

In the movement of toxic compounds researchers have particular interest in mechanisms involving the transport of heavy metal ions and other toxins that happen to be adsorbed on colloidal particles that are transported by the groundwater. In the petroleum industry, many research has been done on the topic to prevent the loss of flow through the formation. They found severe losses in permeability, even when the injected fluid was completely free of particles. The blockage of pores in the geologic substrata often occurs when the injected fluid has a much lower salt content in comparison to the water that was initially present (Hubbe et al., 2009). In the sealing of the ground, permeability reduction can be highly desirable, therefore in the sealing of wastewater lagoons, montmorillonite clay, often called bentonite, showed that very small amounts of the clay is able to decrease permeability of sands by factors of 100 to 1000 (Hubbe et al., 2009).

Fan et al. (1985) concluded that the mechanism of particle retention was quite different, depending on the size ranges of particles; large particles were retained mainly by physical factors, whereas the retention of smaller particles appeared to depend more on attractive forces between surfaces. This means that there are different physical and physical-chemical colloid-porous medium interactions. The physical-chemical colloid-porous medium interactions are blocking and ripening. Blocking is when particle-particle interaction energies are repulsive, so the particles tend to interact with the porous medium (Tosco et al., 2014). The blocking function is described by Schijven and Hassanizadeh (2000):

$$\begin{cases} n\frac{\partial c}{\partial t} + \rho_b \frac{\partial s}{\partial t} = nD\frac{\partial^2 c}{\partial x^2} - q\frac{\partial c}{\partial x} \\ \rho_b \frac{\partial s}{\partial t} = n\psi k_a c - \rho_b k_d s \end{cases} \tag{2.18}$$

where $k_a$ is the attachment rate cofficient, $k_d$ is the detachment rate coefficient and $\psi$ is a dimensionless particle attachment function described by:

$$\psi_i = 1 - \frac{s}{s_{max}} \tag{2.19}$$

where s is the particle concentration in the solid phase, and $s_{max}$ is the maximum particle concentration retainable on the solid phase at given chemical conditions (Tosco and Sethi, 2010).

Ripening occurs when particle-particle interactions are attractive, so particles tend to interact with other particles within the porous medium. From there, there is an increase in attachment kinetics, until the porous medium is completely clogged (Tosco et al., 2014). The ripening kinetics can be defined as:

$$\psi_i = 1 + A_{rip} s^{\beta_{rip}} \tag{2.20}$$

where s is the particle concentration in the solid phase, $A_{rip}$ and $\beta_{rip}$ are the ripening coefficients that define the interaction dynamics. For $A_{rip}$ >0 and $\beta_{rip}$ >0, the deposition rate increases with the increasing concentration of attached particles (Tosco and Sethi, 2010).

The physical interactions are filtration and straining (Tosco et al., 2014). Straining is the trapping the colloid in a down-gradient pore throats, that are too small for the colloid to passage. The straining kinetics can be defined as:

$$\psi_i = (1 + \frac{x}{d_{50,s}})^{-\beta_{str}} \tag{2.21}$$

where x is the length of the path of the particles in the porous media, $\beta_{str}$ (-) is a fitting parameter which controls the shape of the particle spatial distribution, $d_{50,s}$ is the average diameter of the particles (Bianco et al., 2016).

Filtration occurs when particles are larger than the size of the porous medium. When the suspended and colloidal particles collide with the filter grains, attachment could take place (van Halem, 2020). In general the filter material (sand), the suspended and colloidal particles have a negative charge and repulsion takes place. The equation for filtration is formulated as (van Halem, 2020):

$$\frac{\partial c}{\partial t} = -u\frac{\partial c}{\partial y} - \lambda \cdot u \cdot c \tag{2.22}$$

in which c is this concentration of suspended and colloidal solids, y is the depth of the filter bed, v is the filtration rate, p is the porosity, u is the pore velocity (=v/p), $\lambda$ is the filtration coefficient and $\sigma$ is the accumulated solids.

In stationary situation the following is valid (van Halem, 2020):

$$\frac{\partial c}{\partial t} = 0 \tag{2.23}$$

therefore the kinetics equation is transformed into:

$$\frac{\partial c}{\partial y} = -\lambda \cdot c \tag{2.24}$$

Due to pore clogging, the pore velocity increases and fewer solids will accumulate, expressed by a lower filtration coefficient λ. Well-known relationships describing the relationship between filtration coefficient and the accumulated solids, are those of Lerk (2.25) and Maroudas (2.26):

$$\lambda_0 = \frac{k_1}{v \cdot \nu \cdot d^3} \tag{2.25}$$

$$\lambda = \lambda_0 \left(1 - k_2 \frac{\sigma}{\rho_d \cdot p_0}\right) \tag{2.26}$$

The ratio between the accumulated solids $\sigma$ and the density in reduction of pore volume $\sigma_v$ is described by:

$$\frac{\sigma}{\rho_d} = \sigma_v \tag{2.27}$$

in which $\rho_d$ is the density of the flocs and $\sigma_v$ is the volume concentration in the pores.

In equation 2.26 it is assumed that the filtration coefficient decreases linearly as the clogging increases. Although this is a simplification, it can be used to solve the system of equations. With boundary conditions of y=0, c=$c_0$ and the initial condition of t=0, and $\sigma_v$=0 and:

$$\alpha = \frac{v \cdot c_0 \cdot \lambda_0}{n \cdot \rho_d \cdot p_0} \tag{2.28}$$

The general solution becomes:

$$c = c_0 \cdot \frac{e^{a \cdot t}}{e^{\lambda_0 \cdot t} + e^{\alpha \cdot t} - 1} \tag{2.29}$$

with y=L

$$c_e = c_0 \cdot \frac{e^{a \cdot t}}{e^{\lambda_0 \cdot t} + e^{\alpha \cdot t} - 1} \tag{2.30}$$

and the formula for reduction of pore volume is:

$$\sigma_v = n \cdot p_0 \frac{e^{a \cdot t} - 1}{e^{\lambda_0 \cdot t} + e^{\alpha \cdot t} - 1} \tag{2.31}$$

Due to the fact that the clogging increases, the resistance of the filter bed increases as well. The clean bed resistance of a filter bed, $H_0$ can be described by the flow through a pipe and the carman-kozeny equation:

$$I_0 = \frac{H_0}{L} = 180 \frac{\nu}{g} \frac{(1 - p_0)^2}{p_0^3} \cdot \frac{v}{d_0^2} \tag{2.32}$$

in which $I_0$ is the resistance gradient. When clogging occurs the resistance formula changes to:

$$I = I_0 \left(\frac{p_0}{p_0 - \sigma_v}\right)^2 \tag{2.33}$$

## 2.3. Recap on parameters of influence

The permeability reduction method proposed is hydraulic conductivity reduction by Al and OM precipitates. The parameters that influence the flocculation process are pH, the M/C ratio, ionic strength and shear rate. Factors that affect the permeability are the grain size of the porous media, the viscosity of the fluid, the temperature and the porosity of the sand, shown by equation 2.16. The porosity of the sand or the packing density depends on the shape of the particles. It is generally observed that non-spherical particles give a lower random packing density than spherical particles (Chateau, 2012), this is due to the fact that non-spherical particles have more parameters (shape, orientation, size) than spherical ones (Chateau, 2012). For particle retention, the physical interactions, filtration and straining are mostly trapping the colloid in the pore throat. The clogging of the pore throat is mostly influenced by the density of the flocs and with that, the reduction of the pore volume.

# 3

# Material and Methods

To find out if it is feasible to use Al-OM precipitates mixed ex-situ with porous media for a permeability reductive layer, the Al-OM precipitates, and the permeability of the medium should be researched. This chapter explains the different materials and experiments used to answer the research questions. First, the materials and proportions used in the experiments are described. Second, the flocculation experiments are explained. The experiments consist of quantifying the yield of the reaction and measuring the pH over an increasing M/C ratio to test the influence of the Al and OM solutions' concentration. After which the by-products of the reaction are quantified by identifying the amount of potassium chloride (KCl) and the unreacted OM. These experiments are carried out to identify and reduce the variables to explain any discrepancies within test results. Finally, the execution, the experimental cycle, the different ways of adding the Al-OM and porous media and the falling head permeability tests and set-up are explained.

## 3.1. Materials

This section gives a description of the proportions of the prepared solutions and the properties of the chemicals and porous media used in the experiments. First the chemicals with their properties that were selected for the experiments are described after which the used porous media is explained. All solutions were prepared with demineralized water (demi water).

### 3.1.1. HUMIN P775

As a source of OM, potassium humate (HUMIN P775, Humitech, Germany; later on in solution referred to as OM solution) was used. According to the information provided by the supplying company Humitech, HUMIN P775 is a specially selected leonardite material which has been carefully reacted with potassium compounds. This reaction converts the material to water-soluble potassium humates by neutralizing the humic acids. HUMIN P775 has been used in previous experiments in the SoSEAL research program since HUMIN P775, as the OM source, is commercially available and has shown reactivity and high solubility. The result of a CHNS analysis, which analysed the composition of HUMIN P775, is shown in Table 3.1.1. From this CHNS analysis, the amount of organic carbon is derived. The CHNS analysis is important to know the amount of carbon (C) that is present in the HUMIN P775.

Table 3.1.1: CHNS analysis conducted by the University of Amsterdam copied from: (Popma, 2017).

| Sample | N(%) | C(%) | H(%) | S(%) |
|---|---|---|---|---|
| Humin_01 | 1.05 | 41.81 | 3.12 | 0.83 |
| Humin_02 | 1.00 | 42.54 | 3.83 | 0.88 |
| Average | 1.025 | 42.175 | 3.475 | 0.8545 |

When dissolved in water, the resultant OM solution is dark coloured and has a pH value around 9. The molecular weight of the C compound in the OM is 28.87 g/mol. In most experiments, the stock solution was used, which was prepared with 66.4 g/l of the OM source. This corresponds to a concentration of 2.3 mol/l C.

### 3.1.2. Aluminium Chloride Hexahydrate

As the Al source, Aluminium Chloride Hexahydrate ($AlCl_3 \cdot 6\ H_2O$, Sigma Aldrich), was used. $Al^{3+}$ is known to have a primary hydration shell consisting of six water molecules in octahedral coordination. The Al is produced in a solid crystal form. When dissolved a colourless solution is created with a pH value of around 3.5. The molar mass of the $AlCl_3 \cdot 6\ H_2O$ is 242.4 g/mol. In most experiments, the stock solution was used, which was prepared with 242.4 g/l (corresponding to a concentration of 1 mol/l Al).

### 3.1.3. Porous media

Initially, the experiments were done using different grain size distributions by using various sand types to study the importance of the grain size on particle retention. The porous media used were: drainage sand, sand for sandbeds and sands for filling up terrains. The requirements for these sands are found in Table 3.1.2.

Table 3.1.2: Requirements for sand for filling up of terrains, drainage sand and sand from sandbeds (voor Infrabouwproces, 2011).

| Sand | Requirements mineral parts | | | | Requirements on loss on ignition |
|---|---|---|---|---|---|
| | Fraction ≥ 250 um | Fraction ≤ 63 µm | Fraction ≤ 20 µm | Fraction ≤ 2µm | |
| Sand for filling up of terrains | | ≤50% | | ≤ 8% | |
| Drainage sand | ≥50% | ≤5% | | | ≤3% |
| Sand in sandbeds | | ≤15% | ≤3% | | ≤3% |

However, it was observed that the flocs were rinsed out of the sand columns over time. The sands contained some large gravel particles, which had too much influence on the particle retention, especially since the column set-up is with small dimensions. Therefore the sands have been sieved in small ranges to find the optimal grain size for the experiments. These experiments resulted in a favourable grain size that is smaller than 300µm. From TU Delft concrete lab silo 8, silver sand S60 from the company Sibelco was used. This sand has a $D_{50}$ of 230 µm and a high $SiO_2$ content of 99.5 %. In Figure 3.1.1, the cumulative particle size distribution of the used sand is shown in Figure 3.1.1.

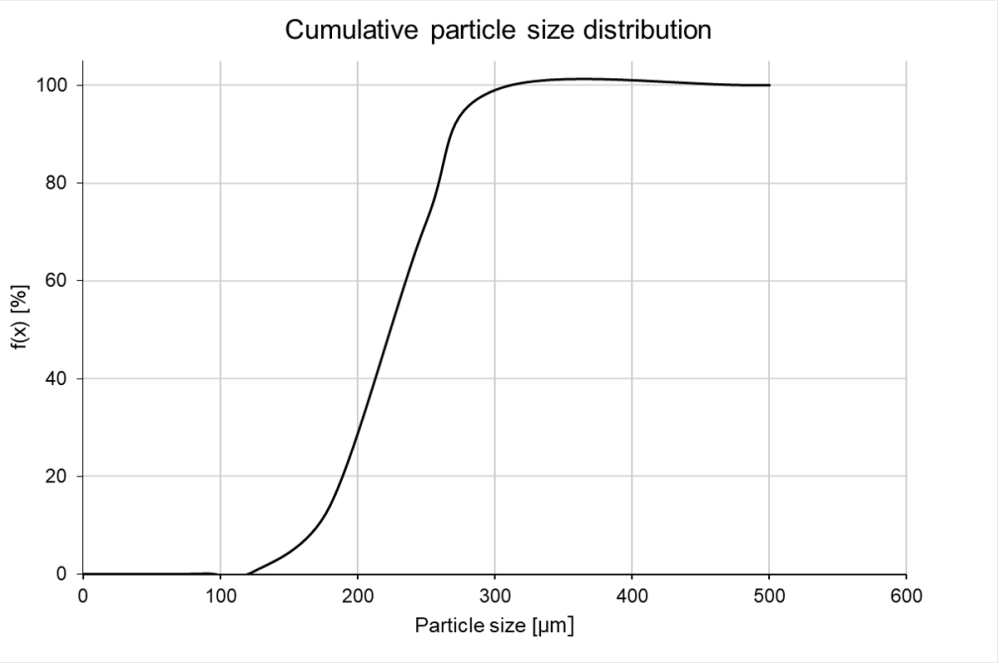


Figure 3.1.1: The cumulative grain-size distribution curve of the used silver sand obtained from ISO sieving retrieved from information provided by Sibelco.

## 3.2. Experiments for mass production of flocs

This section gives an overview of the experiments that were performed to quantify specific parameters for the mass production of flocs. The complexation of the Al-OM is the critical reaction for mass-producing the flocs. Since the Al-OM precipitates have already been injected in large scale field experiments, there is information available for getting the largest and strongest flocs and the fastest flocculation reaction. To be able to answer the research question, a certain amount of flocs had to be made. To be able to produce particular amounts of flocs (based on mass), the yield of the reaction was researched. The aim of the experiments is test the efficiency and identify the byproducts of the flocculation reaction.

### 3.2.1. Yield of the reaction

To mass-produce the flocs, it is necessary to find the yield of the flocculation reaction. The expected mass of dry flocs is 85% of the dry mass of OM used for the reaction (Popma, 2017). In all experiments, the Al and OM were added to each other at a M/C ratio of 0.06. This M/C ratio gives the largest flocs, the largest amount of precipitation and the strongest flocs. Table 3.2.1 gives the amounts in gram and mol of the materials per expected amount of dry flocs in gram.

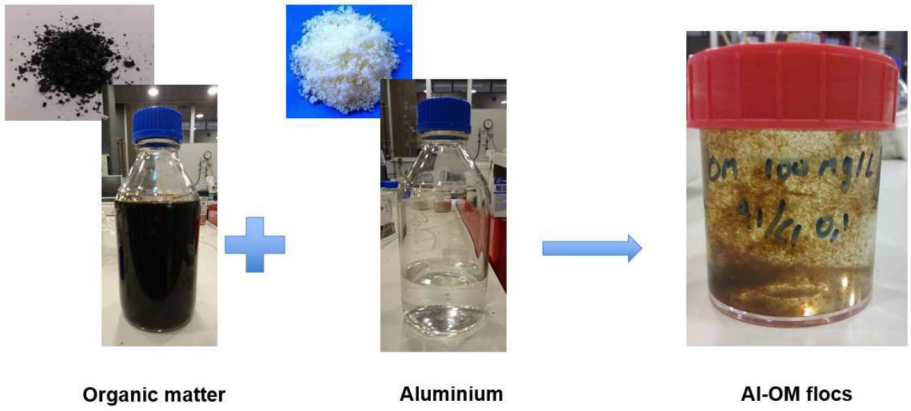


Figure 3.2.1: Visualisation of the materials in powder format, in solution and the Al-OM precipitates.

Table 3.2.1: The necessary amount of chemicals for the expected flocculation.

| Flocculation (g) | OM (g) | Al (g) | OM (mol) | Al (mol) |
|---|---|---|---|---|
| 50 | 57.50 | 28.97 | 1.99 | 0.12 |
| 40 | 46.00 | 23.17 | 1.59 | 0.10 |
| 30 | 34.50 | 17.38 | 1.20 | 0.07 |
| 25 | 28.75 | 14.48 | 1.00 | 0.06 |
| 20 | 23.00 | 11.59 | 0.80 | 0.05 |
| 15 | 17.25 | 8.69 | 0.60 | 0.04 |
| 10 | 11.50 | 5.79 | 0.40 | 0.02 |
| 5 | 5.75 | 2.90 | 0.20 | 0.01 |
| 1 | 1.15 | 0.58 | 0.04 | 0.00 |

First, the stock solutions of 2.3 mol/l OM and 1.0 mol/l Al were made. The experiment was executed by first, weighing the empty measuring cup. The solutions of OM and Al were mixed in the given proportions shown in Table 3.2.1. Constant stirring was applied throughout the addition of the Al solution to the OM solution. The mixture is left to rest overnight. As such, the complexation between Al and OM is expected to be complete. Centrifuging of the mixture was later performed with the Heraeus megafuge 1.0S in order to reduce the electrical conductivity (EC) sufficiently. In order to remove all moisture and obtain the dry weight of the flocs, the flocs mixtures after centrifuging were put into the oven for 21 days at 50 degrees Celsius. Finally, the measuring cup was weighed again, and the empty cup was subtracted from the measured total mass in order to get the dry mass of flocs.

### 3.2.2. Influence of concentration on M/C ratio dependent pH

The influence of the concentration of Al and OM solutions was studied by measuring the pH over an increasing M/C-ratio. This experiment has been performed since the higher the concentrations that can be used, the smaller the volumes of Al and OM solutions necessary for producing the flocs. The M/C ratio often describes the flocculation of OM induced by metal ions. In the thesis of Zhou (2020), a pH-dependent M/C-ratio was found. A critical M/C-ratio was found at a M/C ratio of 0.027 and a pH of 4.5. At the critical M/C ratio and pH, a sharp turning point is expected in the titration curve, which corresponds to the occurrence of flocculation.

First, the stock solutions of 2.3 mol/l OM and 1.0 mol/l Al were made. The pH meter calibration was performed before every test using buffer solutions of pH: 7 and 10. The pH meter is in good condition if the reading difference between the measurement and standard value is $\leq 0.30$. In a OM solution with a volume of 100 ml, 13.8 ml Al was added in different step sizes to obtain 5 gram of dry flocs. After that, half of the concentration and double the volume was used shown in Table 3.2.2.

Table 3.2.2: The concentrations (mol/l), the volume of step sizes and amounts of Al and OM solutions for titration experiments.

| Concentration OM (mol/l) | Volume OM (ml) | Concentration Al (mol/l) | Volume Al (ml) | step size (µl) |
|---|---|---|---|---|
| 2.30 | 100.0 | 1.0 | 13.8 | 200 |
| 2.30 | 100.0 | 1.0 | 13.8 | 500 |
| 2.30 | 100.0 | 1.0 | 13.8 | 1000 |
| 1.15 | 200.0 | 0.5 | 28.0 | 500 |
| 2.30 | 86.6 | 1.0 | 12.0 | 500 |

To obtain the reaction course for even larger concentrations, the titrations have been executed for larger amounts of flocs in different step sizes. The titration experiments were done for different concentrations of solutions, which corresponds to the amount of mol/mol as in Table 3.2.1.

### 3.2.3. Quantifying the ionic strength

HUMIN P775 is a potassium humate. The potassium influences the salinity of the mixture, which could make additional measures mandatory in order to lower the salinity level on-site to the level required by the authorities (commissie bodembescherming, 2007). This experiment aimed to find the relationship between the ionic strength of the flocs solution and salt concentration in the mixture. The ionic strength was measured by the EC of the sample. It should be noted that it was expected that the value of EC in this experiment was mainly influenced by the concentrations of ions ($Cl^-$ and $K^+$) in the floc suspension.

The EC measurements were done on the supernatant of the centrifuged flocs. The flocs were diluted and centrifuged up to an EC value less than 700 µS/cm, which is around the same value as the EC value of tap water. The relationship between the density of flocs and their corresponding ionic strength was then correlated to the concentration of KCl.

### 3.2.4. Quantifying the Dissolved Organic Matter (DOM) from supernatant

The assumption that 85% of the OM can form precipitates by binding Al ions was verified by quantifying the remaining concentration of OM in the supernatant. Samples were taken from the supernatant after centrifuging the flocs in order to quantify the dissolved fraction of OM using UV-VIS spectroscopy at 254 nm wavelength. This approach assumes that the OM concentration is proportional to the UV adsorption at 254 nm. The UV-VIS spectrometer cannot measure the absorbance for high OM concentrations and has a maximum of 3.5 abs.

First, the relationship between the OM and the UV adsorption was established by measuring the UV adsorption of known OM concentrations. Before every use, the UV-VIS spectrophotometer was calibrated with purified $H_2O$, whereafter the in Table 3.2.3 concentrations were tested on their UV adsorption.

Table 3.2.3: The concentrations of OM that are used to establish a relationship between the UV adsorbance and concentration OM

| OM (mol/l) | OM (g/l) |
|---|---|
| 0.3464 | 10 |
| 0.1732 | 5 |
| 0.0693 | 2 |
| 0.0069 | 0.2 |
| 0.0035 | 0.1 |
| 0.0014 | 0.04 |
| 0.0007 | 0.02 |
| 0.0003 | 0.01 |
| 0.0001 | 0.002 |

The flocs were made by the proportions in Table 3.2.1. After resting for a day, the flocs were centrifuged for 15 minutes at 2500 rpm. The samples for the UV adsorption measurements were taken from the supernatant. The mass of the immersed flocs is weighted and diluted with demi-water. After the flocs were diluted and stirred, the mass was noted. In the meantime, the UV adsorption was measured by the spectrometer. The values for UV adsorption were then correlated to the concentration of OM.

## 3.3. Hydraulic conductivity experiments

To prove the principle that adding Al-OM flocs to the porous medium will reduce the porous medium's hydraulic conductivity. Different proportions of flocs and sand and different ways of distributing the flocs through the sand have been tested to find an optimal way to mix the flocs and sand in practice.

### 3.3.1. Different ways of adding flocs

The aim of investigating different ways of adding Al, OM and sand together was to find the optimal method for using the mixture in practice. The hypothesis is that different ways of mixing can influence the resulted permeability reduction. Therefore different ways of adding the Al-(D)OM-sand were explored.

The first method of adding and mixing the Al, (D)OM and porous media has been extensively explained in the previous sections. The Al solution was added to the OM solution, leaving the mixture to rest whereafter the solution was centrifuged. Another way to add the flocs in the mixture is to mix undissolved Al, OM and sand. The undissolved Al, OM and sand were first mixed dry, after which 500 ml of demi-water was added step-by-step while stirring. The third method was to mix dried flocs to the sand and re-wet the mixture with 500 ml of demi-water.

### 3.3.2. Mix design and batching of mixture

In Table 3.2.1 the necessary amount and proportions are given to make up to 50 grams of dry flocs. The floc mixtures for 1 to 50 grams of flocs were made by adding the Al solution to the OM solution and set to rest overnight. The flocs were then diluted and centrifuged at 2500 rpm for 15 minutes until the byproducts were sufficiently removed. After centrifuging, the flocs were set to rest for 12 hours. The total volume of flocs in solution does not exceed the volume of 500 ml. This volume was based on the porosity of the sand, corresponding to the maximum volume to fully saturate the sample. Since the flocs were centrifuged and the higher density of flocs were made by a larger volume, the solution was divided over multiple centrifuge bottles. Due to difficulties with the cleaning of the bottles, some higher floc suspensions exceeded this 500 ml. The volume was reduced to 500 ml by placing it in the oven at 40 degrees Celsius to evaporate the excess water. The cleaning of the centrifuge bottles was done with demi water. Evaporation has an effect on the measured EC value, and in this case that would result in a lower EC value than measured. The floc mixture was added to 1030 gram of dry sand.

The batching of the mixture was established by consistent amounts of raw material, the accuracy of batching and mixing, mixing time and equipment. Batching is the process of measuring and combining required proportions of Al, OM and porous media, either by weight or by volume as per mix design to produce a uniform quality of the mix. Based on batching methods for concrete, traditionally batching is done by volume. However, for granular materials batching on weight is done rather than volume, due to the fact that

the volume of granular materials is less accurate. To start the batching, centrifuged floc suspensions with the correct mass of flocs in 500 ml were made, and mixed with 1030 gram of silver sand with a $D_{50}$ of 230 µm. Hence, uniform water-floc-porous-media mix could be maintained. The mixing procedure consisted of homogenising the sand, by making sure the sand was completely dry and without lumps. The flocs were introduced by pouring the floc suspension over the porous medium. The flocs were kept at 500 ml, since excessive water addition can cause loss of cohesiveness in the mix, which can, in turn, create segregation. The mixture was mixed then by hand for 7 minutes until a homogeneous mixture was achieved. The different steps are visualised in Figure 3.3.1. The testing and sampling of the mixtures were performed at room temperature of 23 ±2 degree Celsius. After the mix has been added to the permeameter, the permeameter was connected to the standpipes. The sample was then submerged with a closed tap for 12 hours.

Figure 3.3.1: Visualisation of different steps of mixing of flocs in the sand. From left to right: Making the flocs, the floc mixture and the clean, dry sand, pouring the solution over the sand, halfway through the mixing, the mixed Al-OM-sand.

### 3.3.3. The falling head test set up

This section explains the method of sample preparation and the set-up for the hydraulic conductivity experiments. The hydraulic conductivity experiment was performed to quantify the change of permeability. Since the hypothesis is that adding flocs will reduce the hydraulic conductivity to a value of a low permeable soil, the chosen method is the falling head test. In Figure 3.3.2 the set-up is shown.

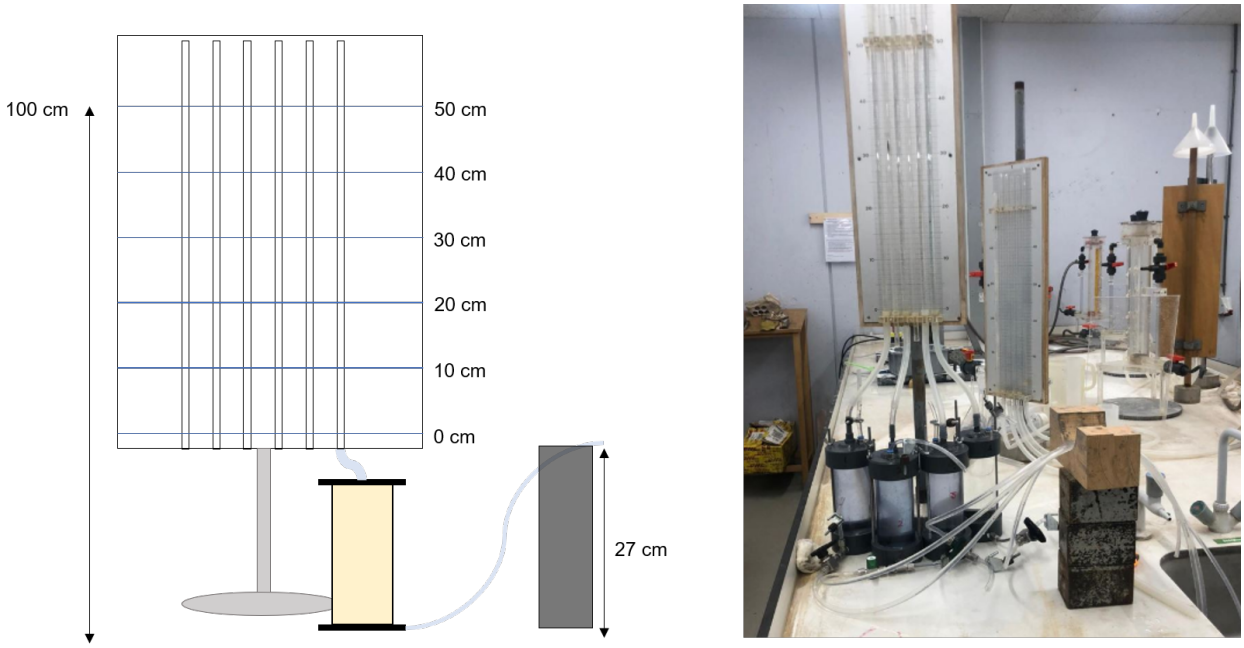


Figure 3.3.2: Schematic representation of the overall falling head test set up with the used dimensions (left), photograph real life set up (right).

The standpipes were exposed to atmospheric pressure, and water started flowing through the sample. The surface area is perpendicular to the flow. The arrangement of the permeameter is given in Figure 3.3.3. The

permeameters used had variating diameter/height dimensions of 6.7/16.6, 6.7/16.5 and 7.2/17.2 cm/cm. The cells consisted of two threaded metal rods in PVC cylinders (ø10 cm) with an inner diameter cut from 7.5 cm. In this inner diameter, there were two rubber O-rings to prevent leakage. In this PVC cylinder, hard plastic transparent cylinders were placed (ø6.7/7.2 cm). Inside the cylinders, on the bottom, a plastic porous cylinder plate (ø 6.7/7.2 cm) with on top a geotextile and a metal filter was placed to prevent clogging of the valve. The sample was constructed by methods elaborated in section 3.3.4. When the transparent column was completely filled with the mixture, a geotextile was placed. The permeameter was cleaned and closed with a lid that can be connected to the standpipes.

Figure 3.3.3: Components of the columns. From left to right: Cells with two metal rods (1), the plastic porous cylinder plate (2), the transparent plastic cylinder (3) and the lid that can be connected to the standpipes (4).

Tap water is used due to the fact that it eased the process since the necessary amount of de-aired water was not available. The standpipes were placed against a measurement board, which gave values from 0-50 cm in steps of 1 mm. This allowed monitoring the head loss over time. The location of the outflow was set at 27 cm, to keep the sample saturated over time. The time that the water in the standpipes had dropped a certain amount of height was logged with a stopwatch, and the value for hydraulic conductivity was determined by equation 2.11

### 3.3.4. Sample construction

The sample construction is a matter of consistency. First, all parts were cleaned, and the permeameter was installed as in Figure 3.3.3. The permeameter was connected to the standpipes and filled with water to prevent unforeseen leakages during testing. No leakages were detected, the columns were emptied and dried. The sample was constructed in a dry permeameter due to separation problems of the mixture. First, a geotextile was added to the permeameter to prevent clogging the tap. As a base layer, a layer of 2 cm of saturated silver sand was added to the column. After that, the mixture was added to the permeameter by layers of 2 cm. After each layer, the mixture was compacted by forty hammer blows, ten hammer blows on top of the column, ten on the right side, ten on the left side and again ten on top. The mixture was added up until the permeameter was overfilled, to make sure the sample was compacted. To prevent leakages from spilt material, the outside of the column was cleaned thoroughly before the lid was placed. The total time for producing the flocs and testing the permeability was approximately two days.

### 3.3.5. Hydraulic Conductivity Reduction

Adding the flocs to the soil structure was expected to reduce the hydraulic conductivity. The hydraulic conductivity reduction (HCR) is defined as the ratio between the hydraulic conductivity, $K_0$ [L/T] of just the silver sand and the hydraulic conductivity with the retained amounts of flocs, K [L/T]:

$$HCR = \frac{K_0}{K} \tag{3.1}$$

the HCR was used as a measure of influence of different concentrations of flocs retained by the sand and their corresponding hydraulic conductivity.

# 4

# Results

This research aims to prove that producing and mixing different concentrations of flocs to sand ex-situ reduces the permeability. First, the key outcomes of the experiments on mass-producing the flocs and quantifying its by-products are shown. In the second part of this chapter, the results and analysis of the falling head test conducted on the different amounts and methods of producing, mixing and distributing the flocs are elaborated.

## 4.1. Results on the mass production of flocs

In this section the results on the experiments on the flocculation reaction and by-products are shown.

### 4.1.1. Yield of the flocculation

To be able to answer the research question, a certain amount of flocs had to be made. The mass of Al-OM precipitates obtained from the reaction was expected to be around 85 % of the mass of OM. In Table 4.1.1 this assumed mass of dry flocs, the obtained dry mass and the absolute and relative error are given.

Table 4.1.1: The results of quantification of flocculation by drying the flocs.

| Expected mass (g) | Mass (g) | Absolute error (-) | Relative error (%) |
|---|---|---|---|
| 1 | 1.13 | 0.13 | 13% |
| 5 | 4.93 | 0.07 | 1% |
| 10 | 10.1 | 0.1 | 1% |
| 15 | 14.57 | 0.43 | 3% |
| 20 | 19.68 | 0.32 | 2% |
| 25 | 24.12 | 0.88 | 4% |
| 30 | 30.63 | 0.63 | 2% |
| 40 | 40.53 | 0.53 | 1% |

The results show that values encountered in practice and the expected mass of flocculation gives an average absolute error of 0.47 g and an average relative error of 4%. The results show that the median of the results is 86 % of the OM with a standard deviation of 4%. There was no relationship found on the deviation between results in higher or lower expected yield.

### 4.1.2. The influence of the M/C ratio on the pH

Based on the knowledge on the pH and M/C ratio dependency and the concept of a critical molar M/C ratio, the titration curve is used as a measure to monitor the flocculation process. The starting values of the pH of the OM solution is always between 9-9.7 and for the Al solution between 3.31-3.01. The pH over an increasing M/C ratio for 5 gram of flocs is shown in Figure 4.1.1.

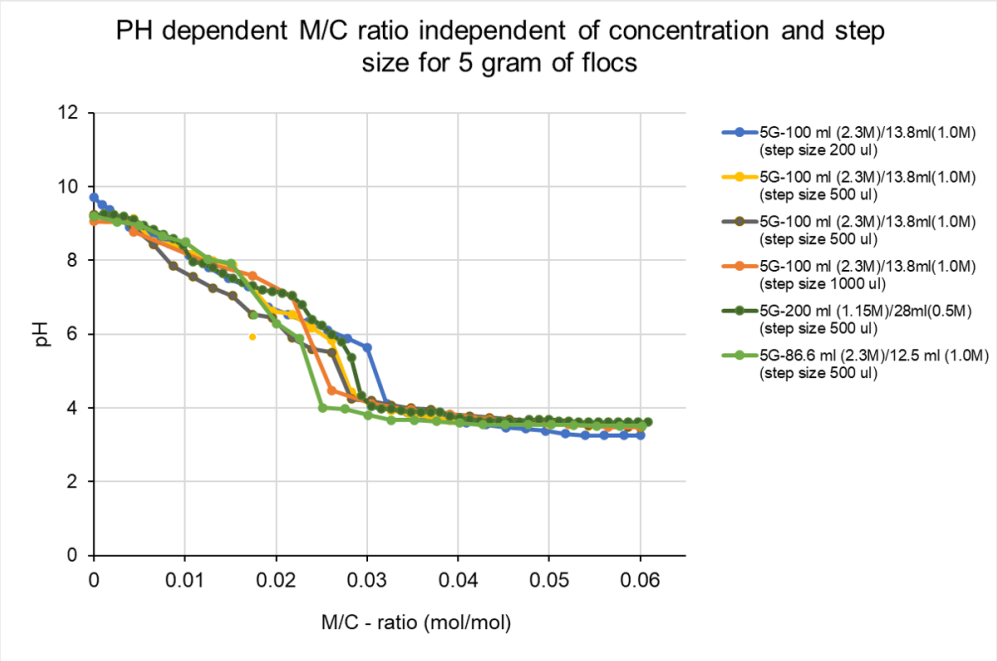


Figure 4.1.1: The relationship between an increasing M/C ratio and a dropping pH, where the Al and OM concentrations and the step size varied but always yielded 5 grams of flocs.

The curve shows a decreasing pH over an increasing M/C ratio. A decrease in pH represents an increase of $H^+$ concentrations. The increase of $H^+$ concentration is a result of the stoichiometry of replacement of $H^+$ by $Al^{3+}$ on OM. For every mol $Al^{3+}$, 3 mol of $H^+$ is released. When charge neutralisation occurs and $H^+$is released, the pH will drop because of the hydrolysis of Al until the acidity is so low that Al can remain in solution. This acidity level, according to Figure 4.1.1, is around pH 4. From Figure 4.1.1 it can be concluded that there is a turning point between pH 7 and pH 4. This turning point is always in a range of an M/C ratio between 0.02 and 0.04. The starting point of the turning point is mostly dependent on the step size. After the turning point, the pH stabilised at a level lower than pH 4. At a pH below 4, the highest free $Al^{3+}$ ion concentration was found, and therefore more chance of flocculation. There is always a fast transition zone between turning points within one addition of Al, which indicates instantaneous flocculation. In practice, these turning points can be detected by eyeballing, where the flocs are visible in the solution.

To make sure that these measurements are not only for the amount of 5 gram of flocs, different amounts of Al were added to OM for different amounts of flocs in different step sizes shown in Figure 4.1.2. For different amount of Al and OM the same trend is shown, even in the high amounts the turning point was within a single step of Al.

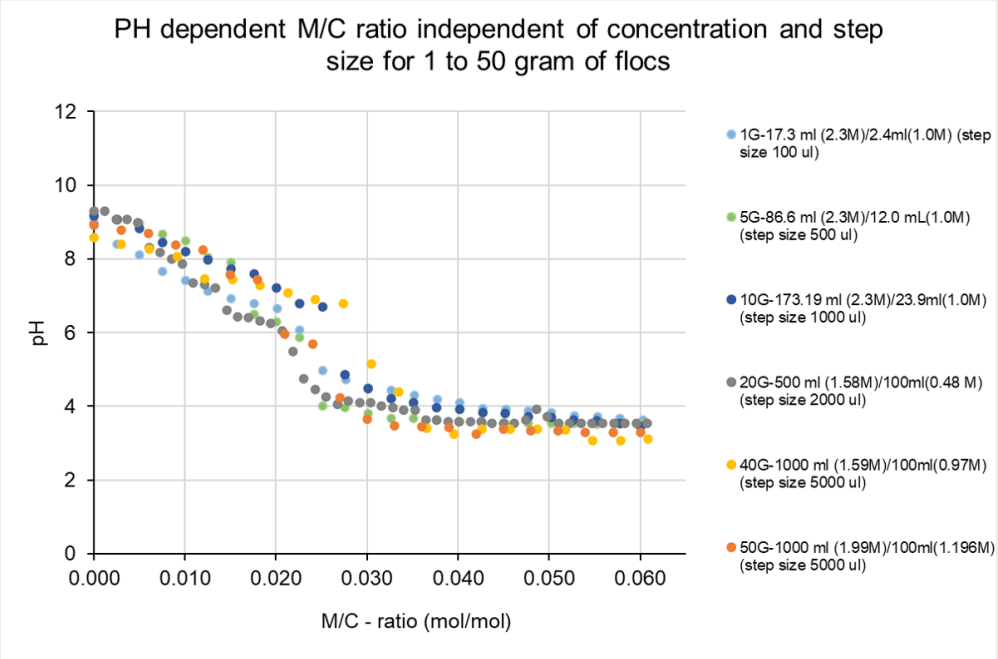


Figure 4.1.2: The relationship between an increasing M/C ratio and a dropping pH, where the Al and OM concentrations, the step size, and the yielded grams of flocs varried from 1-50 grams of flocs.

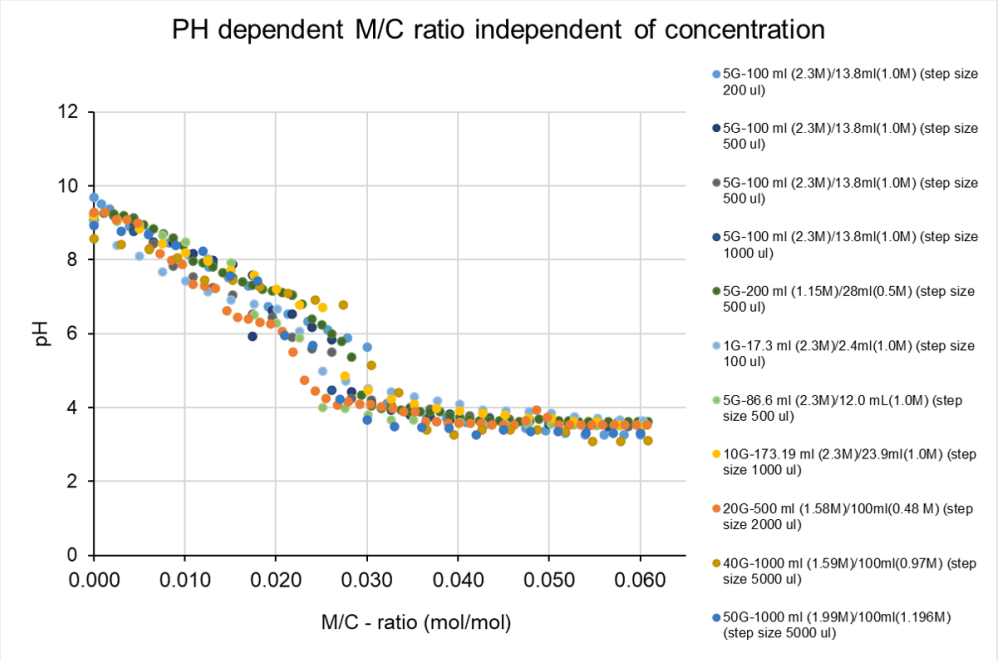


Figure 4.1.3: The relationship between an increasing M/C ratio and a dropping pH, for all pH measurements given in Appendix A.

All pH measurements given in Appendix A are shown in Figure 4.1.3. From here a clear trend of pH over the M/C ratio is shown. The trend is consistent with what is found in literature where 0.027 is the critical M/C ratio and flocculation takes place and where pH < 4.5. The reaction is more M/C ratio dependent than pH with a critical M/C ratio range of 0.025-0.031.

### 4.1.3. Quantification of the ionic strength

All measured EC values of the supernatant after Al-OM precipitation and centrifuging are given in Appendix B.0.1. From these results, a relationship between the initial density of flocs and the ionic strength was found.

The density of flocs is defined by the dry mass of flocs in the solution g/ml. This relationship is given in Figure 4.1.4.

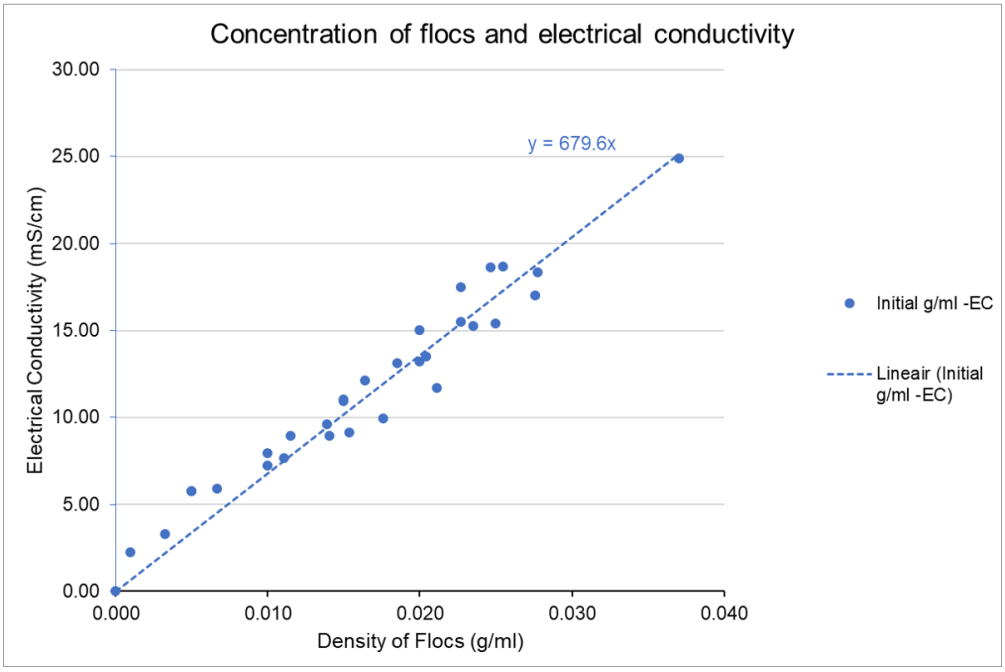


Figure 4.1.4: The relationship of the measured EC of the supernatant of the dry mass of flocs in its initial solution, defined as the density of flocs in g/ml.

The EC of the solution can go up to 24.9 mS/cm at a floc density of 0.037 g/ml. From here, a linear relationship is drawn between the ionic strength and the density of flocs in solution. It was expected that the value of EC is mainly influenced by the concentrations of ions of $Cl^-$ and $K^+$. Therefore an increase of density of flocs in solution shows a linear increase of concentrations of $Cl^-$ and $K^+$, which confirms the theory of stoichiometry.

In practice, this relationship can be used to calculate the dilution factor, to, for example, lower the ionic strength to compile with environmental regulations for bioavailability and toxicity (commissie bodembescherming, 2007; TAW, 1996). The results of the electrical conductivity and the results of the diluted volumes and electrical conductivity are given in Figure 4.1.5. The dilution experiments were carried out until the EC measurement was lower than the EC of tap water (700 µS/cm). This explains the higher density of measurements in the lower EC and density of flocs. From Figure 4.1.5, the diluted ionic strengths show a lower rise in the lower densities. The diluted density of flocs in solution show a lower rise at low densities, and seem to have a steeper rise after a density of flocs of 0.010 g/ml. This can be explained by the fact that the dilution is determined on added mass of water due to the fact that the added volume and the volume of the settled mass were difficult to obtain from the centrifuge bottles. Therefore, this relationship should be seen as an indication of the ability of using the graph to get an estimation of the dilution factor.

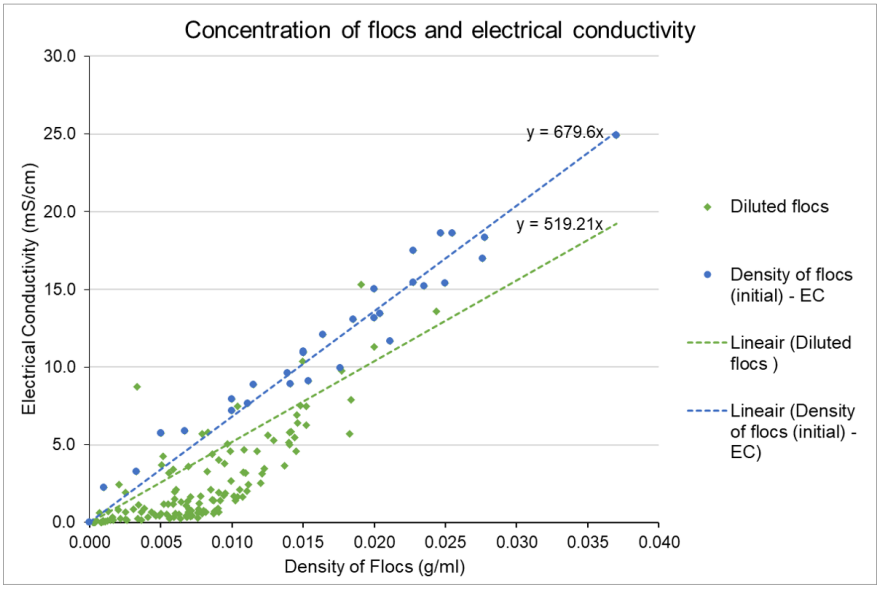


Figure 4.1.5: The relationship of the measured EC of the supernatant of the dry mass of flocs in its initial solution defined as the density of flocs in g/ml (blue dots) compared with the EC of the supernatant of diluted floc densities (green dots).

There is a known linear relationship between the concentration of KCl and its electrical conductivity values. The relationship between the initial concentration of flocs and the relationship between the concentration KCl and the EC are combined in Figure 4.1.6. The x-axis gives the concentration of flocs shown in g/ml. The y-axis on the left shows the electrical conductivity in mS/cm, while the y-axis on the right indicates the concentration of KCl.

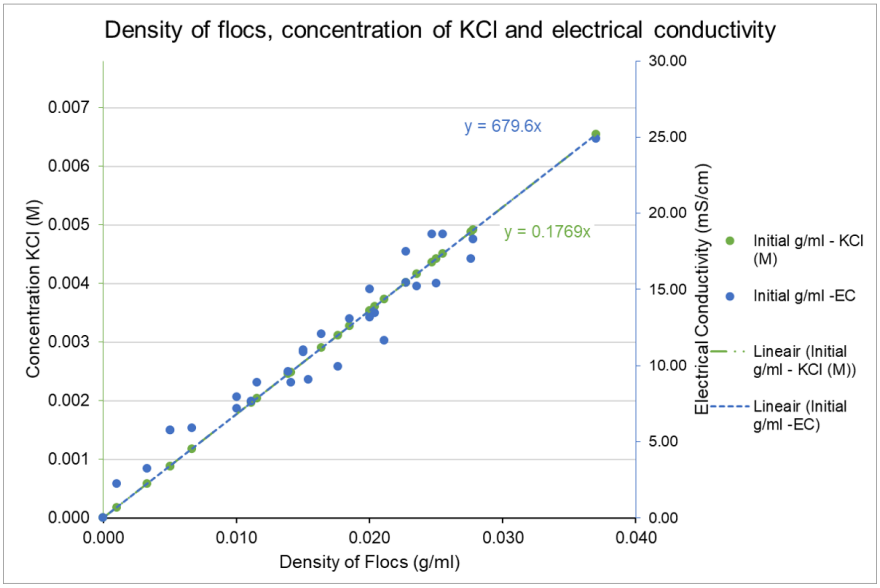


Figure 4.1.6: The relationship of the measured EC and the concentration of KCl in the supernatant and EC of the supernatant of the dry mass of flocs in its initial solution, defined as the density of flocs in g/ml.

The relationship given in Figure 4.1.6 is tested by measuring the EC and the revenue of solid salt in 100 ml supernatant, and using the relationships given in Figure 4.1.6. The results of these tests are given in table 4.1.2. As supportive evidence for the relationship, the calculated and measured concentrations resemble similar values.

Table 4.1.2: Verification of the relationship given in Figure 4.1.6.

| Dry mass in 100 ml in supernatant (g) | KCl (M) | Calculated EC (mS/cm) | Measured EC (mS/cm) |
|---|---|---|---|
| 1.43 | 0.128816 | 15.49 | 17.49 |
| 0.57 | 0.051346 | 6.18 | 6.25 |
| 0.14 | 0.012611 | 1.52 | 2.03 |
| 0.02 | 0.001802 | 0.22 | 0.74 |

### 4.1.4. Quantification of residual OM from the supernantant

To find the relationship between the UV adsorption and the OM. First the relationship between the UV adsorption and known concentrations of OM is established in Figure 4.1.7. A linear relationship was shown, which resembled the relationship found in literature by Popma (2017).

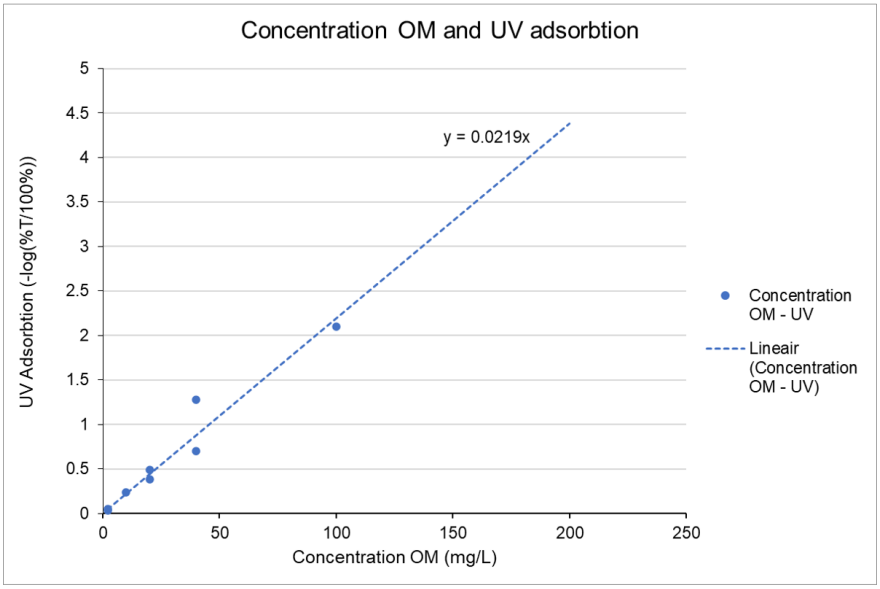


Figure 4.1.7: The relationship between known concentrations of OM and their corresponding UV adsorption.

The measured UV adsorption of the supernatant after Al-OM precipitation and centrifuging are given in Appendix B.0.2. From these results, a relationship between the initial density of flocs and the UV adsorption was sought shown in Figure 4.1.8.

The relationship expected was a linear relationship, but the results are more scattered rather than linear. The differences in UV254 adsorption were caused by dilution errors or variability in OM concentration due to centrifuging. Therefore, the linear relationship is used to back-calculate the concentration of OM. From this back-calculation the results were between 4 and 20 percent of the expected mass OM. Therefore from the supernatant it is hard to quantify the exact mass or concentration of OM in the mixture.

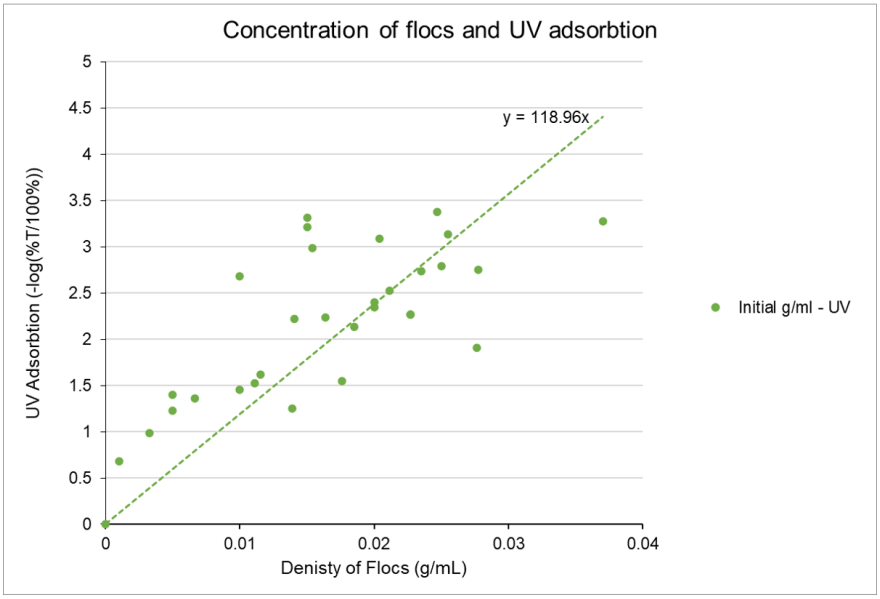


Figure 4.1.8: The relationship of the measured UV adsorption of the supernatant of the dry flocs in its initial solution, defined as the density of flocs in g/ml.

## 4.2. Hydraulic conductivity reduction

The measured hydraulic conductivities per concentration of flocs retained by one kilogram of porous media are given in Figure 4.2.1. Also, the influence of the three different methods is shown. The blue dots are the flocs made under laboratory conditions, where the dissolved Al and OM are combined, and the flocs are cleaned of byproducts by centrifuging the flocs until the ionic strength was below a measured EC value of 700 µm/cm. The green dots show the hydraulic conductivity of the sand as a function of concentration of flocs on sand, in which the Al and OM mass were introduced to the sand in dry powder format. The yellow dots show that the use of only amounts of OM has a negligible influence on the hydraulic conductivity.

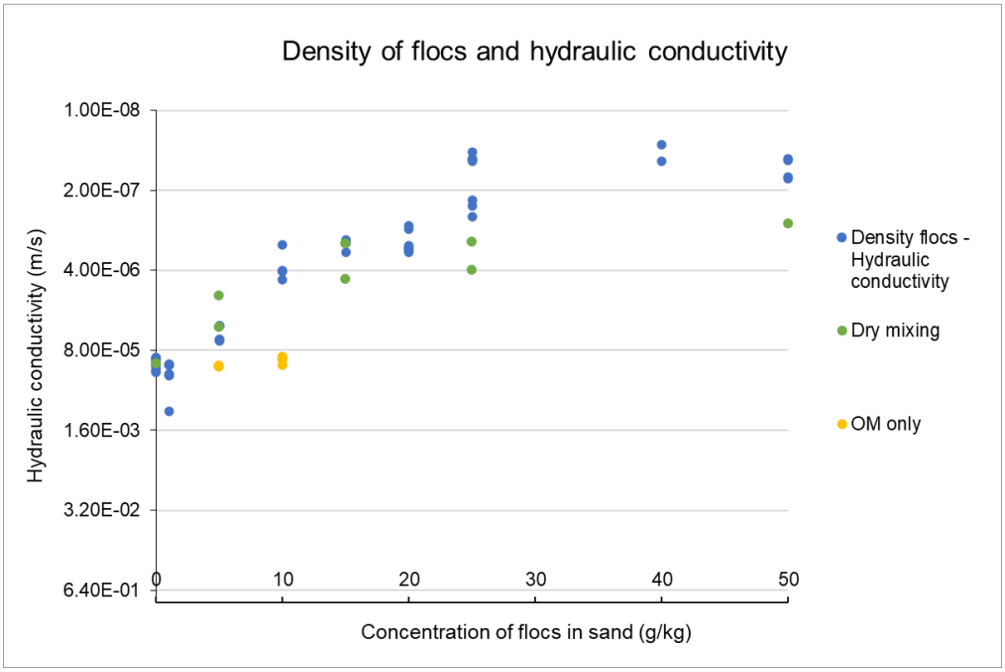


Figure 4.2.1: The measured hydraulic conductivity by conducting a falling head test over increasing concentrations of flocs to the porous medium. The blue dots show the hydraulic conductivity of the sand with Al-OM flocs made in solution. The green dots show the hydraulic conductivity of the sand with Al-OM mixed in the sand in powder format. The yellow dots show the hydraulic conductivity of the sand with only OM added to the sand.

To obtain a relationship between the hydraulic conductivity reduction and the concentration of flocs retained by one kilogram of porous media, the hydraulic conductivity values in Figure 4.2.1 are normalised with the hydraulic conductivity of the sand by equation 3.1. The hydraulic conductivity reduction was calculated for a hydraulic conductivity value of silver sand of $1.31\times10^{-4}$ m/s. The relationship of the hydraulic conductivity reduction and the concentration of flocs retained by one kilogram of porous media is shown in Figure 4.2.2.

From the measurements all shown in Table C.0.1, the highest reduction was $3\times10^{3}$ times achieved by adding 40 gram of flocs to the soil structure. The reduction achieved by making the flocs under laboratory conditions and adding them to the soil structure is showing an exponential increase up to adding 25 gram of flocs. After 25 grams of flocs, any additional increase in flocs concentration does not reduce the permeability of the sand further. At added floc concentrations higher than 25 grams of flocs, the reproducibility of the reduction becomes more difficult, shown in a larger spreading between reduction results.

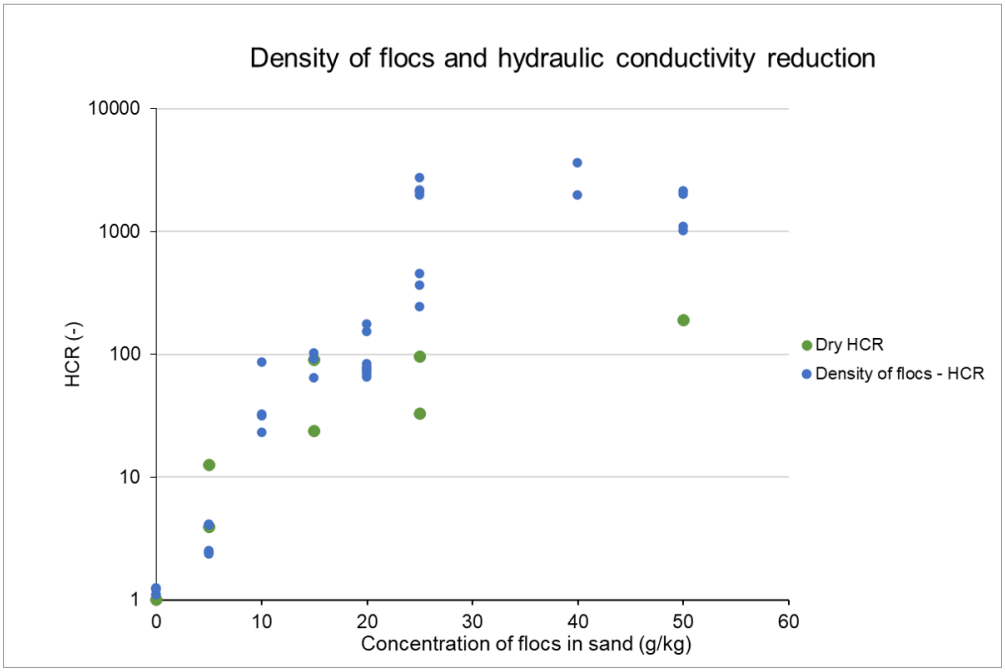


Figure 4.2.2: The HCR, which is the measured hydraulic conductivity by conducting a falling head test normalised over the blanco hydraulic conductivity of the silver sand over the addition of increasing concentrations of flocs to the porous medium. The blue dots show the HCR of the sand with Al-OM flocs made in solution. The green dots show the HCR of the sand with Al-OM mixed in the sand in powder format.

In Figure 4.2.2 the green dots show the reduction of the dry materials mixed in with the porous media after which the mixture was whetted. The increase of the reduction is linear over an increase of concentration of flocs retained by the soil. The highest reduction was 190 times, and was found at 50 grams of flocs retained by the soil.

# 5

# Discussion

In this chapter the limitations of this research are discussed by addressing the experimental implementation and variations within results.

## 5.1. Production of flocs

In the following subsections, the results of the flocculation experiments are discussed. These experiments include the experiments on the yield of the reaction, the M/C ratio-dependent pH, the ionic strength and the unreacted OM.

### 5.1.1. Yield of the reaction

The results on the yield of the reaction experiments were in line with the expected amounts of 85% of the mass of the OM would result in dry mass of flocs. The highest relative error was found for producing 1 gram of flocs. In small quantities, the accuracy and deviation of the materials are of more significant influence. The scale used can be read in two decimal places with a deviation of 0.01 gram. This results in a deviation in a one-litre stock solution of OM of ±0.015% and for a one-litre stock solution of Al ±0.004%. When small amounts of OM solution have to be taken from stock, there is difficulty to obtain a homogeneous amount of OM solution (shown in Table 4.1.1). The small amounts are taken by a pipette which had an accuracy of ±5 µl. Using the smaller amounts resulted in relatively large deviations as indicated in the results (Table 4.1.1). There is no relationship found between the relative errors in the smaller and higher amounts of obtained mass. The larger amounts of obtained mass were produced in larger volumes, which had to be divided into multiple centrifuge bottles. The influence of centrifuging and the number of centrifuge bottles appears to be little as it can not be identified from the results. This means that this error will have little to negligible impact on the large amounts that have to be produced in practise.

### 5.1.2. The influence of the M/C ratio on the pH

The results given in Figure 4.1.1 revealed a range in which the flocculation took place. This range, however, is not caused by the difference in concentrations, rather than it is the result of a non-ideal reaction, meaning that the flocculation is not a homogeneous and instantaneous process. The increasing availability of $H^+$ leads to protonation of the carboxylic groups, which leads to a decrease in the negative surface charge of the molecules. The fraction of the OM that flocculates is determined by the saturation of the surface charge. The distribution of the cations over the different binding sites varies as a function of pH, and subsequently the electrostatic binding in the system is affected by pH.

The ionic strength of the solutions used to obtain 1 - 50 grams of flocs are evaluated to determine the influence of the ionic strength on the flocculation reaction. The highest ionic strength was found for the solution of 50 grams, while the lowest ionic strength was found for the solutions for 20 grams. The relationship between the ionic strength and the path of flocculation could not be found from the measured results (Table B.0.2). From Veerkamp (2018); Zhou (2020), the reaction was therefore expected to be pH dependent. However, results from tests performed in this study suggest that the M/C ratio has a more profound influence comparing with pH. Particularly, the hydrolysis of the used cation, $Al^{3+}$, is known to have an impact on

pH. The M/C ratio was calculated from the used concentrations Al and OM solutions. These stock solutions are prepared with an error margin of 0.015% and 0.004%, and this error margin is derived from the error of pipette (i.e., 5 µl). The pH measurements were done by a pH meter, with a deviation of 0.1. Given that the pH scale is logarithmic, a difference of 1 in pH corresponds to a 10 times difference in proton concentration. As a result, the deviation of 0.1 in pH gives a higher deviation in $H^+$ concentration in the higher pH values. The error bars within the results are given in Figure 5.1.1

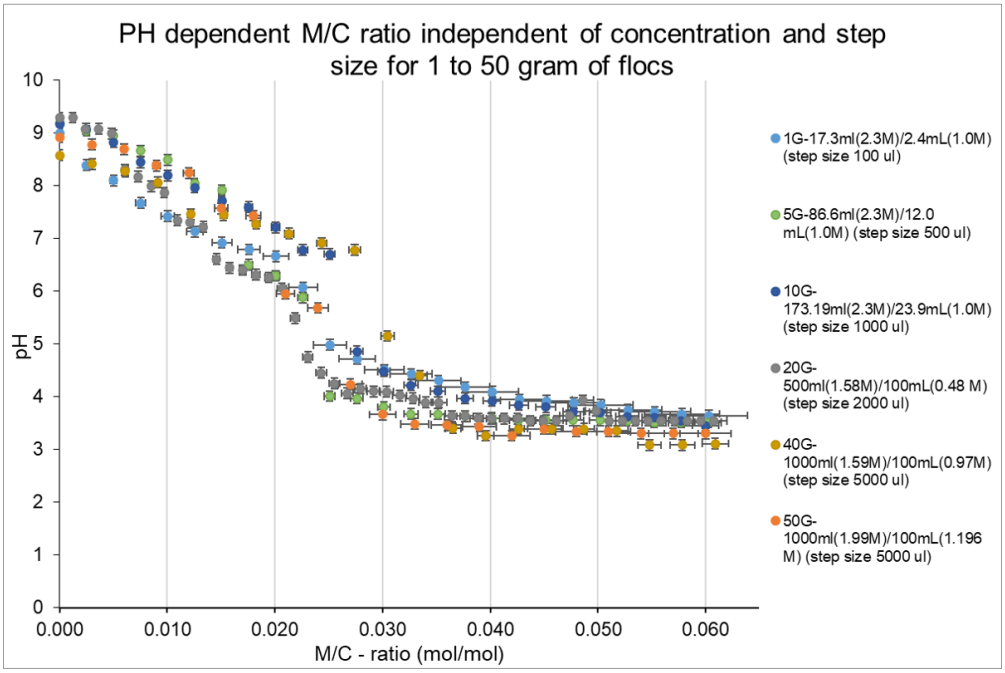


Figure 5.1.1: The titration curve with error bars of 1-50 gram of flocs made by different Al and OM concentrations and different step sizes. The error margin in the horizontal direction is derived from the error of the pipette and error of prepared stock solutions. The error margin in pH is the error of the pH meter, 0.1 pH.

### 5.1.3. The ionic strength

High background concentrations of $K^+$ and $Cl^-$ ions were found. The ionic strength is used as a tracer due to the fact that the $K^+$and $Cl^-$ are non-reactive. The relationship between the ionic strength and the concentration of flocs is linear. The working hypothesis is that the size of the flocs can be increased by reducing the ionic strength in the solution. More experimental data on the floc size are, however, needed to confirm this hypothesis. The diluted densities of the flocs (presented in Figure 4.1.5) were obtained by serial dilution of the settled flocs, from which the supernatant has been removed. The serial dilution method relies on precise measurements of the mass of the centrifuge bottles and added mass of demi-water. As such, this experimental method is not accurate. For instance, large errors in the value of density of flocs can be resulted of the accumulation of errors in each dilution. Therefore, the relationship shown in Figure 4.1.5 should be considered as a relationship for practical application instead of the actual quantification.

### 5.1.4. The OM quantification

The unreacted OM was not able to be quantified from the supernatant. From the linear relationship of the scattered results given in Figure 4.1.7, no valid results could be obtained. One of the possible explanations is that the OM settled during the centrifuging process. The fact that this settled OM is not shown in the yield of the reaction by drying the sample might mean that no unreacted OM was left in the solution by a M/C ratio of 0.06.

## 5.2. Hydraulic conductivity reduction

In this section the results presented in section 4.2 are evaluated. Figure 4.2.2 imply a large variability in the achieved reduction in which the amount of retained flocs dominates this variability.

### 5.2.1. The influence of the porous media

As mentioned in section 3.1.3 the used sand was silversand. From the grain size distribution (Figure 3.1.1) a somewhat steep slope is shown, which indicates a uniform soil (Askarinejad, 2019). Therefore the uniformity coefficient is calculated by equation:

$$Cu = \frac{D_{60}}{D_{10}} \tag{5.1}$$

In which, $C_u$ [-] is the uniformity coefficient; $D_{60}$ is the sieve opening size (mm) through which 60% of aggregate passes and $D_{10}$ the sieve opening size (mm) through which 10% of aggregate passes.

The uniformity coefficient is unity for a material whose particles are all of the same size, and it increases with variety in size. The $C_u$ of the silversand is 1.37. $C_u$ <4 indicates a uniformly graded material having a narrow range of particle size. In case of a highly uniform sand, the effective grainsize ($D_{10}$) is not much different from the mean grain size (Urumović and Urumović, 2014). Granular particles often have various sizes and shapes, which provide variable interstices (space between grains) and are directly responsible for the permeability of the sand. When using the relationships found in section 4.2, the porous media used has a very regular spherical shape and could differ for sands with a larger diameter, irregular shape and non-spherical particles. Diversity of immanent grain size distorts such relations. Since natural materials are mostly non-uniform, divergence between the mean grain and the grain defined by percentage of particles that pass through the sieve is very small, therefore instead of using $D_{50}$, the effective grain size of $D_{10}$ < 300 µm should be used.

### 5.2.2. The influence of different methods of adding the flocs

The results of drying the flocs, re-wet the flocs and add them to the soil structure were not shown since the dried flocs do not adsorb any water. The OM added to the soil structure had a negligible influence on the hydraulic conductivity, because OM has a high dissolving rate and was rinsed out of the sample. This negligible effect of the OM, on the other hand, gives supporting evidence that it is Al-OM flocs that can reduce permeability of soil. The dry mixing technique showed that permeability reduction increases linearly with an increase in concentration of flocs, and the maximum reduction is found to be a magnitude of 2. The relationship between the reduction and the concentration of flocs made by solutions shows an exponential increase up to 25 grams of flocs per kilogram of sand. The hydraulic conductivity was reduced up to 3 orders of magnitude. When mixing the materials dry, a different reaction takes place. This is because the dissolution rate of the $AlCl_3 \cdot 6\ H_2O$ and HUMIN P775 differs dramatically: the Al has a higher dissolution rate than the HUMIN P775. During the dry mixing process, the Al will also interact directly with the solid OM and different floc structures are formed from this interaction. These different structures are shown in Figure 5.2.1, where the dry mixing (shown in Figure 5.2.1 right) results in particles that are visible with the naked eye, while the mixing in solution gives a more slurry-like flocs suspension (Figure 5.2.1 left). The structure obtained by dry mixing and mixing in solution differs. This difference primarily lies in the shear-dependency of the floc size. These difference in floc distribution within the solution indicates a difference within the floc distribution in the soil structure (Figure 5.2.2). This difference is shown in the reduction capacity.

Figure 5.2.1: Floc solution obtained by mixing Al and OM in solution (left) and the floc solution obtained by mixing Al and OM in powder form (right). As shown, the flocs produced by mixing in solution has the shear-dependency feature, while dry mixing created particles that have a constant size.


Figure 5.2.2: The difference in floc distribution after shaking settled flocs produced in powder form and solution. The cups with the red lid are flocs mixed by Al and OM in solution, the cups with the green lid are flocs produced by mixing Al en OM in powder form.

### 5.2.3. The variation in measured HCR

First, the discrepancies within the measurements between the same amount of concentration of flocs added to the soil were attempted to be explained by the differences in ionic strength of the solutions. The influence of the measured end ionic strength of the floc solution on the hydraulic conductivity reduction has not been found. Due to the fact that the ionic strength was lowered below a specific value, only small differences in ionic strength were measured. These small differences showed no visible influence on the measured HCR.

The saturation of the mixture, however, showed a profound influence on the homogeneity of the mixture. Liquefaction caused a separation of flocs from the sand floc mixture. Flocs are lighter than the sand and have the tendency to float on top of the sand with the expelled water (as shown in Figure 5.2.3). This localised presence of flocs in the sand column resulted in a low overall hydraulic conductivity measurement.

The hydraulic conductivity determined by falling head test is controlled by the lowest measured hydraulic conductivity in the system.

Figure 5.2.3: Columns that show heterogeneity in the sample due to separation of flocs from the sand during compaction.

The reduction capacity of mixtures stagnates after a concentration of 25 gram of flocs retained by one kilogram of sand. The results showed that when higher concentrations of flocs were added to reduce the permeability, it became more challenging to get the expected results and to reproduce the same amount of reduction in permeability. In Figure 5.2.4 the logarithmic scale used in 4.2.2 has been made linear to make this spreading between reduction more visible.

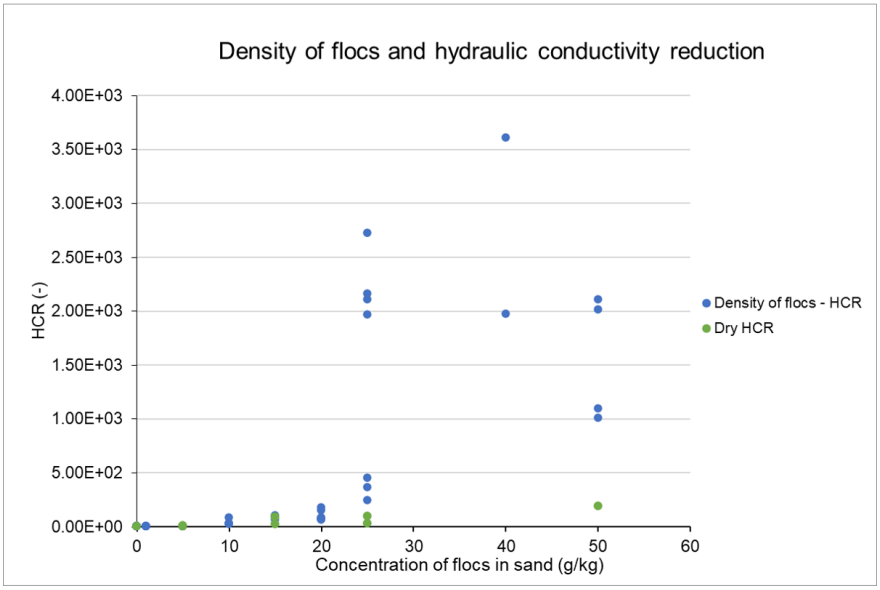


Figure 5.2.4: The results of the HCR and density of flocs given in Figure 4.2.2 with a linear y-axis to show the spreading of results in higher amounts.

The hypothesis that the volume of added flocs exceeds the pore volume in the porous medium was proposed to explain the observed stagnation in permeability reduction. In order to test this hypothesis, the pore volume [$L^3$] was calculated from the porosity of the sand p[-], the volume of the permeameter [$L^3$], the volume of the sand [$L^3$] by:

$$V_{pores} = V_{permeameter} - (V_{sand} * p) \tag{5.2}$$

The pore volume is around $4.5\times10^{-4}$ $m^3$, which resembles the expected volume of 500 ml added independently of the concentration of flocs. A sensitivity analysis on the decrease in the pore space did not give conclusive relations.

However, a large difference was found by packing higher concentrations of flocs, compared to lower concentrations of flocs. The mixtures with higher floc concentrations showed a lower packing density. It was estimated that the packing density of 40 grams of flocs retained in one kilogram of sand was 70% of the packing density of packing the silver sand alone. The mixture was made under saturated conditions to reduce air bubbles that were trapped in the sample. Higher concentrations of flocs show a higher hydraulic conductivity reduction, and this has a large effect on the water within the sample. The low permeability makes it harder for water to flow through the pore space. The flocs will therefore form a barrier within the sample, which resulted in the retention of water within the pore space. Given the fact that water is incompressible, a larger amount of trapped water corresponds to a higher porosity and thus a lower packing density. In addition, this makes the mixture slurry-like. Therefore a decrease of packing density was found without changing the volume added to the soil structure. This hypothesis, i.e., the low permeability did not allow water to flow through the pore space, was validated by the time needed to dry the column. To investigate the influence of higher temperatures and dehydration on the Al-OM-sand mixtures hydraulic conductivity reduction, 3 columns with over 40 grams of flocs per kg of sand were put in the oven. The lid of the columns was removed and put in the oven at 60 degrees Celsius. A higher temperature is not feasible due to the melting point of the PVC used for the columns. After over 3 weeks in the oven, only the top 4 cm of the samples became dry. It was attempted to speed up the process by attaching the samples to a vacuum pump in the oven, however little improvement was seen. In order to evaporate, the water has to move through the sample to the surface. The flow rate depends on the permeability which has become very low. As a result, the evaporation takes a long time.

Figure 5.2.5: Visualisation of drying of the sample.

Another reason for the variation in measured HCR at high floc concentrations could be caused by a larger heterogeneity in the sample, causing very low vertical permeability in the sample leading to preferential flow. For example, reducing the permeability in the sand would force more water to flow along the edges of the sample where the sand particles and the sides of the permeameter are not forming an ideal leakage-free contact. In this case the measurements of permeability in the laboratory is negatively affected by the extent of the wall effect (Kango et al., 2017).

# 6

# Conclusion and implications

## 6.1. Conclusion

Through the work done in this research, it is possible to make a few conclusions. To answer the question 'How to characterise the Al-OM precipitates' complexing behaviour under measurable macro conditions?' experiments have been performed to evaluate the yield of the reaction, the influence of concentration on the M/C ratio-dependent pH, the ionic strength and the unreacted OM. The yield of the reaction was obtained by producing expected masses of flocs by adding certain amounts of Al and OM solutions in which the assumption that 85% of the added mass of OM will result in mass of flocs was confirmed. Based on the knowledge on the pH and M/C ratio dependency and the concept of a critical molar M/C ratio, the titration curve was used as a measure to monitor the flocculation process (Zhou, 2020). This has been done by testing if the flocculation takes place regardless of the input concentrations. Figure 4.1.1 shows that the flocculation occurs at the narrow M/C ratio range between 0.023-0.031 and the pH stabilises at a level lower than 4. This result corroborate the modelling development, in which the fluctuation of OM is shown to be primarily controlled by a critical molar M/C ratio independent of the input concentrations (Veerkamp, 2018; Zhou, 2020). The ionic strength was measured over the supernatant of an increasing density of flocs in solution. The ionic strength increased linearly with an increasing density of flocs which was correlated to the concentration of KCl in figure 4.1.6. Supporting evidence was given for this relationship by drying the supernatant and correlating it to the expected mass of KCl. Therefore the EC can be used as a tracer since the $K^+$ and $Cl^-$ are non-reactive.

To find the most effective method to mix the Al-OM and porous media, the Al, the OM and the silver sand were mixed in different amounts with different methods. In the first method, the Al and OM were added in solution, and the solution containing Al-OM precipitates was centrifuged until the ionic strength was reduced to an EC value less than 700 µS/cm (corresponding to tap water). The flocs in solution were added and mixed with the sand by hand. To find the relationship between the mass of Al-OM precipitates on the permeability reduction of the porous media, a falling head test was conducted over an increasing concentration of flocs retained by one kilogram of sand. The hydraulic conductivity was reduced exponentially over an increasing concentration up to a magnitude of 3. At 20 grams of flocs added to one kilogram of sand, the reproducibility became more difficult, and a large variation between reduction results were found. The other method that was used, where Al and OM were mixed in powder format and added to the sand, after which the mixed sample was wettened. The hydraulic conductivity measurements showed a linear reduction over an increasing concentration up to a magnitude of 2. Mixing the Al and OM in powder compound resulted in a different floc structure than the mixing in solution. Therefore the most effective method to mix the Al-OM and porous media was concluded to add the flocs produced by Al and OM solutions.

Finally, this research showed that it is possible to use Al-OM flocs to reduce the hydraulic conductivity of the layer ex-situ with porous media up to a magnitude of 3. For the layer to be feasible, some recommendations on implementation have to be made.

## 6.2. Recommendations in implementation

To use the layer as geo-engineering tool in practice, the cost-effectiveness and recommendations on design and installation are given in this chapter.

### 6.2.1. Cost analysis

To find out if the layer is a cost-effective alternative for contemporary methods, the cost for 1 $m^3$ of Al-OM-porous media mixture is calculated. The costs were calculated for the addition of 20 grams of flocs per kilogram of sand, which gave the most optimal and reproducible results. The Al source used in this research is the $AlCl_3 \cdot 6H_2O$ by the supplier Sigma Aldrich. This particular Al source is €58,80 (excl. VAT) per kg. The OM source used in this research is the Potassium Humate HUMIN P775 by the firm HUMINTECH. The cost for this OM source is €5,90 per kg. Using these particular Al and OM sources, the cost for 1 $m^3$ is calculated as shown in Table 6.2.1 .

Table 6.2.1: The cost estimation of 1 $m^3$ and the necessary Al, OM and sand.

| Source | Cost (€) | Amount necessary | Cost (€) |
|---|---|---|---|
| Sand | 10 €/$m^3$ | 1 m $^3$ =1600 kg | 10 |
| $AlCl_3 \cdot 6H_2O$ | 58,80 €/kg | 18.6 kg | 1093.68 |
| HUMIN P775 | 5,90 €/kg | 36.8 kg | 217.12 |
| Flocs | | 32 kg | 1310.8 |
| | | | 1320.8 |

This, of course, is not cost-effective. The layer would become far too expensive per $m^3$. Most of the costs are in the Al source that was used. Therefore alternative Al sources are sought. The first alternative is a highly concentrated Al solution, where in water treatment, polyaluminium chloride is often used. The poly aluminium choride of the company Breustadt Chemie B.V., which has 5% active substance of Al, costs 0.85 €/L. From experiences of Zhou (2020), less pure $AlCl_3 \cdot 6\ H_2O$ powder showed good reactivity in the large field experiment. The used $AlCl_3 \cdot 6\ H_2O$ were from the companies Alfa Aesar and Honeywell. The prices from Honeywell were 7 €/ kg. As for the OM source, no alternatives have been researched, which could be explored in future research.

Using the current sources of Al and OM would make the layer cost-ineffective. However, the adaptation of alternative Al source can lower price for the layer to around 370 €/$m^3$. The costs for the layer were calculated for the highest reduction and for a M/C ratio of 0.06. As shown in Figure 4.1.3 flocculation takes place after a M/C ratio of 0.031. The ratio of 0.06 has been taken to ensure the largest and strongest flocs, future research could be done to see the influence of lowering the M/C ratio on the permeability reduction and with that the reduction of costs. The advantage of the layer is that the reduction can be adjusted to the required reduction in practice by adding a lower density of flocs. The Al-OM layer is used to improve the soil conditions of the sand and allows the soil to perform better in the retention of water. The prices of the alternatives, such as bentonite clay and geosynthetics, are per $m^2$ 2 orders of magnitude lower. Additionally, Al-OM can improve the lifetime of a certain application and therefore save short-term maintenance costs. It is therefore recommended to have the cost-effectiveness of the layer evaluated for particular engineering practices.

### 6.2.2. Recommendations on design

The following recommendations are given to evaluate the performance of the layer in a given design. The largest opportunities for the Al-OM layer are as a horizontal liner (i.e., landfill liners, channel liners, tank farm liners and dike covers). For the Al-OM-sand layer to be a competitor, smaller amounts of the layer should be as effective as larger amounts of alternatives. Used over a specific area, this could be achieved if a thinner layer of Al-OM-sand will reduce the permeability the same as a thicker layer of the alternative. For the design of the layer, the expected flow through the liner under specific site conditions should be determined. The site conditions are probably not similar to the test conditions used in this research. It has to be taken into account that for using the Al-OM as a liner, the hydraulic conductivity measured in this research should be evaluated for the following aspects. The first parameter to check is the hydraulic gradient on-site. This

can be calculated by dividing the force that the water column exerts over one square meter by the density of water which is approximately equal to 9.81 kN/m$^3$ (Davies and Mander, 2007). The necessary thickness of the layer could be calculated as shown:

$$Q = kiA \tag{6.1}$$

Where Q is the total leakage [L$^3$/T]; i is the hydraulic gradient (hydraulic head+barrier thickness)/barrier thickness [L/L]; A the area which the leakage occurs [L$^2$] and k is the permeability in [L/T].

Another design issue that has to be taken into account is the lower the layer's hydraulic conductivity, the more difficult it becomes to get uniform packing. Trying to achieve a certain hydraulic conductivity reduction in the layer could give technical issues. Therefore the designer should take into account that a compromise should be made between its designed degree of compaction and the maximum reduction in hydraulic conductivity.

### 6.2.3. Recommendations on installation

As mentioned, the layer has the most potential as a horizontal liner. Another proposed method of using the Al-OM layer is underwater as a channel liner. Installing a channel liner is conventionally done by a spray pontoon or by normal discharge such as rainbowing. A spray pontoon is chosen over normal discharge due to the fact that it discharges the material in a more precise and controlled way (Dickhof, 2016). One of the most influential factors in the settlement process is the fall velocity. The fall velocity is often calculated as:

$$G = (\rho_s - \rho_w)\frac{1}{6}\pi D_p^3 g \tag{6.2}$$

Where the G is the submerged weight [MLT$^{-2}$]; $\rho_s$ the density of the sediment [M/L$^3$]; $\rho_w$ is the density of the water [M/L$^3$]; $D_p$ is the particle diameter [L] and g is the accelaration due to gravity [L/T$^2$] (van Ieperen, 1987).

When using a spray pontoon, the heavier particles settle close to the spray head, and the lighter particles stay in the water column and settle further on. The difference in the fall velocity of the flocs and the sand particles' fall velocity makes it almost impossible to spread a layer of a uniform Al-OM-sand mixture underwater. As an illustration, the sand Al-OM mixture was added to a large column filled with water, shown in Figure 6.2.1. For the approach to be successful, the spray head should be as close to the ground as possible, and the water flow rate should be as low as possible from preventing the Al-OM from separating from the mixture.

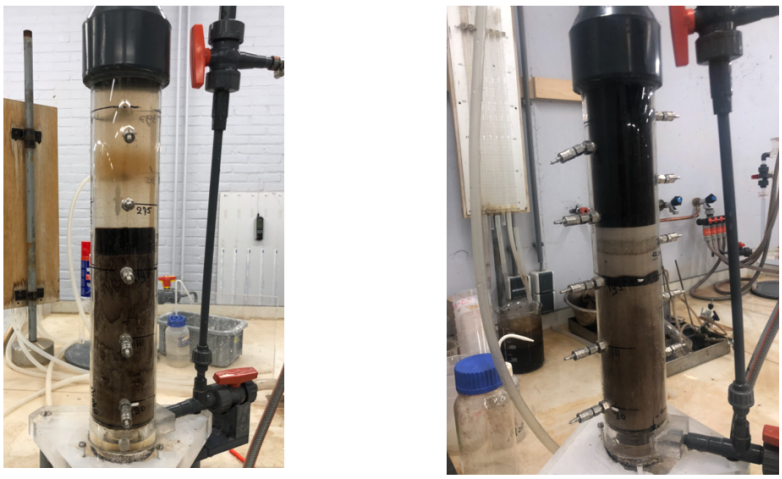

Figure 6.2.1: Performance of the mixture installed under water (left) and after a current from below the layer (right)

Another technique in which the Al-OM-sand mixture could be used is the mixed-in-place method (MIP). During this process, a triple auger is used to break up the soil, in which the existing soil is mixed with a binder slurry, in this case Al-OM. The relevant parameters in this case are drilling depth, volume of slurry,

rate of flow, auger speed and time of installation. Especially the rate of flow could influence the size of the flocs, due to their shear dependency. The important parameters for the mixture when used in this method is the permeability and compressive strength.

## 6.3. Recommendations for future research

The major challenge encountered in this research is the variability within test results at higher floc densities. In chapter 5 explanations for this spreading are given. To increase the packing density, a different sample construction is recommended, especially for higher floc amounts. First, using a smaller volume for the floc solution could increase the compaction of the layer because the water content is reduced. Another method that could increase the layer's compaction is using a drain, for example, a rod giving the trapped water a flow path. To reduce the influence of wall effect and the influence of preferential flow paths along the edges of the sample, it is recommended to use a larger area for the sample. or seal the sides of the sample. Another recommendation is to use image analysis on CT tests to investigate the heterogeneity within the samples with higher floc densities.

For using the layer in practice, additional research on strength parameters and compaction of the layer is needed. To use the mixture as a dyke cover for example, the shear strength of the layer is very interesting. The shear strength includes the slippage of soil particles, one on another, which may lead to the sliding of one body of soil relative to the surrounding mass. Therefore it is recommended to investigate the shear strength of the mixture over an increasing floc concentration. To obtain the required packing density, the sample needs to be compacted. At lower permeability, the packing density became lower. This could imply that the compaction requires more time at higher floc densities. Additional research on the compaction of the layer over time is therefore recommended. The costs for the layer are calculated for the highest reduction and for a M/C ratio of 0.06. As shown in figure 4.1.3 flocculation takes place after a M/C ratio of 0.031. The ratio of 0.06 has been taken to ensure the largest and strongest flocs, future research could be done to see the influence of lowering the M/C ratio on the reduction. Another recommendation is researching the influence of using alternative, cheaper Al and OM sources, such as proposed in section 6.2.1.

# Bibliography


Alice Gomes de Melo, B., Lopes Motta, F., and Adrade Santana, M. H. (2016). Humic acids : Structural properties and multiple functionalities for novel technological developments. *Materials Science & Engineering C*, 62:967–974.

Askarinejad, A. (2019). Experimental methods in Geotechnical Engineering Soil Classification and permeability tests Contents ….

Bear, J. and Cheng, A. H. (2010). *Modeling Groundwater Flow and Contaminant Transport*. Springer International Publishing, Haifa, 23 edition.

Bianco, C., Tosco, T., and Sethi, R. (2016). A 3-dimensional micro- and nanoparticle transport and fi ltration model ( MNM3D ) applied to the migration of carbon-based nanomaterials in porous media. *Journal of Contaminant Hydrology*, 193:10–20.

Blauw, M., Lambert, J., and Latil, M.-N. (2016). Biosealing : A Method for in situ Sealing of Leakages. Number July, pages 125–130, Delft. Deltares.

Bonfiglio, C. (2016). MSc. Thesis: Hydraulic conductivity reduction induced by precipitation of aluminium-organic matter flocs in porous. Master's thesis, Delft University of Technology.

Chateau, X. (2012). *Particle packing and the rheology of concrete*. Woodhead Publishing Limited.

Chu, J., Stabnikov, V., and Ivanov, V. (2012). Microbially Induced Calcium Carbonate Precipitation on Surface or in the Bulk of Soil. *Geomicrobiology Journal*, 29(6):544–549.

commissie bodembescherming, T. (2007). TCB S34(2007) Advies Monitoren. Technical Report 2006.

Daniel, D. E. (1993). *Clay liners*, pages 137–163. Springer US, Boston, MA.

Davies, N. and Mander, E. (2007). GeoSynthetic Clay Liners ( GCLS ) – The Cost Effective Alternative for Waste Management. (September):197–201.

Dickhof, R. (2016). Design and construction of a spray pontoon and maintenance of HAM 310. (January).

Duan, J. and Gregory, J. (2003). Coagulation by hydrolysing metal salts. *Advances in Colloid and Interface Science*, 100-102(SUPPL.):475–502.

Fan, L., Hwang, S., Nassar;, R., and Chou, S. (1985). An experimental study of deep-bed filtration: Stochastic analysis. *Powder Technol*.

Fitts, C. R. (2013). *Groundwater Science*. Elsevier, 2nd edition.

Ghernaout, D. and Ghernaout, B. (2012). Sweep flocculation as a second form of charge neutralisation — a review. *Desalination and water treatment*, 44:15–28.

Hazen, R. A. (1892). Some physical properties of sand and gravels, with special reference to their use in filtration. *Massachusetts State Board of Health*.

Head, K. (2018). Chapter 10: Permeability and erodibility tests. *Manual of Soil Laboratory Testing*, 2:80–164.

Head, K. H. and Epps, R. J. (2011). Direct Shear Tests. *Manual of Soil Laboratory Testing*, pages 208–300.

Holtz, W. G. (1974). Soil as an Engineering Material. Technical report, United States Department of the Interior, Washington.

Hommel, J., Coltman, E., and Class, H. (2018). Porosity–Permeability Relations for Evolving Pore Space: A Review with a Focus on (Bio-)geochemically Altered Porous Media. *Transport in Porous Media*, 124(2):589–629.

Hopman, J. (2016). *First insights into Al-OM complexation and the effect of Al-OM flocs on porous media-permeability*. Bachelor thesis, Delft University of Technology.

Hubbe, M. A., Chen, H., and Heitmann, J. A. (2009). Permeability reduction phenomena in packed beds, fiber mats, and wet webs of paper exposed to flow of liquids and suspensions: a review. *Bioresources*, 4(1):405–451.

Jansen, B., Nierop, K. G., and Verstraten, J. M. (2002). Influence of pH and metal/carbon ratios on soluble organic complexation of Fe(II), Fe(III) and Al(III) in soil solutions determined by diffusive gradients in thin films. *Analytica Chimica Acta*, 454(2):259–270.

Jarvis, P., Jefferson, B., and Parsons, S. A. (2005). Breakage, regrowth, and fractal nature of natural organic matter flocs. *Environmental Science and Technology*, 39(7):2307–2314.

Jarvis, P., Jefferson, B., and Parsons, S. A. (2006). Floc structural characteristics using conventional coagulation for a high doc, low alkalinity surface water source. *Water Research*, 40(14):2727–2737.

Kango, R., Alam, M. A., and Shankar, V. (2017). Investigations of wall effect on permeability through porous media at low flow rates. *Water Supply*, 18(1):233–239.

Kipton, H., Powell, J., and Town, R. M. (1992). Solubility and fractionation of humic acid; effect of pH and ionic medium. *Analytica Chimica Acta*, 267(1):47–54.

Laumann, S., Zhou, J., and Heimovaara, T. (2016). Aluminium-organic matter precipitation as a geoengineering tool for in situ permeability reduction in a porous media. *26th Goldschmidt Conference*.

Laumann, S., Zhou, J., and Heimovaara, T. (2018). Laboratory investigations on the interaction between aluminum and organic matter and its impact on soil permeability. Technical report, Delft University of Technology, Faculty of Civil Engineering and Geosciences, Section of geo-engineering.

Lundstrom, U. S., Van Breemen, N., and Bain, D. (2000). The podzolization process. A review. *Geoderma*, 94:91–107.

McRory, J. (2005). *Polymer Treatment of Bentonite Clay for Contaminant Resistant Barriers*, pages 1–11. American Society of Civil Engineers.

Met, I., Akgun, H., and Turkmenoglu, A. (2005). Environmental geological and geotechnical investigations related to the potential use of Ankara clay as a compacted landfill liner material , Turkey. *Environmental Geology*, 47:225–236.

Nagy, L., Tabácks, A., Huszák, T., Mahler, A., and Varga, G. (2013). Comparison of permeability testing methods. *18th International Conference on Soil Mechanics and Geotechnical Engineering: Challenges and Innovations in Geotechnics, ICSMGE 2013*, 1:399–402.

Nierop, K. G., Jansen, B., and Verstraten, J. M. (2002). Dissolved organic matter, aluminium and iron interactions: Precipitation induced by metal/carbon ratio, pH and competition. *Science of the Total Environment*, 300(1-3):201–211.

Owa, Y. and Husar, P. E.-c. J. (1987). United States Patent.

Popma, J. (2017). Engineering a horizontal layer of reduced permeability using Al-DOM precipitation Msc. Thesis. Technical report, TU Delft.

Proto, C. J., DeJong, J. T., and Nelson, D. C. (2016). Biomediated permeability reduction of saturated sands. *Journal of Geotechnical and Geoenvironmental Engineering*, 142(12):1–11.

Richens, D. T. (1997). *The Chemistry of Aqua Ions: Synthesis, Structure and Reqactivity: ATour Trough the Periodic Table of the Elements*. Wiley.

Sanna, V. (2020). Mobility of aluminium-OM flocs in porous media and their ability to reduce the hydraulic conductivity. Technical report, Politecnico di Torino.

Schijven, J. and Hassanizadeh, S. M. (2000). Removal of Viruses by Soil Passage : Overview of Modeling , Processes , and. *Environmental Science and Technology*, 30(January):49–127.

Stevenson, F. J. (1995). Humus Chemistry: Genesis, Composition, Reactions. *J. Chem. Educ.*, 72(4):A93.

TAW (1996). Technisch Rapport Klei Voor Dijken. *Taw*, page 81.

Tipping, E. (2002). *Cation Binding by Humic Substances*. Cambridge Environmental Chemistry Series. Cambridge University Press.

Tosco, T., Patrangeli Papini, M., Cruz Viggi, C., and Sethi, R. (2014). Nanoscale zerovalent iron particles for groundwater remediation : a review. *Journal of Cleaner Production*, 77:10–21.

Tosco, T. and Sethi, R. (2010). Transport of Non-Newtonian Suspensions of Highly Concentrated Micro- And Nanoscale Iron Particles in Porous Media: A Modeling Approach. *Environmental Science and Technology*, 44(23):9062–9068.

Ural, N. (2018). We are IntechOpen , the world ' s leading publisher of Open Access books Built by scientists , for scientists TOP 1 %. In *The Importance of Clay in Geotechnical Engineering*, pages 83–102.

Urumović, K. and Urumović, K. (2014). The effective porosity and grain size relations in permeability functions. *Hydrology and Earth System Sciences Discussions*, 11(6):6675–6714.

van Halem, D. D. (2020). Granular filtration.

van Ieperen, H. (1987). The falll velocity of grain particles. Technical report, Department of Hydraulics and Cathcment Hydroogy Agricultural University Wageningen.

Veerkamp, M. (2018). *The suitability of gibbsite as aluminum source to complex with dissolved organic matter*. Msc. thesis, Delft University of Technology.

Vis, R. (2015). *Control of Subsurface Flow The Effect of Al-OM Interactions on Hydraulic Conductivity*. Msc. thesis, Delft Univestiy of Technology.

voor Infrabouwproces, R. (2011). *RAW-systematiek*. CROW.

Weng, L., Temminghoff, E., and Riemsdijk, W. (2002). Interpretation of humic acid coagulation and soluble soil organic matter using a calculated electrostatic potential. *European Journal of Soil Science*, 53(December):575–587.

Wiersma, W. (2019). *Effect of shear stress on breakage and re-growth of aluminum- organic matter flocs*. PhD thesis, University of Wageningen.

Yu, W.-Z., Gregory, J., and Campos, L. (2010). Breakage and Regrowth of Al-Humic Flocs - Effect of Additional Coagulant Dosage. *Environmental Science & Technology*, 44(16):6371–6376.

Zhou, J. (2017). In situ soil permeability reduction through Al and OM precipitation as a geoengineering tool Al for dike In situ soil permeability reduction through OM stabilization precipitation as a geoengineering tool for dike stabilization. *25th Meeting of the European WOkring Group on INternal Erosion*, pages 42–43.

Zhou, J. (2020). *Development of a nature-based Geo-engineering solution to reduce soil permeability in-situ GEO - ENGINEERING SOLUTION TO REDUCE SOIL*. PhD thesis, Delft University of Technology.

Zhou, J., Laumann, S., and Heimovaara, T. J. (2019). Applying aluminum-organic matter precipitates to reduce soil permeability in-situ: A field and modeling study. *Science of the Total Environment*, 662:99–109.

Zsolnay, A. (2003). Dissolved organic matter: artefact, definitions and functions. *Geoderma*, 113:187–209.

# A

# Tables and plots for quantification of flocculation

Table A.0.1: Titration results for 5 gram of flocs with 100 ml 2.3 M OM, 13.8 ml 1.0 M Al (Table 1)

| OM 2.3 M (ml) | Al 1.0 M (µl) | pH | M/C -ratio | Al 1.0 M (µl) | pH | M/C -ratio | Al 1.0 M (µl) | pH | M/C -ratio | Al 1.0 M (µl) | pH | M/C -ratio | Al 1.0 M (µl) | pH | M/C -ratio |
|---|---|---|---|---|---|---|---|---|---|---|---|---|---|---|---|
| 100 | 0 | 9.7 | 0 | 0 | 9.71 | 0 | 0 | 9.33 | 0 | 0 | 9.14 | 0 | 0 | 9.14 | 0 |
| 100 | 200 | 9.51 | 0.001 | 500 | 9.64 | 0.002 | 495 | 9.33 | 0.002 | 500 | 9.1 | 0.002 | 500 | 8.42 | 0.002 |
| 100 | 400 | 9.38 | 0.002 | 1000 | 9.59 | 0.004 | 990 | 9.24 | 0.004 | 1000 | 8.95 | 0.004 | 1000 | 8.5 | 0.004 |
| 100 | 900 | 8.91 | 0.004 | 1500 | 9.38 | 0.007 | 1485 | 9.08 | 0.006 | 1500 | 8.34 | 0.007 | 1500 | 8.5 | 0.007 |
| 100 | 1400 | 8.74 | 0.006 | 2000 | 9.3 | 0.009 | 2000 | 8.87 | 0.009 | 2000 | 8.09 | 0.009 | 2000 | 7.53 | 0.009 |
| 100 | 1900 | 8.45 | 0.008 | 2500 | 9.17 | 0.011 | 2500 | 8.75 | 0.011 | 2500 | 7.17 | 0.011 | 2500 | 7.08 | 0.011 |
| 100 | 2400 | 8.15 | 0.01 | 3000 | 9.08 | 0.013 | 3000 | 8.66 | 0.013 | 3000 | 7.08 | 0.013 | 3000 | 7.12 | 0.013 |
| 100 | 2900 | 7.81 | 0.013 | 3500 | 8.96 | 0.015 | 3500 | 8.45 | 0.015 | 3500 | 7 | 0.015 | 3500 | 7.06 | 0.015 |
| 100 | 3400 | 7.51 | 0.015 | 4000 | 8.87 | 0.017 | 4000 | 8.24 | 0.017 | 4000 | 6.88 | 0.017 | 4000 | 6.39 | 0.017 |
| 100 | 3900 | 7.3 | 0.017 | 4500 | 8.79 | 0.02 | 4500 | 8 | 0.02 | 4500 | 6.6 | 0.02 | 4500 | 6.43 | 0.02 |
| 100 | 4400 | 6.74 | 0.019 | 5000 | 8.66 | 0.022 | 5000 | 7.54 | 0.022 | 5000 | 6.43 | 0.022 | 5000 | 6.15 | 0.022 |
| 100 | 4900 | 6.53 | 0.021 | 5500 | 8.53 | 0.024 | 5500 | 7.25 | 0.024 | 5500 | 5.99 | 0.024 | 5500 | 5.14 | 0.024 |
| 100 | 5400 | 6.32 | 0.023 | 6000 | 8.27 | 0.026 | 6000 | 5.75 | 0.026 | 6000 | 5.87 | 0.026 | 6000 | 5.1 | 0.026 |
| 100 | 5900 | 6.11 | 0.026 | 6500 | 8.02 | 0.028 | 6500 | 5.59 | 0.028 | 6500 | 5.38 | 0.028 | 6500 | 4.29 | 0.028 |
| 100 | 6400 | 5.89 | 0.028 | 7000 | 7.89 | 0.03 | 7000 | 5.38 | 0.03 | 7000 | 4.73 | 0.03 | 7000 | 4.13 | 0.03 |
| 100 | 6900 | 5.64 | 0.03 | 7500 | 7.64 | 0.033 | 7500 | 4.18 | 0.033 | 7500 | 4.49 | 0.033 | 7500 | 4.05 | 0.033 |
| 100 | 7400 | 4.11 | 0.032 | 8000 | 7.42 | 0.035 | 8000 | 3.97 | 0.035 | 8000 | 4.21 | 0.035 | 8000 | 3.97 | 0.035 |
| 100 | 7900 | 3.89 | 0.034 | 8500 | 7.3 | 0.037 | 8500 | 3.8 | 0.037 | 8500 | 4.09 | 0.037 | 8500 | 3.92 | 0.037 |
| 100 | 8400 | 3.72 | 0.037 | 9000 | 7.17 | 0.039 | 9000 | 3.72 | 0.039 | 9000 | 4.01 | 0.039 | 9000 | 3.86 | 0.039 |
| 100 | 8900 | 3.7 | 0.039 | 9500 | 7.04 | 0.041 | 9500 | 3.63 | 0.041 | 9500 | 3.97 | 0.041 | 9500 | 3.84 | 0.041 |
| 100 | 9400 | 3.6 | 0.041 | 10000 | 6.32 | 0.043 | 10000 | 3.72 | 0.043 | 10000 | 3.88 | 0.043 | 10000 | 3.76 | 0.043 |
| 100 | 9900 | 3.55 | 0.043 | 10500 | 5.55 | 0.046 | 10500 | 3.63 | 0.046 | 10500 | 3.76 | 0.046 | 10500 | 3.76 | 0.046 |
| 100 | 10400 | 3.47 | 0.045 | 11000 | 5.04 | 0.048 | 11000 | 3.62 | 0.048 | 11000 | 3.84 | 0.048 | 11000 | 3.8 | 0.048 |
| 100 | 10900 | 3.43 | 0.047 | 11500 | 4.57 | 0.05 | 11500 | 3.51 | 0.05 | 11500 | 3.76 | 0.05 | 11500 | 3.8 | 0.05 |
| 100 | 11400 | 3.38 | 0.05 | 12000 | 4.46 | 0.052 | 12000 | 3.47 | 0.052 | 12000 | 3.72 | 0.052 | 12000 | 3.68 | 0.052 |
| 100 | 11900 | 3.3 | 0.052 | 12500 | 4.32 | 0.054 | 12500 | 3.43 | 0.054 | 12500 | 3.76 | 0.054 | 12500 | 3.68 | 0.054 |
| 100 | 12400 | 3.26 | 0.054 | 13000 | 4.15 | 0.057 | 13000 | 3.47 | 0.057 | 13000 | 3.68 | 0.057 | 13000 | 3.68 | 0.057 |
| 100 | 12900 | 3.26 | 0.056 | 13500 | 4.06 | 0.059 | 13500 | 3.51 | 0.059 | 13500 | 3.65 | 0.059 | 13500 | 3.64 | 0.059 |
| 100 | 13400 | 3.26 | 0.058 | 13800 | 3.98 | 0.06 | 13800 | 3.43 | 0.06 | 13800 | 3.64 | 0.06 | 13800 | 3.64 | 0.06 |

Table A.0.2: Titration results for 5 gram of flocs with 100 ml 2.3 M OM, 13.8 ml 1.0 M Al (Table 2)

| OM 2.3 M (ml) | Al 1.0 M (µl) | pH | M/C -ratio | Al 1.0 M (µl) | pH | M/C -ratio | Al 1.0 M (µl) | pH | M/C -ratio |
|---|---|---|---|---|---|---|---|---|---|
| 100 | 0 | 9.04 | 0 | 0 | 9.2 | 0 | 0 | 9.24 | 0 |
| 100 | 500 | 8.5 | 0.002 | 500 | 9.19 | 0.002 | 500 | 9.2 | 0.002 |
| 100 | 1000 | 8.12 | 0.004 | 1000 | 9.12 | 0.004 | 1000 | 8.9 | 0.004 |
| 100 | 1500 | 8 | 0.007 | 1500 | 8.49 | 0.007 | 1500 | 8.44 | 0.007 |
| 100 | 2000 | 7.92 | 0.009 | 2000 | 8.45 | 0.009 | 2000 | 7.84 | 0.009 |
| 100 | 2500 | 7.79 | 0.011 | 2500 | 8.16 | 0.011 | 2500 | 7.55 | 0.011 |
| 100 | 3000 | 7.46 | 0.013 | 3000 | 7.99 | 0.013 | 3000 | 7.25 | 0.013 |
| 100 | 3500 | 7.29 | 0.015 | 3500 | 7.87 | 0.015 | 3500 | 7.04 | 0.015 |
| 100 | 4000 | 7.12 | 0.017 | 4000 | 5.92 | 0.017 | 4000 | 6.53 | 0.017 |
| 100 | 4500 | 6.46 | 0.02 | 4500 | 6.62 | 0.02 | 4500 | 6.45 | 0.02 |
| 100 | 5000 | 6.25 | 0.022 | 5000 | 6.54 | 0.022 | 5000 | 5.9 | 0.022 |
| 100 | 5500 | 5.3 | 0.024 | 5500 | 6.18 | 0.024 | 5500 | 5.6 | 0.024 |
| 100 | 6000 | 4.74 | 0.026 | 6000 | 5.83 | 0.026 | 6000 | 5.51 | 0.026 |
| 100 | 6500 | 4.22 | 0.028 | 6500 | 4.42 | 0.028 | 6500 | 4.24 | 0.028 |
| 100 | 7000 | 4.09 | 0.03 | 7000 | 4.09 | 0.03 | 7000 | 4.2 | 0.03 |
| 100 | 7500 | 4.01 | 0.033 | 7500 | 3.94 | 0.033 | 7500 | 4.07 | 0.033 |
| 100 | 8000 | 3.93 | 0.035 | 8000 | 3.8 | 0.035 | 8000 | 3.99 | 0.035 |
| 100 | 8500 | 3.88 | 0.037 | 8500 | 3.76 | 0.037 | 8500 | 3.96 | 0.037 |
| 100 | 9000 | 3.8 | 0.039 | 9000 | 3.67 | 0.039 | 9000 | 3.82 | 0.039 |
| 100 | 9500 | 3.72 | 0.041 | 9500 | 3.72 | 0.041 | 9500 | 3.78 | 0.041 |
| 100 | 10000 | 3.64 | 0.043 | 10000 | 3.67 | 0.043 | 10000 | 3.74 | 0.043 |
| 100 | 10500 | 3.51 | 0.046 | 10500 | 3.63 | 0.046 | 10500 | 3.69 | 0.046 |
| 100 | 11000 | 3.51 | 0.048 | 11000 | 3.59 | 0.048 | 11000 | 3.65 | 0.048 |
| 100 | 11500 | 3.47 | 0.05 | 11500 | 3.55 | 0.05 | 11500 | 3.61 | 0.05 |
| 100 | 12000 | 3.47 | 0.052 | 12000 | 3.55 | 0.052 | 12000 | 3.57 | 0.052 |
| 100 | 12500 | 3.47 | 0.054 | 12500 | 3.51 | 0.054 | 12500 | 3.52 | 0.054 |
| 100 | 13000 | 3.43 | 0.057 | 13000 | 3.51 | 0.057 | 13000 | 3.52 | 0.057 |
| 100 | 13500 | 3.43 | 0.059 | 13500 | 3.5 | 0.059 | 13500 | 3.48 | 0.059 |
| 100 | 13800 | 3.42 | 0.06 | 13800 | 3.47 | 0.06 | 13800 | 3.47 | 0.06 |

Table A.0.3: Titration results for 5 gram of flocs with 200 ml 1.15 M OM, 28 ml 0.5 M Al

| OM 1.15 M (ml) | Al 0.5 M(µl) | pH | M/C -ratio | OM 1.15 M (ml) | Al 0.5 M(µl) | pH | M/C -ratio |
|---|---|---|---|---|---|---|---|
| 200 | 0 | 9.19 | 0.000 | 200 | 14000 | 4.05 | 0.030 |
| 200 | 500 | 9.27 | 0.001 | 200 | 14500 | 3.97 | 0.032 |
| 200 | 1000 | 9.23 | 0.002 | 200 | 15000 | 3.97 | 0.033 |
| 200 | 1500 | 9.19 | 0.003 | 200 | 15500 | 3.93 | 0.034 |
| 200 | 2000 | 9.11 | 0.004 | 200 | 16000 | 3.89 | 0.035 |
| 200 | 2500 | 8.95 | 0.005 | 200 | 16500 | 3.89 | 0.036 |
| 200 | 3000 | 8.83 | 0.007 | 200 | 17000 | 3.89 | 0.037 |
| 200 | 3500 | 8.71 | 0.008 | 200 | 17500 | 3.89 | 0.038 |
| 200 | 4000 | 8.59 | 0.009 | 200 | 18000 | 3.77 | 0.039 |
| 200 | 4500 | 8.4 | 0.010 | 200 | 18500 | 3.73 | 0.040 |
| 200 | 5000 | 7.96 | 0.011 | 200 | 19000 | 3.69 | 0.041 |
| 200 | 5500 | 7.92 | 0.012 | 200 | 19500 | 3.65 | 0.042 |
| 200 | 6000 | 7.8 | 0.013 | 200 | 20000 | 3.65 | 0.043 |
| 200 | 6500 | 7.64 | 0.014 | 200 | 20500 | 3.65 | 0.045 |
| 200 | 7000 | 7.52 | 0.015 | 200 | 21000 | 3.65 | 0.046 |
| 200 | 7500 | 7.4 | 0.016 | 200 | 21500 | 3.61 | 0.047 |
| 200 | 8000 | 7.32 | 0.017 | 200 | 22000 | 3.68 | 0.048 |
| 200 | 8500 | 7.2 | 0.018 | 200 | 22500 | 3.68 | 0.049 |
| 200 | 9000 | 7.16 | 0.020 | 200 | 23000 | 3.69 | 0.050 |
| 200 | 9500 | 7.12 | 0.021 | 200 | 23500 | 3.65 | 0.051 |
| 200 | 10000 | 7.04 | 0.022 | 200 | 24000 | 3.65 | 0.052 |
| 200 | 10500 | 6.8 | 0.023 | 200 | 24500 | 3.61 | 0.053 |
| 200 | 11000 | 6.4 | 0.024 | 200 | 25000 | 3.61 | 0.054 |
| 200 | 11500 | 6.24 | 0.025 | 200 | 25500 | 3.61 | 0.055 |
| 200 | 12000 | 6 | 0.026 | 200 | 26000 | 3.61 | 0.057 |
| 200 | 12500 | 5.8 | 0.027 | 200 | 26500 | 3.61 | 0.058 |
| 200 | 13000 | 5.36 | 0.028 | 200 | 27000 | 3.61 | 0.059 |
| 200 | 13500 | 4.33 | 0.029 | 200 | 27500 | 3.61 | 0.060 |
| | *table continues on the right* | | | 200 | 28000 | 3.61 | 0.061 |

Table A.0.4: Titration results for 10 gram of flocs with 200 ml 2.23 M OM, 28 ml 1.0 M Al

| OM 2.3 M (ml) | Al 1.0 M (µl) | pH | M/C -ratio | Al 1.0 M (µl) | pH | M/C -ratio | Al 1.0 M (µl) | pH | M/C -ratio | Al 1.0 M (µl) | pH | M/C -ratio |
|---|---|---|---|---|---|---|---|---|---|---|---|---|
| 200 | 0 | 9.13 | 0.000 | 0 | 9.06 | 0.000 | 0 | 9.46 | 0.000 | 0 | 9.23 | 0.000 |
| 200 | 500 | 9.15 | 0.001 | 500 | 9.06 | 0.001 | 500 | 9.51 | 0.001 | 500 | 9.36 | 0.001 |
| 200 | 1000 | 9.15 | 0.002 | 1000 | 9.06 | 0.002 | 1000 | 9.47 | 0.002 | 1000 | 8.6 | 0.002 |
| 200 | 1500 | 9.02 | 0.003 | 1500 | 9.02 | 0.003 | 1500 | 9.43 | 0.003 | 1500 | 8.56 | 0.003 |
| 200 | 2000 | 8.94 | 0.004 | 2000 | 9.01 | 0.004 | 2000 | 9.17 | 0.004 | 2000 | 8.43 | 0.004 |
| 200 | 2500 | 8.81 | 0.005 | 2500 | 8.89 | 0.005 | 2500 | 9.09 | 0.005 | 2500 | 8.22 | 0.005 |
| 200 | 3000 | 8.68 | 0.007 | 3000 | 8.64 | 0.007 | 3000 | 8.95 | 0.007 | 3000 | 8.18 | 0.007 |
| 200 | 3500 | 8.52 | 0.008 | 3500 | 8.56 | 0.008 | 3500 | 8.79 | 0.008 | 3500 | 8.05 | 0.008 |
| 200 | 4000 | 8.39 | 0.009 | 4000 | 7.97 | 0.009 | 4000 | 6.31 | 0.009 | 4000 | 6.24 | 0.009 |
| 200 | 4500 | 8.26 | 0.010 | 4500 | 7.88 | 0.010 | 4500 | 5.8 | 0.010 | 4500 | 6.11 | 0.010 |
| 200 | 5000 | 8.14 | 0.011 | 5000 | 7.8 | 0.011 | 5000 | 5.42 | 0.011 | 5000 | 5.02 | 0.011 |
| 200 | 5500 | 8.01 | 0.012 | 5500 | 7.67 | 0.012 | 5500 | 5.2 | 0.012 | 5500 | 4.89 | 0.012 |
| 200 | 6000 | 7.88 | 0.013 | 6000 | 7.46 | 0.013 | 6000 | 5.08 | 0.013 | 6000 | 4.85 | 0.013 |
| 200 | 6500 | 7.72 | 0.014 | 6500 | 7.34 | 0.014 | 6500 | 4.95 | 0.014 | 6500 | 4.89 | 0.014 |
| 200 | 7000 | 7.59 | 0.015 | 7000 | 6.66 | 0.015 | 7000 | 4.82 | 0.015 | 7000 | 4.85 | 0.015 |
| 200 | 7500 | 6.62 | 0.016 | 7500 | 6.62 | 0.016 | 7500 | 4.69 | 0.016 | 7500 | 4.64 | 0.016 |
| 200 | 8000 | 6.49 | 0.017 | 8000 | 6.58 | 0.017 | 8000 | 4.65 | 0.017 | 8000 | 4.51 | 0.017 |
| 200 | 8500 | 6.24 | 0.018 | 8500 | 6.16 | 0.018 | 8500 | 4.73 | 0.018 | 8500 | 4.43 | 0.018 |
| 200 | 9000 | 6.16 | 0.020 | 9000 | 6.07 | 0.020 | 9000 | 4.62 | 0.020 | 9000 | 4.39 | 0.020 |
| 200 | 9500 | 6.03 | 0.021 | 9500 | 5.82 | 0.021 | 9500 | 4.6 | 0.021 | 9500 | 4.39 | 0.021 |
| 200 | 10000 | 5.9 | 0.022 | 10000 | 5.74 | 0.022 | 10000 | 4.39 | 0.022 | 10000 | 4.56 | 0.022 |
| 200 | 10500 | 5.87 | 0.023 | 10500 | 5.61 | 0.023 | 10500 | 4.35 | 0.023 | 10500 | 4.64 | 0.023 |
| 200 | 11000 | 5.86 | 0.024 | 11000 | 5.57 | 0.024 | 11000 | 4.39 | 0.024 | 11000 | 4.34 | 0.024 |
| 200 | 11500 | 5.82 | 0.025 | 11500 | 5.44 | 0.025 | 11500 | 4.35 | 0.025 | 11500 | 4.34 | 0.025 |
| 200 | 12000 | 5.74 | 0.026 | 12000 | 5.35 | 0.026 | 12000 | 4.22 | 0.026 | 12000 | 4.22 | 0.026 |
| 200 | 12500 | 5.61 | 0.027 | 12500 | 5.02 | 0.027 | 12500 | 4.09 | 0.027 | 12500 | 4.26 | 0.027 |
| 200 | 13000 | 5.4 | 0.028 | 13000 | 4.81 | 0.028 | 13000 | 4.31 | 0.028 | 13000 | 4.05 | 0.028 |
| 200 | 13500 | 5.19 | 0.029 | 13500 | 4.47 | 0.029 | 13500 | 4.14 | 0.029 | 13500 | 4.18 | 0.029 |
| 200 | 14000 | 4.89 | 0.030 | 14000 | 4.3 | 0.030 | 14000 | 3.97 | 0.030 | 14000 | 4.05 | 0.030 |
| 200 | 14500 | 4.56 | 0.032 | 14500 | 4.22 | 0.032 | 14500 | 3.88 | 0.032 | 14500 | 3.92 | 0.032 |
| 200 | 15000 | 4.68 | 0.033 | 15000 | 4.09 | 0.033 | 15000 | 3.81 | 0.033 | 15000 | 3.83 | 0.033 |
| 200 | 15500 | 4.68 | 0.034 | 15500 | 4.05 | 0.034 | 15500 | 3.79 | 0.034 | 15500 | 3.8 | 0.034 |
| 200 | 16000 | 4.43 | 0.035 | 16000 | 3.97 | 0.035 | 16000 | 3.79 | 0.035 | 16000 | 3.75 | 0.035 |
| 200 | 16500 | 4.47 | 0.036 | 16500 | 4.01 | 0.036 | 16500 | 3.75 | 0.036 | 16500 | 3.71 | 0.036 |
| 200 | 17000 | 4.18 | 0.037 | 17000 | 3.88 | 0.037 | 17000 | 3.71 | 0.037 | 17000 | 3.71 | 0.037 |
| 200 | 17500 | 4.01 | 0.038 | 17500 | 3.88 | 0.038 | 17500 | 3.71 | 0.038 | 17500 | 3.71 | 0.038 |
| 200 | 18000 | 4.01 | 0.039 | 18000 | 3.84 | 0.039 | 18000 | 3.67 | 0.039 | 18000 | 3.67 | 0.039 |
| 200 | 18500 | 3.97 | 0.040 | 18500 | 3.84 | 0.040 | 18500 | 3.62 | 0.040 | 18500 | 3.63 | 0.040 |
| 200 | 19000 | 4.05 | 0.041 | 19000 | 3.92 | 0.041 | 19000 | 3.62 | 0.041 | 19000 | 3.59 | 0.041 |
| 200 | 19500 | 3.88 | 0.042 | 19500 | 3.8 | 0.042 | 19500 | 3.62 | 0.042 | 19500 | 3.58 | 0.042 |
| 200 | 20000 | 3.84 | 0.043 | 20000 | 3.76 | 0.043 | 20000 | 3.62 | 0.043 | 20000 | 3.54 | 0.043 |
| 200 | 20500 | 3.76 | 0.045 | 20500 | 3.76 | 0.045 | 20500 | 3.58 | 0.045 | 20500 | 3.54 | 0.045 |
| 200 | 21000 | 3.84 | 0.046 | 21000 | 3.76 | 0.046 | 21000 | 3.58 | 0.046 | 21000 | 3.54 | 0.046 |
| 200 | 21500 | 3.71 | 0.047 | 21500 | 3.75 | 0.047 | 21500 | 3.58 | 0.047 | 21500 | 3.5 | 0.047 |
| 200 | 22000 | 3.63 | 0.048 | 22000 | 3.71 | 0.048 | 22000 | 3.58 | 0.048 | 22000 | 3.5 | 0.048 |
| 200 | 22500 | 3.67 | 0.049 | 22500 | 3.71 | 0.049 | 22500 | 3.58 | 0.049 | 22500 | 3.5 | 0.049 |
| 200 | 23000 | 3.63 | 0.050 | 23000 | 3.71 | 0.050 | 23000 | 3.57 | 0.050 | 23000 | 3.5 | 0.050 |
| 200 | 23500 | 3.54 | 0.051 | 23500 | 3.8 | 0.051 | 23500 | 3.58 | 0.051 | 23500 | 3.46 | 0.051 |
| 200 | 24000 | 3.5 | 0.052 | 24000 | 3.71 | 0.052 | 24000 | 3.54 | 0.052 | 24000 | 3.46 | 0.052 |
| 200 | 24500 | 3.5 | 0.053 | 24500 | 3.71 | 0.053 | 24500 | 3.54 | 0.053 | 24500 | 3.46 | 0.053 |
| 200 | 25000 | 3.46 | 0.054 | 25000 | 3.67 | 0.054 | 25000 | 3.54 | 0.054 | 25000 | 3.46 | 0.054 |
| 200 | 25500 | 3.46 | 0.055 | 25500 | 3.59 | 0.055 | 25500 | 3.54 | 0.055 | 25500 | 3.46 | 0.055 |
| 200 | 26000 | 3.47 | 0.057 | 26000 | 3.59 | 0.057 | 26000 | 3.54 | 0.057 | 26000 | 3.46 | 0.057 |
| 200 | 26500 | 3.46 | 0.058 | 26500 | 3.54 | 0.058 | 26500 | 3.5 | 0.058 | 26500 | 3.63 | 0.058 |
| 200 | 27000 | 3.42 | 0.059 | 27000 | 3.5 | 0.059 | 27000 | 3.51 | 0.059 | 27000 | 3.51 | 0.059 |
| 200 | 27500 | 3.42 | 0.060 | 27500 | 3.5 | 0.060 | 27500 | 3.5 | 0.060 | 27500 | 3.46 | 0.060 |
| 200 | 27600 | 3.46 | 0.060 | 27600 | 3.5 | 0.060 | 27600 | 3.5 | 0.060 | 27600 | 3.46 | 0.060 |

Table A.0.5: Titration results for 1-15 grams of flocs with varying concentrations and step sizes

| 1G | | | | | 5G | | | | 10G | | | | 15G | | | |
|---|---|---|---|---|---|---|---|---|---|---|---|---|---|---|---|---|
| OM 2.3 M (ml) | Al 1.0 M (µl) | pH | pH | M/C-ratio | OM 2.3 M (ml) | Al 1.0 M (µl) | pH | M/C-ratio | OM 2.3 M (ml) | Al 1.0 M (ml) | pH | M/C-ratio | OM 2.3 M (ml) | Al 1.5 M (ml) | pH | M/C-ratio |
| 17.3 | 0 | 9.28 | 8.99 | 0 | 86.6 | 0 | 9.2 | 0 | 173.19 | 0 | 9.17 | 0 | 259.79 | 0 | 9.25 | 0 |
| 17.3 | 100 | 9.24 | 8.39 | 0.003 | 86.6 | 500 | 9.04 | 0.003 | 173.19 | 1 | 9.08 | 0.003 | 259.79 | 5 | 6 | 0.013 |
| 17.3 | 200 | 9.2 | 8.1 | 0.005 | 86.6 | 1000 | 8.95 | 0.005 | 173.19 | 2 | 8.83 | 0.005 | 259.79 | 6 | 5.93 | 0.015 |
| 17.3 | 300 | 9.12 | 7.67 | 0.008 | 86.6 | 1500 | 8.66 | 0.008 | 173.19 | 3 | 8.44 | 0.008 | 259.79 | 7 | 5.92 | 0.018 |
| 17.3 | 400 | 8.79 | 7.42 | 0.01 | 86.6 | 2000 | 8.49 | 0.01 | 173.19 | 4 | 8.19 | 0.01 | 259.79 | 8 | 5.5 | 0.02 |
| 17.3 | 500 | 8.04 | 7.13 | 0.013 | 86.6 | 2500 | 8.04 | 0.013 | 173.19 | 5 | 7.97 | 0.013 | 259.79 | 9 | 5.42 | 0.023 |
| 17.3 | 600 | 7.54 | 6.92 | 0.015 | 86.6 | 3000 | 7.91 | 0.015 | 173.19 | 6 | 7.72 | 0.015 | 259.79 | 10 | 5.03 | 0.025 |
| 17.3 | 700 | 7.37 | 6.79 | 0.018 | 86.6 | 3500 | 6.5 | 0.018 | 173.19 | 7 | 7.59 | 0.018 | 259.79 | 11 | 4.61 | 0.028 |
| 17.3 | 800 | 6.75 | 6.66 | 0.02 | 86.6 | 4000 | 6.29 | 0.02 | 173.19 | 8 | 7.21 | 0.02 | 259.79 | 12 | 4.35 | 0.03 |
| 17.3 | 900 | 6.33 | 6.07 | 0.023 | 86.6 | 4500 | 5.88 | 0.023 | 173.19 | 9 | 6.78 | 0.023 | 259.79 | 13 | 4.05 | 0.033 |
| 17.3 | 1000 | 5.92 | 4.98 | 0.025 | 86.6 | 5000 | 4.01 | 0.025 | 173.19 | 10 | 6.7 | 0.025 | 259.79 | 14 | 3.97 | 0.035 |
| 17.3 | 1100 | 5.21 | 4.72 | 0.028 | 86.6 | 5500 | 3.97 | 0.028 | 173.19 | 11 | 4.86 | 0.028 | 259.79 | 15 | 3.92 | 0.038 |
| 17.3 | 1200 | 4.13 | 4.51 | 0.03 | 86.6 | 6000 | 3.8 | 0.03 | 173.19 | 12 | 4.48 | 0.03 | 259.79 | 16 | 3.84 | 0.04 |
| 17.3 | 1300 | 3.76 | 4.43 | 0.033 | 86.6 | 6500 | 3.67 | 0.033 | 173.19 | 13 | 4.22 | 0.033 | 259.79 | 17 | 3.81 | 0.043 |
| 17.3 | 1400 | 3.8 | 4.3 | 0.035 | 86.6 | 7000 | 3.67 | 0.035 | 173.19 | 14 | 4.1 | 0.035 | 259.79 | 18 | 3.8 | 0.045 |
| 17.3 | 1500 | 3.67 | 4.18 | 0.038 | 86.6 | 7500 | 3.63 | 0.038 | 173.19 | 15 | 3.97 | 0.038 | 259.79 | 19 | 3.75 | 0.048 |
| 17.3 | 1600 | 3.67 | 4.09 | 0.04 | 86.6 | 8000 | 3.59 | 0.04 | 173.19 | 16 | 3.92 | 0.04 | 259.79 | 20 | 3.75 | 0.05 |
| 17.3 | 1700 | 3.61 | 3.94 | 0.043 | 86.6 | 8500 | 3.55 | 0.043 | 173.19 | 17 | 3.84 | 0.043 | 259.79 | 21 | 3.72 | 0.053 |
| 17.3 | 1800 | 3.59 | 3.92 | 0.045 | 86.6 | 9000 | 3.55 | 0.045 | 173.19 | 18 | 3.8 | 0.045 | 259.79 | 22 | 3.71 | 0.055 |
| 17.3 | 1900 | 3.55 | 3.88 | 0.048 | 86.6 | 9500 | 3.55 | 0.048 | 173.19 | 19 | 3.71 | 0.048 | 259.79 | 23 | 3.67 | 0.058 |
| 17.3 | 2000 | 3.54 | 3.84 | 0.05 | 86.6 | 10000 | 3.55 | 0.05 | 173.19 | 20 | 3.7 | 0.05 | 259.79 | 24 | 3.54 | 0.06 |
| 17.3 | 2100 | 3.51 | 3.75 | 0.053 | 86.6 | 10500 | 3.54 | 0.053 | 173.19 | 21 | 3.62 | 0.053 | 259.79 | 24.41 | 3.5 | 0.061 |
| 17.3 | 2200 | 3.51 | 3.71 | 0.055 | 86.6 | 11000 | 3.51 | 0.055 | 173.19 | 22 | 3.61 | 0.055 | | | | |
| 17.3 | 2300 | 3.51 | 3.67 | 0.058 | 86.6 | 11500 | 3.51 | 0.058 | 173.19 | 23 | 3.54 | 0.058 | | | | |
| 17.3 | 2400 | 3.46 | 3.64 | 0.06 | 86.6 | 12000 | 3.51 | 0.06 | 173.19 | 23.9 | 3.45 | 0.06 | | | | |

Table A.0.6: Titration results for 20-50 grams of flocs with varying concentrations and step sizes

| 20 G | | | | | 40 G | | | | 50 G | | | |
|---|---|---|---|---|---|---|---|---|---|---|---|---|
| OM 1.58 M (ml) | Al 0.48 M (ml) | pH | pH | M/C-ratio | OM 1.59 M (ml) | Al 0.97 M (ml) | pH | M/C-ratio | OM 1.99 M (ml) | Al 1.196 M (ml) | pH | M/C -ratio |
| 500 | 0 | 9.48 | 9.29 | 0 | 1000 | 0 | 8.58 | 0 | 1000 | 0 | 8.92 | 0 |
| 500 | 2 | 9.42 | 9.29 | 0.001 | 1000 | 5 | 8.41 | 0.003 | 1000 | 5 | 8.78 | 0.003 |
| 500 | 4 | 9.38 | 9.08 | 0.002 | 1000 | 10 | 8.27 | 0.006 | 1000 | 10 | 8.69 | 0.006 |
| 500 | 6 | 9.29 | 9.08 | 0.004 | 1000 | 15 | 8.06 | 0.009 | 1000 | 15 | 8.38 | 0.009 |
| 500 | 8 | 9.21 | 8.99 | 0.005 | 1000 | 20 | 7.46 | 0.012 | 1000 | 20 | 8.24 | 0.012 |
| 500 | 10 | 9.16 | 8.3 | 0.006 | 1000 | 25 | 7.44 | 0.015 | 1000 | 25 | 7.57 | 0.015 |
| 500 | 12 | 9.08 | 8.17 | 0.007 | 1000 | 30 | 7.28 | 0.018 | 1000 | 30 | 7.43 | 0.018 |
| 500 | 14 | 8.9 | 7.99 | 0.009 | 1000 | 35 | 7.09 | 0.021 | 1000 | 35 | 5.95 | 0.021 |
| 500 | 16 | 8.75 | 7.87 | 0.01 | 1000 | 40 | 6.91 | 0.024 | 1000 | 40 | 5.68 | 0.024 |
| 500 | 18 | 8.51 | 7.34 | 0.011 | 1000 | 45 | 6.78 | 0.027 | 1000 | 45 | 4.23 | 0.027 |
| 500 | 20 | 8.25 | 7.3 | 0.012 | 1000 | 50 | 5.15 | 0.03 | 1000 | 50 | 3.66 | 0.03 |
| 500 | 22 | 7.97 | 7.22 | 0.013 | 1000 | 55 | 4.4 | 0.033 | 1000 | 55 | 3.48 | 0.033 |
| 500 | 24 | 7.35 | 6.61 | 0.015 | 1000 | 60 | 3.4 | 0.037 | 1000 | 60 | 3.46 | 0.036 |
| 500 | 26 | 6 | 6.44 | 0.016 | 1000 | 65 | 3.26 | 0.04 | 1000 | 65 | 3.43 | 0.039 |
| 500 | 28 | 6.87 | 6.4 | 0.017 | 1000 | 70 | 3.39 | 0.043 | 1000 | 70 | 3.26 | 0.042 |
| 500 | 30 | 5.54 | 6.31 | 0.018 | 1000 | 75 | 3.39 | 0.046 | 1000 | 75 | 3.39 | 0.045 |
| 500 | 32 | 5.49 | 6.26 | 0.019 | 1000 | 80 | 3.39 | 0.049 | 1000 | 80 | 3.34 | 0.048 |
| 500 | 34 | 5.14 | 6.05 | 0.021 | 1000 | 85 | 3.35 | 0.052 | 1000 | 85 | 3.34 | 0.051 |
| 500 | 36 | 5.1 | 5.49 | 0.022 | 1000 | 90 | 3.08 | 0.055 | 1000 | 90 | 3.3 | 0.054 |
| 500 | 38 | 5.1 | 4.75 | 0.023 | 1000 | 95 | 3.08 | 0.058 | 1000 | 95 | 3.3 | 0.057 |
| 500 | 40 | 5.14 | 4.45 | 0.024 | 1000 | 100 | 3.11 | 0.061 | 1000 | 100 | 3.3 | 0.06 |
| 500 | 42 | 5.01 | 4.25 | 0.026 | | | | | | | | |
| 500 | 44 | 5.01 | 4.06 | 0.027 | | | | | | | | |
| 500 | 46 | 4.79 | 4.15 | 0.028 | | | | | | | | |
| 500 | 48 | 4.75 | 4.1 | 0.029 | | | | | | | | |
| 500 | 50 | 4.49 | 4.09 | 0.03 | | | | | | | | |
| 500 | 52 | 4.46 | 4.02 | 0.032 | | | | | | | | |
| 500 | 54 | 4.06 | 3.97 | 0.033 | | | | | | | | |
| 500 | 56 | 3.84 | 3.89 | 0.034 | | | | | | | | |
| 500 | 58 | 3.58 | 3.89 | 0.035 | | | | | | | | |
| 500 | 60 | 3.6 | 3.63 | 0.036 | | | | | | | | |
| 500 | 62 | 3.5 | 3.63 | 0.038 | | | | | | | | |
| 500 | 64 | 3.93 | 3.58 | 0.039 | | | | | | | | |
| 500 | 66 | 4.02 | 3.58 | 0.04 | | | | | | | | |
| 500 | 68 | 3.57 | 3.58 | 0.041 | | | | | | | | |
| 500 | 70 | 3.54 | 3.58 | 0.043 | | | | | | | | |
| 500 | 72 | 3.94 | 3.54 | 0.044 | | | | | | | | |
| 500 | 74 | 3.83 | 3.54 | 0.045 | | | | | | | | |
| 500 | 76 | 3.77 | 3.54 | 0.046 | | | | | | | | |
| 500 | 78 | 4.15 | 3.64 | 0.047 | | | | | | | | |
| 500 | 80 | 3.76 | 3.93 | 0.049 | | | | | | | | |
| 500 | 82 | 3.97 | 3.73 | 0.05 | | | | | | | | |
| 500 | 84 | 3.75 | 3.54 | 0.051 | | | | | | | | |
| 500 | 86 | 3.79 | 3.54 | 0.052 | | | | | | | | |
| 500 | 88 | 3.66 | 3.54 | 0.053 | | | | | | | | |
| 500 | 90 | 3.58 | 3.54 | 0.055 | | | | | | | | |
| 500 | 92 | 3.97 | 3.54 | 0.056 | | | | | | | | |
| 500 | 94 | 3.64 | 3.54 | 0.057 | | | | | | | | |
| 500 | 96 | 3.76 | 3.54 | 0.058 | | | | | | | | |
| 500 | 98 | 2.75 | 3.54 | 0.06 | | | | | | | | |
| 500 | 100 | 3.09 | 3.54 | 0.061 | | | | | | | | |

# B

# Tables and plots for the quantification of potassium chloride

Table B.0.1: The results of the measured electrical conductivity and UV adsorption over the density of flocs and the dilution of the floc mix.

| Sample | Mass I (g) | Mass II (g) | EC (mS/cm) | UV | Remarks |
|---|---|---|---|---|---|
| 1.1 | 1000.00 | 500.00 | 2.24 | 0.68 | |
| | 1000.00 | 500.00 | 0.63 | 0.24 | Filtered by coffee filter |
| | 1000.00 | 500.00 | 0.13 | 0.24 | Stirring and settling |
| | 1000.00 | 500.00 | 0.03 | 0.53 | Stirring and settling |
| | 1000.00 | 500.00 | 0.01 | 1.97 | Stirring and settling |
| | 1000.00 | 500.00 | 0.04 | 1.49 | Stirring and settling |
| | 1000.00 | 500.00 | 0.01 | 3.05 | Stirring and settling |
| | 1000.00 | 500.00 | 0.01 | 3.09 | Stirring and settling |
| 1.2 | 150.00 | 20.00 | 5.90 | 1.36 | |
| | 485.00 | 150.00 | 2.45 | 1.14 | |
| | 485.00 | 197.00 | 0.73 | 0.78 | |
| | 485.00 | 197.00 | 0.10 | 0.56 | |
| 1.3 | 305.00 | 28.69 | 3.27 | 0.99 | |
| | 355.00 | 27.10 | 0.37 | 1.12 | |
| 5.1 | 1000.00 | 500.00 | 5.76 | 1.40 | Stirring and settling |
| | 1000.00 | 500.00 | 8.75 | 2.00 | Stirring and settling |
| | 1000.00 | 500.00 | 1.95 | 0.62 | Stirring and settling |
| | 1000.00 | 500.00 | 0.80 | 0.48 | Centrifuge |
| | 1000.00 | 500.00 | 0.16 | 0.89 | Centrifuge |
| | 1000.00 | 500.00 | 0.17 | 1.05 | Centrifuge |
| | 1000.00 | 500.00 | 0.12 | 0.85 | Centrifuge |
| | 1000.00 | 500.00 | 0.07 | 0.69 | Centrifuge |
| | 1000.00 | 500.00 | 0.08 | 0.64 | Centrifuge |
| | 1000.00 | 500.00 | 0.06 | 0.64 | Centrifuge |
| | 1000.00 | 500.00 | 0.01 | 1.44 | Centrifuge |
| | 1000.00 | 500.00 | 0.03 | 0.85 | Centrifuge |
| 5.2 | 1000.00 | 560.00 | 5.76 | 1.23 | |
| | 485.00 | 500.00 | 3.70 | 1.31 | |
| | 485.00 | 500.00 | 4.27 | 1.47 | |
| | 485.00 | 160.00 | 0.90 | 0.88 | |
| | 485.00 | 160.00 | 0.88 | 0.80 | |
| | 485.00 | 130.00 | 0.19 | 0.69 | |
| | 485.00 | 130.00 | 0.24 | 0.77 | |
| 5.3 | 305.00 | 87.33 | 12.10 | 2.24 | |
| | 355.00 | 80.00 | 4.38 | 1.82 | |
| | 405.00 | 82.88 | 1.16 | 1.66 | |
| | 405.00 | 81.09 | 0.35 | 2.65 | |
| 10.1 | 900.00 | 197.09 | 7.66 | 1.52 | Average of 4 bottles |
| | 1300.00 | 500.00 | 3.43 | 1.18 | Average of 4 bottles |
| | 1260.00 | 220.00 | 0.66 | 0.81 | Average of 4 bottles |
| | 1300.00 | 192.00 | 0.18 | 0.55 | Average of 4 bottles |
| 10.2 | 405.00 | 183.12 | 18.62 | 3.38 | |
| | 405.00 | 142.00 | 10.36 | 2.67 | |
| | 405.00 | 151.40 | 4.67 | 1.88 | |
| | 405.00 | 150.83 | 2.12 | 1.31 | |
| | 405.00 | 150.24 | 0.84 | 0.49 | |
| | 405.00 | 146.50 | 0.34 | 1.19 | |
| 10.3 | 1000 | 366.66 | 7.93 | 2.68 | |
| | 1002.11 | 357.31 | 2.10 | 1.24 | |
| | 1019.7 | 357.31 | 0.68 | 1.02 | |
| | 1004.94 | 353.86 | 0.25 | 0.95 | |
| 15.1 | 1300.00 | 285.00 | 8.90 | 1.62 | Average of 4 bottles |
| | 1260.00 | 660.00 | 5.73 | 1.82 | Average of 4 bottles |
| | 1260.00 | 660.00 | 1.52 | 1.11 | Average of 4 bottles |
| | 1300.00 | 500.00 | 0.52 | 0.97 | Average of 4 bottles |
| | 1300.00 | 500.00 | 0.15 | 1.09 | Average of 4 bottles |
| 15.2 | 405.00 | 199.60 | 24.90 | 3.28 | |
| | 405.00 | 194.12 | 13.60 | 2.57 | |
| | 405.00 | 200.60 | 5.70 | 1.76 | |
| | 405.00 | 199.20 | 6.40 | 1.80 | |
| | 405.00 | 194.34 | 3.12 | 1.72 | |
| | 425.00 | 182.83 | 1.72 | 0.53 | |
| | 425.00 | 183.34 | 1.41 | 1.85 | |
| | 425.00 | 183.45 | 0.84 | 1.21 | |
| | 425.00 | 183.25 | 0.42 | 0.97 | |
| 15.3 | 1000 | 418.66 | 10.91 | 3.32 | |
| | 1001.3 | 420.16 | 3.78 | 1.45 | |
| | 1004.16 | 411.62 | 1.39 | 1.36 | |
| | 1015.98 | 424.21 | 0.55 | 1.06 | |
| 20.1 | 1420.00 | 540.00 | 8.92 | 2.22 | |
| | 1420.00 | 420.00 | 3.29 | 1.39 | |
| | 1420.00 | 420.00 | 1.18 | 1.23 | |
| | 1420.00 | 780.00 | 0.42 | 1.15 | |
| 20.2 | 850.00 | 282.00 | 15.23 | 2.74 | |
| | 850.00 | 279.13 | 5.79 | 1.06 | |
| | 850.00 | 254.03 | 2.70 | 0.65 | |
| | 850.00 | 266.00 | 1.21 | 1.79 | |
| | 850.00 | 275.70 | 0.54 | 0.51 | |
| 25.1 | 905.00 | 500.00 | 17.00 | 1.91 | |
| | 905.00 | 500.00 | 15.30 | 1.55 | |
| | 905.00 | 500.00 | 6.90 | 0.90 | |

| | | | | | |
|---|---|---|---|---|---|
| | 905.00 | 500.00 | 4.60 | 0.80 | |
| | 905.00 | 500.00 | 4.58 | 0.81 | |
| 25.2 | 1800.00 | 1200.00 | 9.61 | 1.25 | Stirring and settling |
| | 1800.00 | 1200.00 | 7.50 | 1.04 | Stirring and settling |
| | 1800.00 | 1200.00 | 5.80 | 0.76 | Stirring and settling |
| | 1800.00 | 1200.00 | 3.60 | 0.61 | Stirring and settling |
| | 1800.00 | | 1.98 | 1.10 | |
| | 1800.00 | | 1.18 | 1.05 | |
| | 1800.00 | | 0.45 | 0.92 | |
| 25.3 | 1420.00 | 856.53 | 9.94 | 1.55 | Average of 4 bottles (500 mL) |
| | 1220.00 | 856.53 | 5.15 | 0.93 | Average of 4 bottles (500 mL) |
| | 1620.00 | 756.38 | 1.73 | 1.38 | Average of 4 bottles (500 mL) |
| | 1620.00 | 749.90 | 0.51 | 1.12 | Average of 4 bottles (500 mL) |
| 30.1 | 1420.00 | 660.00 | 11.67 | 2.53 | Average of 4 bottles (500 mL) |
| | 1420.00 | 519.80 | 5.31 | 1.79 | Average of 4 bottles (500 mL) |
| | 1420.00 | 436.38 | 1.92 | 1.50 | Average of 4 bottles (500 mL) |
| | 1420.00 | 400.00 | 0.69 | 1.48 | Average of 4 bottles (500 mL) |
| | 1420.00 | 400.00 | 0.27 | 1.48 | Average of 4 bottles (500 mL) |
| 30.2 | 1620.00 | 905.47 | 13.09 | 2.14 | Average of 4 bottles (500 mL) |
| | 1620.00 | 841.66 | 5.62 | 1.84 | Average of 4 bottles (500 mL) |
| | 1620.00 | 874.85 | 1.89 | 1.38 | Average of 4 bottles (500 mL) |
| | 1620.00 | 826.25 | 0.64 | 1.12 | Average of 4 bottles (500 mL) |
| | 1620.00 | 846.29 | 0.26 | 1.12 | Average of 4 bottles (500 mL) |
| 40.1 | 1960.00 | 1800.00 | 13.47 | 3.09 | Average of 4 bottles (500 mL) |
| | 2000.00 | 1132.54 | 5.84 | 2.36 | Average of 4 bottles (500 mL) |
| | 2000.00 | 1132.54 | 3.26 | 2.37 | Average of 4 bottles (500 mL) |
| | 2000.00 | 1052.96 | 1.47 | 1.84 | Average of 4 bottles (500 mL) |
| | 2000.00 | 1032.17 | 0.77 | 1.30 | Average of 4 bottles (500 mL) |
| 40.2 | 2000.00 | 1177.84 | 13.19 | 2.35 | Average of 4 bottles (500 mL) |
| | 2000.00 | 1223.14 | 5.48 | 1.31 | Average of 4 bottles (500 mL) |
| | 2000.00 | 989.78 | 2.11 | 1.14 | Average of 4 bottles (500 mL) |
| | 2000.00 | 897.99 | 0.67 | 0.99 | Average of 4 bottles (500 mL) |
| 40.3 | 2000.00 | 1211.82 | 15.02 | 2.40 | Average of 4 bottles (500 mL) |
| | 2000.00 | 1155.19 | 5.03 | 1.34 | Average of 4 bottles (500 mL) |
| | 2000.00 | 1116.14 | 1.67 | 1.14 | Average of 4 bottles (500 mL) |
| | 2000.00 | 1131.26 | 0.58 | 1.08 | Average of 4 bottles (500 mL) |
| 50.1 | 1800.00 | 1300.00 | 18.32 | 2.75 | Average of 4 bottles (500 mL) |
| | 1900.00 | 1200.00 | 11.32 | 2.47 | Average of 4 bottles (500 mL) |
| | 1980.00 | 1200.00 | 7.50 | 2.04 | Average of 4 bottles (500 mL) |
| | 2000.00 | 1200.00 | 3.46 | 2.26 | Average of 4 bottles (500 mL) |
| | 1800.00 | 1080.00 | 1.63 | 1.30 | Average of 4 bottles (500 mL) |
| | 1800.00 | 1080.00 | 0.69 | 1.02 | Average of 4 bottles (500 mL) |
| | 1800.00 | 1080.00 | 0.74 | 1.44 | Average of 4 bottles (500 mL) |
| | 1800.00 | 1080.00 | 0.43 | 1.64 | Average of 4 bottles (500 mL) |
| | 1800.00 | 1470.00 | 0.32 | 1.19 | Average of 4 bottles (500 mL) |
| 50.2 | 2000.00 | 1200.00 | 15.39 | 2.79 | Average of 4 bottles (500 mL) |
| | 1800.00 | 1080.00 | 7.88 | 1.93 | Average of 4 bottles (500 mL) |
| | 1800.00 | 1080.00 | 4.59 | 1.89 | Average of 4 bottles (500 mL) |
| | 1800.00 | 1080.00 | 2.56 | 1.55 | Average of 4 bottles (500 mL) |
| | 1800.00 | 1080.00 | 1.44 | 1.70 | Average of 4 bottles (500 mL) |
| | 1800.00 | 1080.00 | 0.82 | 1.13 | Average of 4 bottles (500 mL) |
| | 1800.00 | 1080.00 | 0.59 | 1.69 | Average of 4 bottles (500 mL) |
| | 1800.00 | 1080.00 | 0.41 | 0.92 | Average of 4 bottles (500 mL) |
| 50.3 | 1960.00 | 1800.00 | 18.64 | 3.14 | Average of 4 bottles (500 mL) |
| | 2000.00 | 1133.21 | 9.76 | 3.43 | Average of 4 bottles (500 mL) |
| | 2000.00 | 1178.63 | 3.68 | 1.36 | Average of 4 bottles (500 mL) |
| | 2000.00 | 1089.10 | 3.21 | 1.45 | Average of 4 bottles (500 mL) |
| | 2000.00 | 1096.56 | 1.44 | 1.70 | Average of 4 bottles (500 mL) |
| | 2000.00 | 1055.69 | 1.68 | 1.47 | Average of 4 bottles (500 mL) |
| | 2000.00 | 1055.69 | 1.09 | 1.20 | Average of 4 bottles (500 mL) |
| | 2000.00 | 1055.69 | 0.56 | 1.09 | Average of 4 bottles (500 mL) |
| 50.4 | 2200.00 | 1076.80 | 15.46 | 2.27 | Average of 4 bottles (500 mL) |
| | 2200.00 | 1024.02 | 7.53 | 1.51 | Average of 4 bottles (500 mL) |
| | 2200.00 | 1089.47 | 2.45 | 1.12 | Average of 4 bottles (500 mL) |
| | 2200.00 | 1150.70 | 0.91 | 1.11 | Average of 4 bottles (500 mL) |
| | 2200.00 | 1161.26 | 0.29 | 0.85 | Average of 4 bottles (500 mL) |
| 50.5 | 2200.00 | 992.35 | 17.49 | 2.27 | Average of 4 bottles (500 mL) |
| | 2200.00 | 1119.03 | 6.25 | 1.48 | Average of 4 bottles (500 mL) |
| | 2200.00 | 960.68 | 2.03 | 1.26 | Average of 4 bottles (500 mL) |
| | 2200.00 | 1025.61 | 0.74 | 0.97 | Average of 4 bottles (500 mL) |

Table B.0.2: The density of flocs in gram of flocs in initial volume with their corresponding EC and UV values.

| Sample | g | mL | g/mL | EC (mS/cm) | UV |
|---|---|---|---|---|---|
| 0.0 | 0.00 | 0 | 0.000 | 0.00 | 1.00 |
| 1.1 | 1.00 | 1000 | 0.001 | 2.24 | 0.68 |
| 1.2 | 1.00 | 150 | 0.007 | 5.90 | 1.36 |
| 1.3 | 1.00 | 305 | 0.003 | 3.27 | 0.99 |
| 5.1 | 5.00 | 1000 | 0.005 | 5.76 | 1.40 |
| 5.2 | 5.00 | 1000 | 0.005 | 5.76 | 1.23 |
| 5.3 | 5.00 | 305 | 0.016 | 12.10 | 2.24 |
| 10.1 | 10.00 | 900 | 0.011 | 7.66 | 1.52 |
| 10.2 | 10.00 | 405 | 0.025 | 18.62 | 3.38 |
| 15.1 | 15.00 | 1300 | 0.012 | 8.90 | 1.62 |
| 15.2 | 15.00 | 405 | 0.037 | 24.90 | 3.28 |
| 20.1 | 20.00 | 1420 | 0.014 | 8.92 | 2.22 |
| 20.2 | 20.00 | 850 | 0.024 | 15.23 | 2.74 |
| 25.1 | 25.00 | 905 | 0.028 | 17.00 | 1.91 |
| 25.2 | 25.00 | 1800 | 0.014 | 9.61 | 1.25 |
| 25.3 | 25.00 | 1420 | 0.018 | 9.94 | 1.55 |
| 30.1 | 30.00 | 1420 | 0.021 | 11.67 | 2.53 |
| 30.2 | 30.00 | 1620 | 0.019 | 13.09 | 2.14 |
| 40.1 | 40.00 | 1960 | 0.020 | 13.47 | 3.09 |
| 40.2 | 40.00 | 2000 | 0.020 | 13.19 | 2.35 |
| 40.3 | 40.00 | 2000 | 0.020 | 15.02 | 2.40 |
| 50.1 | 50.00 | 1800 | 0.028 | 18.32 | 2.75 |
| 50.2 | 50.00 | 2000 | 0.025 | 15.39 | 2.79 |
| 50.3 | 50.00 | 1960 | 0.026 | 18.64 | 3.14 |
| 50.4 | 50.00 | 2200 | 0.023 | 15.46 | 2.27 |
| 50.5 | 50.00 | 2200 | 0.023 | 17.49 | 2.27 |

# C

# Tables and plots for the permeability reduction coefficient

Table C.0.1: The used parameters, the results of the falling head tests and the reduction of hydraulic conductivity.

| Sample | Amount of flocs (g/kg) | Area sample A (m) | Length L (m) | Area of burrette a (m^2) | h (m) | h0 (m) | t (s) | k (m/s) | k0 (m/s) | HCR (-) |
|---|---|---|---|---|---|---|---|---|---|---|
| 0.1 | 0 | 3.53E-03 | 0.166 | 5.03E-05 | 0.23 | 0.73 | 23.05 | 1.19E-04 | 1.31E-04 | 1.11 |
| 0.1 | 0 | 3.53E-03 | 0.166 | 5.03E-05 | 0.23 | 0.73 | 22.95 | 1.19E-04 | 1.31E-04 | 1.10 |
| 0.1 | 0 | 3.53E-03 | 0.166 | 5.03E-05 | 0.23 | 0.73 | 19.71 | 1.39E-04 | 1.31E-04 | 0.95 |
| 0.2 | 0 | 3.53E-03 | 0.167 | 5.03E-05 | 0.23 | 0.73 | 14.95 | 1.84E-04 | 1.31E-04 | 0.71 |
| 0.2 | 0 | 3.53E-03 | 0.167 | 5.03E-05 | 0.23 | 0.73 | 15.44 | 1.78E-04 | 1.31E-04 | 0.74 |
| 0.2 | 0 | 3.53E-03 | 0.167 | 5.03E-05 | 0.23 | 0.73 | 25.93 | 1.06E-04 | 1.31E-04 | 1.24 |
| 0.3 | 0 | 3.53E-03 | 0.166 | 5.03E-05 | 0.23 | 0.73 | 25.18 | 1.09E-04 | 1.31E-04 | 1.21 |
| 0.3 | 0 | 3.53E-03 | 0.166 | 5.03E-05 | 0.23 | 0.73 | 25.45 | 1.07E-04 | 1.31E-04 | 1.22 |
| 0.3 | 0 | 3.53E-03 | 0.166 | 5.03E-05 | 0.23 | 0.73 | 19.1 | 1.43E-04 | 1.31E-04 | 0.92 |
| 0.4 | 0 | 3.53E-03 | 0.166 | 5.03E-05 | 0.23 | 0.73 | 17.17 | 1.59E-04 | 1.31E-04 | 0.83 |
| 0.4 | 0 | 3.53E-03 | 0.166 | 5.03E-05 | 0.23 | 0.73 | 25.48 | 1.07E-04 | 1.31E-04 | 1.22 |
| 0.4 | 0 | 3.53E-03 | 0.166 | 5.03E-05 | 0.23 | 0.73 | 25.68 | 1.06E-04 | 1.31E-04 | 1.23 |
| 1.1 | 1 | 3.85E-03 | 0.172 | 5.03E-05 | 0.23 | 0.73 | 17.63 | 1.47E-04 | 1.31E-04 | 0.89 |
| 1.1 | 1 | 3.85E-03 | 0.172 | 5.03E-05 | 0.23 | 0.73 | 17.48 | 1.48E-04 | 1.31E-04 | 0.89 |
| 1.1 | 1 | 3.85E-03 | 0.172 | 5.03E-05 | 0.23 | 0.73 | 18.11 | 1.43E-04 | 1.31E-04 | 0.92 |
| 1.1 | 1 | 3.85E-03 | 0.172 | 5.03E-05 | 0.23 | 0.73 | 17.74 | 1.46E-04 | 1.31E-04 | 0.90 |
| 1.1 | 1 | 3.85E-03 | 0.172 | 5.03E-05 | 0.23 | 0.73 | 17.64 | 1.47E-04 | 1.31E-04 | 0.89 |
| 1.2 | 1 | 3.53E-03 | 0.167 | 5.03E-05 | 0.23 | 0.73 | 13.83 | 1.99E-04 | 1.31E-04 | 0.66 |
| 1.2 | 1 | 3.53E-03 | 0.167 | 5.03E-05 | 0.23 | 0.73 | 13.37 | 2.06E-04 | 1.31E-04 | 0.64 |
| 1.2 | 1 | 3.53E-03 | 0.167 | 5.03E-05 | 0.23 | 0.73 | 13.8 | 1.99E-04 | 1.31E-04 | 0.66 |
| 1.2 | 1 | 3.53E-03 | 0.167 | 5.03E-05 | 0.23 | 0.73 | 13.28 | 2.07E-04 | 1.31E-04 | 0.63 |
| 1.2 | 1 | 3.53E-03 | 0.167 | 5.03E-05 | 0.23 | 0.73 | 3.51 | 7.83E-04 | 1.31E-04 | 0.17 |
| 5.1 | 5 | 3.85E-03 | 0.172 | 5.03E-05 | 0.23 | 0.73 | 45.08 | 5.76E-05 | 1.31E-04 | 2.28 |
| 5.1 | 5 | 3.85E-03 | 0.172 | 5.03E-05 | 0.23 | 0.73 | 45.27 | 5.73E-05 | 1.31E-04 | 2.29 |
| 5.1 | 5 | 3.85E-03 | 0.172 | 5.03E-05 | 0.23 | 0.73 | 45.43 | 5.71E-05 | 1.31E-04 | 2.30 |
| 5.1 | 5 | 3.85E-03 | 0.172 | 5.03E-05 | 0.23 | 0.73 | 46.73 | 5.55E-05 | 1.31E-04 | 2.37 |
| 5.1 | 5 | 3.85E-03 | 0.172 | 5.03E-05 | 0.23 | 0.73 | 43.98 | 5.90E-05 | 1.31E-04 | 2.23 |
| 5.2 | 5 | 3.53E-03 | 0.167 | 5.03E-05 | 0.23 | 0.73 | 84.87 | 3.24E-05 | 1.31E-04 | 4.05 |
| 5.2 | 5 | 3.53E-03 | 0.167 | 5.03E-05 | 0.23 | 0.73 | 83.93 | 3.28E-05 | 1.31E-04 | 4.01 |
| 5.2 | 5 | 3.53E-03 | 0.167 | 5.03E-05 | 0.23 | 0.73 | 83.41 | 3.30E-05 | 1.31E-04 | 3.98 |
| 5.2 | 5 | 3.53E-03 | 0.167 | 5.03E-05 | 0.23 | 0.73 | 83.37 | 3.30E-05 | 1.31E-04 | 3.98 |
| 10.1 | 10 | 3.53E-03 | 0.167 | 5.03E-05 | 0.23 | 0.73 | 585 | 4.76E-06 | 1.31E-04 | 27.59 |
| 10.1 | leakage rate | 3.53E-03 | 0.167 | 5.03E-05 | 0.58 | 0.63 | 61.12 | 3.22E-06 | 1.31E-04 | 40.78 |
| | | 3.53E-03 | 0.167 | | | | | 1.54E-06 | 1.31E-04 | 85.26 |
| 10.2 | 10 | 3.85E-03 | 0.172 | 5.03E-05 | 0.23 | 0.73 | 613.63 | 4.28E-06 | 1.31E-04 | 30.67 |
| 10.2 | 10 | 3.85E-03 | 0.172 | 5.03E-05 | 0.23 | 0.73 | 428.13 | 6.06E-06 | 1.31E-04 | 21.68 |
| 10.3 | 10 | 3.85E-03 | 0.172 | 5.03E-05 | 0.23 | 0.73 | 585 | 4.44E-06 | 1.31E-04 | 29.62 |
| 15.1 | 15 | 3.53E-03 | 0.167 | 5.03E-05 | 0.23 | 0.73 | 611.14 | 4.56E-06 | | 0.00 |
| | leakage rate | 3.53E-03 | 0.167 | 5.03E-05 | 0.68 | 0.73 | 61.12 | 2.50E-06 | | 0.00 |
| | | | | | | | | 2.06E-06 | 1.31E-04 | 63.70 |
| 15.1 | 15 | 3.53E-03 | 0.167 | 5.03E-05 | 0.23 | 0.73 | 722.94 | 3.80E-06 | | 0.00 |
| | leakage rate | 3.53E-03 | 0.167 | 5.03E-05 | 0.68 | 0.73 | 61.12 | 2.50E-06 | | 0.00 |
| | | | | | | | | 1.31E-06 | 1.31E-04 | 100.47 |
| 15.1 | 15 | 3.53E-03 | 0.167 | 5.03E-05 | 0.23 | 0.73 | 695.27 | 3.96E-06 | | 0.00 |
| | leakage rate | 3.53E-03 | 0.167 | 5.03E-05 | 0.68 | 0.73 | 61.12 | 2.50E-06 | | 0.00 |
| | | | | | | | | 1.46E-06 | 1.31E-04 | 90.04 |
| 15.2 | 15 | 3.85E-03 | 0.172 | 5.03E-05 | 0.23 | 0.73 | 1083.68 | 2.39E-06 | 1.31E-04 | 54.87 |
| 15.2 | 15 | 3.85E-03 | 0.172 | 5.03E-05 | 0.23 | 0.73 | 314.73 | 8.24E-06 | 1.31E-04 | 15.94 |
| 15.3 | 15 | 3.85E-03 | 0.172 | 5.03E-05 | 0.23 | 0.73 | 1562 | 1.66E-06 | 1.31E-04 | 79.09 |
| 15.3 | 15 | 3.85E-03 | 0.172 | 5.03E-05 | 0.23 | 0.73 | 1612 | 1.61E-06 | 1.31E-04 | 81.62 |
| 20.1 | 20 | 3.85E-03 | 0.172 | 5.03E-05 | 0.23 | 0.73 | 1212.68 | 2.14E-06 | 1.31E-04 | 61.40 |
| 20.1 | 20 | 3.85E-03 | 0.172 | 5.03E-05 | 0.23 | 0.73 | 1420.32 | 1.83E-06 | 1.31E-04 | 71.91 |
| 20.1 | 20 | 3.85E-03 | 0.172 | 5.03E-05 | 0.23 | 0.73 | 1362.56 | 1.90E-06 | 1.31E-04 | 68.99 |
| 20.1 | 20 | 3.85E-03 | 0.172 | 5.03E-05 | 0.23 | 0.73 | 1286.13 | 2.02E-06 | 1.31E-04 | 65.12 |
| 20.2 | 20 | 3.85E-03 | 0.172 | 5.03E-05 | 0.23 | 0.73 | 1456.29 | 1.78E-06 | 1.31E-04 | 73.73 |
| 20.2 | 20 | 3.85E-03 | 0.172 | 5.03E-05 | 0.23 | 0.73 | 1564.31 | 1.66E-06 | 1.31E-04 | 79.20 |
| 20.3 | 20 | 3.85E-03 | 0.172 | 5.03E-05 | 0.23 | 0.73 | 2864.31 | 9.06E-07 | 1.31E-04 | 145.02 |
| 20.3 | 20 | 3.85E-03 | 0.172 | 5.03E-05 | 0.23 | 0.73 | 3300 | 7.86E-07 | 1.31E-04 | 167.08 |
| 25.1 | 25 | 3.85E-03 | 0.172 | 5.03E-05 | 0.23 | 0.73 | 4529.27 | 5.73E-07 | 1.31E-04 | 229.32 |
| 25.1 | 25 | 3.85E-03 | 0.172 | 5.03E-05 | 0.23 | 0.73 | 8446.74 | 3.07E-07 | 1.31E-04 | 427.67 |
| 25.1 | 25 | 3.85E-03 | 0.172 | 5.03E-05 | 0.23 | 0.78 | 7174.64 | 3.82E-07 | 1.31E-04 | 343.55 |
| 25.2 | 25 | 3.85E-03 | 0.172 | 5.03E-05 | 0.29 | 0.79 | 44020.37 | 5.08E-08 | 1.31E-04 | 2585.44 |
| 25.2 | 25 | 3.85E-03 | 0.172 | 5.03E-05 | 0.23 | 0.73 | 40560.21 | 6.40E-08 | 1.31E-04 | 2053.61 |
| 25.3 | 25 | 3.85E-03 | 0.172 | 5.03E-05 | 0.23 | 0.73 | 36840.65 | 7.04E-08 | 1.31E-04 | 1865.29 |
| 25.3 | 25 | 3.85E-03 | 0.172 | 5.03E-05 | 0.23 | 0.73 | 39450.87 | 6.58E-08 | 1.31E-04 | 1997.44 |
| 30.1 | 30 | 3.85E-03 | 0.172 | 5.03E-05 | 0.27 | 0.81 | 2340 | 1.05E-06 | 1.31E-04 | 125.69 |
| 30.1 | 30 | 3.85E-03 | 0.172 | 5.03E-05 | 0.23 | 0.73 | 3327.81 | 7.80E-07 | 1.31E-04 | 168.49 |
| 30.1 | 30 | 3.85E-03 | 0.172 | 5.03E-05 | 0.23 | 0.73 | 4504.7 | 5.76E-07 | 1.31E-04 | 228.08 |
| 30.2 | 30 | 3.85E-03 | 0.172 | 5.03E-05 | 0.29 | 0.81 | 3360 | 6.80E-07 | 1.31E-04 | 193.23 |
| 30.2 | 30 | 3.85E-03 | 0.172 | 5.03E-05 | 0.23 | 0.73 | 4062.63 | 6.39E-07 | 1.31E-04 | 205.70 |
| 40.1 | 40 | 3.85E-03 | 0.172 | 5.03E-05 | 0.43 | 0.73 | 16962 | 7.01E-08 | 1.31E-04 | 1874.11 |
| 40.2 | 40 | 3.85E-03 | 0.172 | 5.03E-05 | 0.53 | 0.73 | 18744 | 3.84E-08 | 1.31E-04 | 3423.51 |
| 50.1 | 50 | 3.85E-03 | 0.172 | 5.03E-05 | 0.59 | 0.78 | 9344.16 | 6.89E-08 | 1.31E-04 | 1907.86 |
| 50.2 | 50 | 3.85E-03 | 0.172 | 5.03E-05 | 0.51 | 0.73 | 12276.97 | 6.56E-08 | 1.31E-04 | 2001.83 |
| 50.3 | 50 | 3.53E-03 | 0.167 | 5.03E-05 | 0.445 | 0.788 | 11253.22 | 1.21E-07 | 1.31E-04 | 1086.60 |
| 50.4 | 50 | 3.53E-03 | 0.166 | 5.03E-05 | 0.41 | 0.73 | 10540.6 | 1.30E-07 | 1.31E-04 | 1014.23 |